

Purdue University
Purdue e-Pubs

ECE Technical Reports

Electrical and Computer Engineering

12-1-1993

MODELING AND ANALYSIS OF DISTRIBUTION LOAD CURRENTS PRODUCED BY AN AD JUSTABLE SPEED DRIVE HEAT PUMP

Stephen Paul Hoffman

Purdue University School of Electrical Engineering

Follow this and additional works at: <http://docs.lib.purdue.edu/ecetr>

Hoffman, Stephen Paul, "MODELING AND ANALYSIS OF DISTRIBUTION LOAD CURRENTS PRODUCED BY AN AD JUSTABLE SPEED DRIVE HEAT PUMP" (1993). *ECE Technical Reports*. Paper 258.

<http://docs.lib.purdue.edu/ecetr/258>

This document has been made available through Purdue e-Pubs, a service of the Purdue University Libraries. Please contact epubs@purdue.edu for additional information.

MODELING AND ANALYSIS OF
DISTRIBUTION LOAD CURRENTS
PRODUCED BY AN ADJUSTABLE
SPEED DRIVE HEAT PUMP

STEPHEN PAUL HOFFMAN

TR-EE 93-51
DECEMBER 1993



SCHOOL OF ELECTRICAL ENGINEERING
PURDUE UNIVERSITY
WEST LAFAYETTE, INDIANA 47907-1285

**MODELING AND ANALYSIS OF DISTRIBUTION
LOAD CURRENTS PRODUCED BY AN
ADJUSTABLE SPEED DRIVE HEAT PUMP**

Stephen Paul Hoffman

Purdue Electric Power Center
School of Electrical Engineering
Purdue University
1285 Electrical Engineering Building
West Lafayette, IN 47907-1285

December 1993

TABLE OF CONTENTS

	Page
LIST OF TABLES.....	v
LIST OF FIGURES.....	vi
NOMENCLATURE.....	x
ABSTRACT.....	xx
CHAPTER 1. INTRODUCTION.....	1
1.1 Motivation.....	1
1.2 Scope.....	3
1.3 Adjustable speed drives.....	4
1.4 Transformers.....	8
1.4.1 Distribution transformers.....	8
1.4.2 Transformer losses.....	9
1.4.3 Transformer thermal damage.....	9
1.4.4 American National Standard Institute document C57.110.....	10
CHAPTER 2. ADJUSTABLE SPEED DRIVE HEAT PUMPS.....	13
2.1 Refrigeration cycle.....	13
2.2 Adjustable speed drive heat pumps.....	18

	Page
CHAPTER 3. MODELING OF THE ASD HEAT PUMP.....	22
3.1 Introduction.....	22
3.2 Modeling of the electric motor.....	23
3.3 Modeling of the adjustable speed drive.....	34
3.3.1 Introduction.....	34
3.3.2 VSI-ASD inverter.....	36
3.3.3 VSI-ASD rectifier operation.....	40
3.4 Modeling of the distribution transformer.....	42
3.5 Modeling of the compressor shaft load.....	44
3.6 ACSL program explanation and listing.....	45
 CHAPTER 4. SIMULATION RESULTS AND ANALYSIS.....	 54
4.1 Introduction.....	54
4.2 Simulation results.....	55
4.3 Field measurement cases.....	75
4.4 Transformer derating calculations.....	80
4.4.1 ANSI C57.110 example calculation.....	80
4.4.2 Transformer derating of actual system.....	81
4.4.3 Transformer derating for simulation results.....	83
4.5 IEEE Standard 519-1992.....	86
 CHAPTER 5. CONCLUSIONS AND RECOMMENDATIONS.....	 89
5.1 Conclusions.....	89
5.2 Recommendations.....	90
 BIBLIOGRAPHY.....	 92

LIST OF TABLES

Table		Page
4.1	ASD figure description, no load case.....	56
4.2	Simulated motor load torque cases.....	58
4.3	Figure descriptions of field measurements.....	75
4.4	ANSI C57.110 transformer derating example.....	81
4.5	Transformer active power loss estimates for the actual measurements.....	82
4.6	Transformer active power loss estimates for the simulation results, load 3.....	84
4.7	Transformer primary and secondary current total harmonic distortion and derating for the five load cases.....	85
4.8	Transformer derating for the five load cases, transformer at rated load, one-half ASD and full ASD load cases.....	86
4.9	IEEE Standard 519-1992 Current distortion limits for general distribution systems (120 volts through 69,000 volts) [11]	87
5.1	THD and transformer derating results for simulated and measured waveforms.....	90

LIST OF FIGURES

Figure	Page
1.1 Drive system showing controller, converter, motor, and process.....	4
1.2 Simplified diagram of adjustable speed drive.....	5
1.3 Voltage source inverter adjustable speed drive.....	7
1.4 Transformer configuration.....	8
2.1 Refrigeration cycle block diagram.....	14
2.2 Reversible refrigeration cycle in cooling mode.....	15
2.3 Reversible refrigeration cycle in heating mode.....	16
2.4 Block diagram of ASD heat pump.....	21
3.1 Side view of motor with stator winding.....	24
3.2 Winding turns density versus θ_r	25
3.3 Cross-sectional view of induction motor showing the locations of the rotor and stator windings.....	25
3.4 Equivalent circuit of induction machine.....	26
3.5 Figure showing relationship between (abc) and (qdo) variables.....	31
3.6 Voltage source inverter adjustable speed drive.....	34
3.7 Six step voltage waveform.....	35
3.8 Voltage source inverter, 3-phase.....	36
3.9 Inverter switching strategy.....	38

Figure	Page
3.10	Six step inverter waveform.....39
3.11	Single phase rectifier with LC filter..... 41
3.12	Transformer equivalent circuit diagram..... 44
3.13	Transformer and drive with ACSL program parameters..... 53
4.1	Transformer primary voltage versus time..... 59
4.2	Transformer input current versus time.....59
4.3	Transformer instantaneous power versus time..... 59
4.4	Phase a inverter six step output voltage versus time..... 60
4.5	Phase b inverter six step output voltage versus time..... 60
4.6	Phase c inverter six step output voltage versus time..... 60
4.7	Induction motor speed versus time..... 61
4.8	Induction motor electrical torque versus time.....61
4.9	Inverter input voltage V_{inv} versus time..... 61
4.10	Frequency spectrum of inverter output voltage V_{as}62
4.11	Frequency spectrum of transformer secondary current..... 62
4.12	Frequency spectrum of phase a motor stator current..... 62
4.13	Induction motor speed versus time..... 63
4.14	Induction motor electrical torque versus time..... 63
4.15	Applied load torque versus time..... 63
4.16	Transformer secondary current versus time..... 64
4.17	Transformer primary instantaneous power versus time..... 64
4.18	Inverter input voltage versus time..... 64
4.19	Load 1. Transformer primary current versus time.....65
4.20	Load 1. Transformer secondary current versus time..... 65

Figure	Page
4.21 Load 1. Transformer primary instantaneous power.....	65
4.22 Load 1. Frequency spectrum of transformer secondary current expressed as a percentage of the fundamental.....	66
4.23 Load 1. Frequency spectrum of transformer primary current expressed as a percentage of the fundamental.....	66
4.24 Load 2. Transformer primary current versus time.....	67
4.25 Load 2. Transformer secondary current versus time.....	67
4.26 Load 2. Transformer primary instantaneous power.....	67
4.27 Load 1. Frequency spectrum of transformer secondary current expressed as a percentage of the fundamental.....	68
4.28 Load 1. Frequency spectrum of transformer primary current expressed as a percentage of the fundamental.....	68
4.29 Load 3. Transformer primary current versus time.....	69
4.30 Load 3. Transformer secondary current versus time.....	69
4.31 Load 3. Transformer primary instantaneous power.....	69
4.32 Load 3. Frequency spectrum of transformer secondary current expressed as a percentage of the fundamental.....	70
4.33 Load 3. Frequency spectrum of transformer primary current expressed as a percentage of the fundamental.....	70
4.34 Load 4. Transformer primary current versus time.....	71
4.35 Load 4. Transformer secondary current versus time.....	71
4.36 Load 4. Transformer primary instantaneous power.....	71

Figure	Page
4.37 Load 4. Frequency spectrum of transformer secondary current expressed as a percentage of the fundamental.....	72
4.38 Load 4. Frequency spectrum of transformer primary current expressed as a percentage of the fundamental.....	72
4.39 Load 5. Transformer primary current versus time.....	73
4.40 Load 5. Transformer secondary current versus time.....	73
4.41 Load 5. Transformer primary instantaneous power.....	73
4.42 Load 5. Frequency spectrum of transformer secondary current expressed as a percentage of the fundamental.....	74
4.43 Load 5. Frequency spectrum of transformer primary current expressed as a percentage of the fundamental.....	74
4.44 Phase a current and voltage snapshot. heat pump off.....	76
4.45 Phase a instantaneous power. heat pump off.....	76
4.46 Phase a voltage amplitude spectrum. heat pump off.....	77
4.47 Phase a current amplitude spectrum. heat pump off.....	77
4.48 Phase a current and voltage snapshot. heat pump on.....	78
4.49 Phase a instantaneous power. heat pump on.....	78
4.50 Phase a voltage amplitude spectrum. heat pump on.....	79
4.51 Phase a current amplitude spectrum. heat pump on.....	79

NOMENCLATURE

ac	alternating current
ACSL	Advanced Continuous Simulation Language
alpha	rectifier firing delay angle variable
ANSI	American National Standards Institute
ANSI C57.110	Recommended Practice for Establishing Transformer Capability when Supplying Nonsinusoidal Load Currents
ar	subscript to denote the a rotor phase winding
as	subscript to denote the a stator phase winding
ASD	adjustable speed drive
br	subscript to denote the b rotor phase winding
bs	subscript to denote the b stator phase winding
C_f	capacitance of parallel capacitor
cint	ACSL variable to determine data logging rate
COP	coefficient of performance
cr	subscript to denote the c rotor phase winding
cs	subscript to denote the c stator phase winding
dc	direct current
DSM	demand side management
EER	energy efficiency ratio
f_{abcr}	3 by 1 column vector of a, b, and c rotor parameters
f_{abcr}	3 by 1 column vector of a, b, and c rotor parameters referred to the stator windings

f_{abc}	3 by 1 column vector of a, b, and c stator parameters
FFT	fast Fourier transform
f_h	harmonic current distribution factor for harmonic h
F_{me}	frequency of the inverter ac output waveform
	frequency of fundamental component
f_{qdr}	3 by 1 column vector of a, b, and c rotor parameters referred to the stator windings
gtzero	logical variable used to determine rectifier state
h	harmonic order
HP	heat pump
HVAC	heating, ventilation, and air conditioning
I_{abr}	3 by 1 column vector of a, b, and , rotor phase currents
i_{abc}	3 by 1 column vector of a, b, and c rotor phase currents referred to the stator windings
I_{abc}	3 by 1 column vector of a, b, and , stator phase currents
ialg	ACSL constant to determine integration algorithm
i_{ar}	current into phase a or induction motor rotor winding
i_{as}	current into phase a of induction motor stator winding
i_{br}	current into phase b of induction motor rotor winding
i_{bs}	current into phase b of induction motor stator winding
i_{cr}	current into phase c of induction motor rotor winding
i_{cs}	current into phase c of induction motor stator winding
i_{dr}	d axis rotor current referred to the stator windings
idrs	current through d rotor winding
i_{ds}	current through d stator winding
idss	current through d stator winding

i_{inv}	current into the inverter
I_l	current through the inductor L_f
i_{lic}	current through inductor L_f initial condition
$I_{max}(pu)$	rms load current
i'_{qdor}	3 by 1 column vector of q, d, and 0 rotor currents referred to the stator windings
i_{qdos}	3 by 1 column vector of q, d, and 0 stator currents
i'_{qr}	q axis rotor current referred to the stator windings
i_{drs}	current through d rotor winding
i_{qs}	current through q stator winding
i_{qss}	current through q stator winding
I_{rec}	current drawn by the rectifier
I_s	induction motor stator winding current
i'_{0r}	0 axis rotor current referred to the stator windings
i_{0s}	current through 0 stator winding
I_1	current into the transformer primary winding
I_2	current into the transformer secondary winding
i'_2	transformer secondary current referred to the primary
i_{2pr}	transformer secondary current referred to the primary
J	induction motor rotor inertia
kA	kiloamps
K_r	3 by 3 rotor arbitrary reference frame transformation
K_s	3 by 3 stator arbitrary reference frame transformation
kV	kilovolts
kVA	kilovolt-amps
L_f	inductance of series smoothing inductor

L_r	induction motor rotor leakage inductance
L'_r	induction motor rotor leakage inductance referred to the stator windings
L_s	induction motor stator leakage inductance
L'_{12}	transformer secondary leakage inductance referred to the primary
L_{mr}	induction motor rotor mutual inductance
L_{ms}	induction motor stator mutual inductance
L_r	3 by 3 matrix of rotor leakage and mutual inductances
L'_r	3 by 3 matrix of rotor leakage and mutual inductances referred to the stator windings
L_s	3 by 3 matrix of stator leakage and mutual inductances
L_{sr}	maximum mutual inductance between stator and rotor
L'_{sr}	maximum mutual inductance between stator and rotor referred to the stator windings
L_{srm}	mutual inductance between stator and rotor windings
max_t	ACSL maximum integration step size constant
$mint$	ACSL minimum integration step size constant
N_r	number of turns in rotor phase winding
N_1	number of turns in transformer primary winding
N_2	number of turns in transformer secondary winding
M	1.5 times the stator mutual inductance
N_s	number of turns in stator phase winding
p	derivative with respect to time operator
P	number of poles in induction motor
pil	time derivative of the inductor current
$pilon$	time derivative of the inductor current when switch is on
$pilonmns$	time derivative of the inductor current when $V_{rec} < 0$

pilonplus	time derivative of the inductor current when $V_{rec} > 0$
$P_{EC-R}(pu)$	per unit winding eddy current loss for rated conditions
$P_{LL-R}(pu)$	per unit load loss density under rated conditions
pramp	time derivative of ramp to determine inverter switching
prampp	time derivative of ramp to determine rectifier switching
pSidrs	time derivative of rotor d axis flux linkage per second
pSidss	time derivative of stator d axis flux linkage per second
pSiqrs	time derivative of rotor q axis flux linkage per second
pSiqss	time derivative of stator q axis flux linkage per second
pSi1	time derivative of the transformer primary flux linkage per second
pSi2pr	time derivative of the transformer secondary flux linkage per second
pVinv	time derivative of the voltage across the capacitor C_f
pwr	time derivative of rotor angular velocity
rampic	inverter switching ramp function initial condition
ramppic	rectifier switching ramp function initial condition
Rload	resistance of load across transformer secondary
rms	root mean square
Ron	logical variable used to determine rectifier state
r_r	induction motor rotor phase winding resistance
	induction motor rotor phase winding resistance referred to the stator windings
r_{rm}	3 by 3 diagonal matrix with diagonal entries equal to r_r
r'_{rm}	3 by 3 diagonal matrix with diagonal entries equal to r'_r
r_s	induction motor stator phase winding resistance
r_{sm}	3 by 3 diagonal matrix with diagonal entries equal to r_s
r_1	resistance of transformer primary winding

$r'2$	transformer secondary resistance referred to the primary
$r2pr$	transformer secondary resistance referred to the primary
SA	logical variable used to determine inverter state
SB	logical variable used to determine inverter state
SC	logical variable used to determine inverter state
SCR	silicon controlled rectifier
Sidrs	induction motor d axis rotor flux linkage per second
Sidrsic	induction motor d axis rotor flux linkage per second initial condition
Sidss	induction motor d axis stator flux linkage per second
Sidssic	induction motor d axis stator flux linkage per second initial condition
Sirn	transformer mutual flux linkage per second
simd	induction motor flux linkage per second parameter
simq	induction motor flux linkage per second parameter
Siqrs	induction motor q axis rotor flux linkage per second
Siqrsic	induction motor q axis rotor flux linkage per second initial condition
Siqss	induction motor q axis stator flux linkage per second
Siqssic	induction motor q axis stator flux linkage per second initial condition
Si1	transformer primary flux linkage per second
Silic	transformer primary flux linkage per second initial condition
Si2pr	transformer secondary flux linkage per second referred to the primary
$()^T$	transpose
Si2pric	transformer secondary flux linkage per second initial condition referred to the primary winding
t	time in ACSL simulation
Tconstant	constant component of compressor load torque

TDD	total harmonic distortion
THD	total harmonic distortion
T_e	electrical torque produced by the motor
T_m	inverter output waveform period
t_{stop}	ACSL variable to determine simulation stop time
T_l	load torque applied to the induction motor
T_{var}	time-varying component in compressor load torque
$two\pi$	constant equal to two times pi
V	volts
V_{abcr}	3 by 1 column vector of a, b, and c rotor phase voltages
V'_{abcr}	3 by 1 column vector of a, b, and c rotor phase voltages referred to the stator windings
V_{abcs}	3 by 1 column vector of a, b, and c stator phase voltages
V_{ag}	voltage from node a to ground in Figure (3.8)
V_{ap}	voltage from nodes a to p in Figure (3.8)
V_{ar}	voltage across induction motor phase a rotor winding
V_{as}	voltage across induction motor phase a stator winding
V_{bg}	voltage from node b to ground in Figure (3.8)
V_{bp}	voltage from nodes b to p in Figure (3.8)
V_{br}	voltage across induction motor phase b rotor winding
V_{bs}	voltage across induction motor phase b stator winding
v_{cg}	voltage from node c to ground in Figure (3.8)
V_{cp}	voltage from nodes c to p in Figure (3.8)
V_{cr}	voltage across induction motor phase c rotor winding
V_{cs}	voltage across induction motor phase c stator winding
V'_{dr}	d axis rotor voltage referred to the stator windings

v_{drs}	voltage across d rotor winding
V_{ds}	voltage across d stator winding
v_{dss}	voltage across d stator winding
v_{inv}	voltage applied to the inverter and across capacitor C_f
V_{invic}	voltage applied to the inverter initial condition
V_m	transformer reference voltage
V_{mag}	magnitude of the sinusoidal transformer primary voltage
V_{ng}	voltage from node n to ground in Figure (3.8)
V_{np}	voltage from nodes n to p in Figure (3.8)
V'_{qdor}	3 by 1 column vector of q, d, and 0 rotor voltages referred to the stator windings
V_{qdos}	3 by 1 column vector of q, d, and 0 stator voltages
V'_{qr}	q axis rotor voltage referred to the stator winding
v_{qrs}	voltage across d rotor winding
V_{qs}	voltage across q stator winding
v_{qss}	voltage across q stator winding
V_{rec}	voltage applied to the single phase rectifier
V_{SI}	voltage source inverter
V'_{0r}	0 axis rotor voltage referred to the rotor windings
v_{os}	voltage across 0 stator winding
V_1	voltage applied to the transformer primary winding
V_2	voltage applied to the transformer secondary winding
V'_2	transformer secondary voltage referred to the primary
v_{2pr}	transformer secondary voltage referred to the primary
ω_b	base frequency in radians per second
ω_e	source electrical frequency in radians per second

w_r	induction motor rotor angular velocity
w_{rb}	induction motor rotor base frequency
w_{ric}	induction motor rotor angular velocity initial condition
w_{sl}	induction motor slip frequency in radians per second
X_{ad}	induction motor d axis reactance constant
x_{capm}	transformer reactance constant
X_{aq}	induction motor q axis reactance constant
X_{lr}	induction motor rotor leakage reactance
X_{ls}	induction motor stator leakage reactance
x_{l1}	transformer primary leakage reactance
x_{l2pr}	transformer secondary leakage reactance referred to the primary winding
X_M	induction motor mutual reactance
x_{mtran}	transformer mutual reactance
β	rotor arbitrary reference frame transformation angle
θ	stator arbitrary reference frame transformation angle
θ_r	induction motor rotor angle
λ_{abc_r}	3 by 1 column vector of a, b, and c rotor flux linkages
λ'_{abc_r}	3 by 1 column vector of a, b, and c rotor flux linkages referred to the stator windings
λ_{abc_s}	3 by 1 column vector of a, b, and c stator flux linkages
λ'_{dqr}	3 by 1 column vector with entries λ'_{dr} , $-\lambda'_{qr}$, and 0
λ_{dq_s}	3 by 1 column vector with entries λ_{ds} , $-\lambda_{qs}$, and 0
λ'_{dr}	flux linking d rotor winding referred to the stator winding
λ_{ds}	flux linking d stator winding

λ'_{qd0r}	3 by 1 column vector of q, d, and 0 rotor flux linkages referred to stator windings
λ_{qd0s}	3 by 1 column vector of q, d, and 0 stator flux linkages
λ'_{qr}	flux linking q rotor winding referred to the stator winding
λ_{qs}	flux linking q axis stator winding
λ'_{0r}	flux linking 0 rotor winding referred to the stator winding
λ_{0s}	flux linking 0 stator winding
ω	arbitrary reference frame velocity
ω_r	induction machine rotor velocity
ω_{shaft}	velocity of compressor shaft
Ψ_m	transformer mutual flux linkage per second

ABSTRACT

A number of demand side management techniques have been **proposed** for the efficient use of electric power in the commercial and residential sector;. The adjustable **speed drive** heat pump is a technology which has the prospect of decreasing power demands for space heating. This design has the advantage over conventional designs of higher efficiency and, potentially, reduction of peak power demand. Its **main** disadvantage is higher cost. Further, it has the disadvantage that it produces a load current with a substantial harmonic content. This load current waveform is injected into the distribution system and causes extra losses in the distribution transformer. These high efficiency heat pumps are being promoted by some utility rebate programs to encourage residential customers to install the high efficiency devices. This thesis presents an introduction to adjustable speed drives as they are applied to the refrigeration cycle. **The** impact of these devices on distribution transformers and the significant transformer **derating** is discussed. In addition, an Advanced Continuous Simulation Language, (ACSL), simulation is presented that models the induction motor, six step adjustable speed drive, and distribution transformer. The results of this simulation are **presented** to show typical system waveforms, such as the load current and its frequency spectrum. These **waveforms** are compared to results obtained from an actual installation. In addition, the ANSI

Standard C57.110 is used to assess the **transformer** derating. The main contribution of the thesis is the presentation of a detailed method for the analysis of adjustable speed drive heat pump loads. General conclusions are drawn concerning the **applicability** of the high efficiency, adjustable speed drive heat pump including the added losses in the distribution system.

CHAPTER 1

INTRODUCTION

1.1 Motivation

In recent years, due to the high cost of adding power generation, transmission, and distribution capacity, many electric utility companies have instituted various programs with the intent of forestalling system expansion. Also, in many jurisdictions, regulatory agencies critically examine applications for system expansion because they are under pressure from consumer groups to minimize all costs which are placed in the rate base, including those costs for system expansion. Among these efforts are programs to reduce the peak demand. One class of such programs are termed demand side management (DSM) programs. Demand side management programs include such efforts as control of air conditioners and electric water heaters during peak periods. Other commonly used techniques for reducing the electrical peak demand are making use of interconnections with neighbors, applications of cogeneration, conservation, and taking advantage of the modern technologies which increase the efficiency of loads. These programs are designed to reduce both the peak demand and the total electric energy consumed. If the electrical demand, or its growth, is reduced the presently installed generation, transmission, and distribution capacity may be sufficient to supply the load for a longer time. In this way, electric utility companies can get the maximum use from their installed facilities.

The three most frequently used programs for peak demand reduction and total energy use reduction are demand side management, conservation, and increased efficiency.

Demand side management refers to direct control of loads by the electric utility company. Using direct control, the peak demand can be reduced by shifting loads in time from on-peak to off-peak hours. Conservation programs refer to voluntary reduction of the load during both on-peak and off-peak hours by the elimination of electric energy use by some non-critical loads that would have otherwise been required. Conservation includes such measures as a decreased household heating temperature, a higher household cooling set-point temperature, reduced lighting load, and a lower water heater temperature setting. The third demand reduction program, improvement of load efficiencies, may be the most important method to achieve a reduction in the load. Unlike the first two methods, improving load efficiencies does not entail sacrifice or change of life style by individual residential or commercial consumers. Improvements of load efficiencies have been implemented or are being studied in diverse applications such as electric clothes dryers (a microwave clothes dryer has been proposed), high efficiency motors, electric ballasts for fluorescent lighting, novel lighting designs to replace the conventional incandescent lamp, high efficiency refrigerators, water heaters, dishwashers, and heat pumps. Demand side management, conservation, and improved efficiency programs for many utilities include rebates and other incentives.

The energy required to heat or cool a residential and commercial building represents a significant percentage of the total electric energy consumed in the United States. Within a given region of the country, the heating and cooling load depends largely on weather related factors. Most utilities in the United States, except for those in the far North, experience their peak load during the summer months due to the extra energy required to serve air conditioning loads. An improvement in the efficiency of air conditioners would reduce the peak load served by these utilities. Although the utility may lose revenue due to increased efficiency, a reduction in peak load is an advantage for a utility because generation and transmission installation requirements are determined from

the peak load. If a utility can limit its peak load the need for new generating units can be postponed. In this manner, a company whose business is to sell electric power can justify encouraging consumers to install **energy-efficient** air conditioning units. Utilities are also under regulatory pressure to promote energy conservation, and it is a **prudent** practice to conserve energy and resources whenever possible.

This thesis focuses on the high efficiency, adjustable speed drive heat pump and air conditioner. The high efficiency heat pump is used and promoted as a key element in energy efficiency improvement programs by electric utilities. Some of these high efficiency heat pumps produce a large amount of currents at harmonic frequencies, which can cause additional losses in the distribution system. This thesis will present a model of the adjustable speed drive heat pump and show how the harmonic currents affect the distribution system, in particular the distribution transformer.

1.2 Scope

The adjustable speed drive has been successfully applied to heat pumps for a resulting gain in efficiency. This thesis examines how the adjustable speed drive has been applied to the refrigeration cycle. Although the power drawn by one residential heat pump is not significant, a large number of ASD heat pumps and other nonlinear loads present on a distribution circuit could have a resulting larger effect on the distribution system. Some electric utility companies have developed rebate programs which encourage the installation of the high efficiency heat pump. If these programs are instituted without considering the distorted load currents in the distribution system, the utility company may encounter problems associated with the distortion and the will not be compensated for extra losses incurred.

This thesis presents the operation and modeling of the induction motor, adjustable speed drive, distribution transformer, and compressor shaft load. This is accomplished through analysis and simulation. The simulation is used to obtain **characteristics** of the

system behavior during various operating conditions. The fast Fourier transform, **FFT**, is also used to obtain the frequency spectrum of selected waveforms. The simulation results are compared to waveforms obtained from an operating adjustable speed drive heat pump. Calculations are presented which show the transformer derating for typical operating conditions with a nonlinear load.

1.3 Adjustable speed drives

An adjustable speed drive (ASD) is a solid state device which controls the energy flow to a rotating machine for the purpose of controlling its operation. A motor drive consists of the controller, power electronic converter, electric motor, and possibly speed and position sensors. A block diagram of a power electronic drive system is shown in Figure (1.1). The purpose of the drive is to directly control the voltage, current, and frequency applied to the electric motor so that the motor outputs, such as speed and torque, are as desired for a particular application. Power electronic drives are typically connected to an alternating current supply and are used to control synchronous, direct current, induction, and stepper motors. Motor drives are in operation that can supply and control motors ranging in size from several watts up to several thousand horsepower [12].

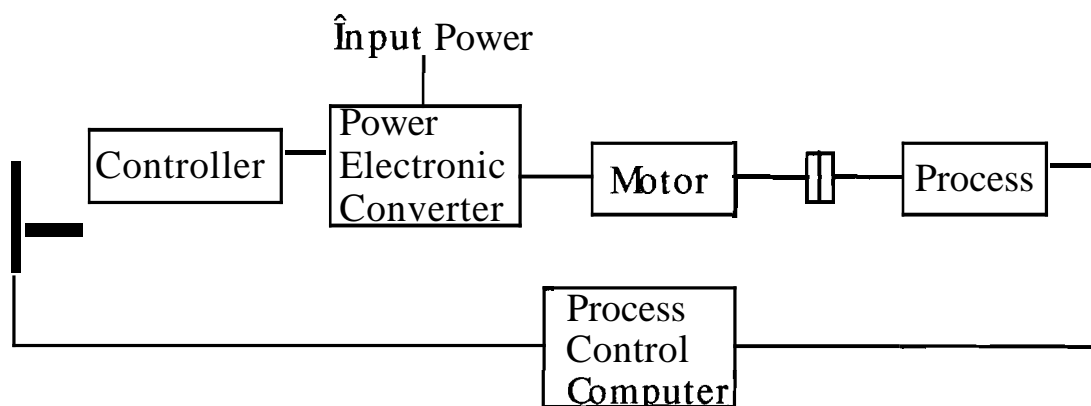


Figure 1.1 Drive system showing controller, converter, motor, and process

The power electronic converters in an adjustable speed drive employ several switching strategies and circuit configurations to achieve control of the motor. The most common power electronic drive schemes employ the following general operating strategy: the input ac waveform is changed into a dc voltage by a one-phase or a three-phase rectifier; a capacitor is also typically used to provide a more constant dc voltage, an inverter is then used to change the dc voltage back into an ac voltage and current which is then fed into the machine. This process is shown in block diagram form in Figure (1.2). The advantage of switching from ac to dc and then back to ac is that the output ac voltage and frequency can be different from the input waveform. Further, the output can have a different number of phases than the input.

Perhaps the most important advantage of the **ASD** is the improvement in overall, process efficiency. Also, an **ASD** affords greater design flexibility. For example, if a single-speed motor is driving a pump and the output of the pump needs to be reduced, a commonly used method is to install a throttle at the output of the pump. This is not the best solution because energy is lost by the throttle. If the motor speed can be easily varied to change the output of the pump, then the energy wasting throttle is not needed. The **ASD** solution to this application affords both improvement of overall efficiency and a more flexible electrical solution.

Several switching schemes are used by the inverters to construct an ac waveform. These methods include square-wave pulse switching, current-regulated modulation, the

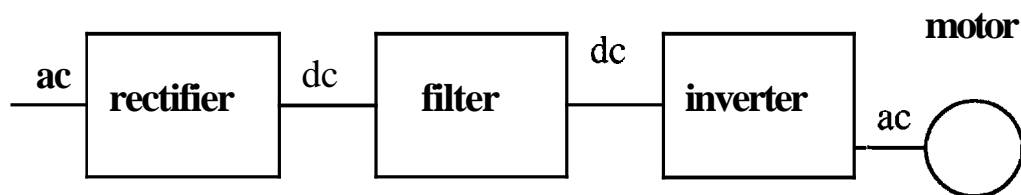


Figure 1.2 Simplified diagram of adjustable speed drive

voltage-cancellation technique, and pulse-width modulation [7]. This last method has the advantage that the output frequency and voltage magnitude is controllable and the harmonics in the output waveform are lower than with other methods. More information on other novel and proposed drive topologies, such as the matrix converter, the current link converter, the resonant link converter, can be found in [12].

The voltage source inverter employs one of the simplest switching strategies and is favored because of its low switching frequency requirements. This adjustable speed drive design is also rugged, but has the disadvantages of a poor power factor at low speeds and low speed pulsations. The circuit diagram for the voltage source inverter is shown in Figure (1.3). The single phase, usually 60 hertz supply is connected to a rectifier. The rectifier can be constructed with diodes to give an uncontrolled dc output voltage. For induction motor drives the rectifier is usually constructed with thyristors. Thyristors can be controlled to yield a variable output voltage. The series inductor and parallel capacitor between the rectifier and inverter reduces the pulsations in the dc voltage which supplies the inverter. The inverter uses thyristors or some other controllable switch to produce a three phase, six-step waveform which is fed into the machine. Referring to Figure (1.3), the inverter is controlled such that a switch is turned on for 180 electrical degrees. The resulting output of this switching pattern is a three phase, six step output voltage waveform which is used to drive a machine. The intermediate dc voltage isolates the input ac from the output ac, which is why the output can have a different number of phases, voltage level, and frequency than the input waveform.

The thyristor, which can be used in a voltage source inverter ASD, is a solid state switch which has a high power transmitting capability. It can block voltages up to 7kV in the reverse direction and can block voltages of up to 5kV in the forward direction **until** a voltage signal is applied to the gate terminal. Then the device turns on **and** can **carry** up to **2kA** of current with a forward voltage drop of 1-3 volts. The thyristor will then stay in the conducting mode until the voltage across the device becomes negative. The thyristor has a controllable turn-on time and must be turned off by the voltage across the device.

Depending on the application and device characteristics desired, the switches used in power converter circuits are: bipolar junction transistors, monolithic darlingtons, **metal-oxide semiconductor field effect transistors** , thyristors, **triacs**, **gate-turn-off** thyristors, and insulated gate bipolar transistors. The thyristor and **triac** can be turned on by a control signal but must be turned off by the external circuit voltage. Controllable switches can be turned on and off by control signals, which provides many more circuit configurations in which they are useful.

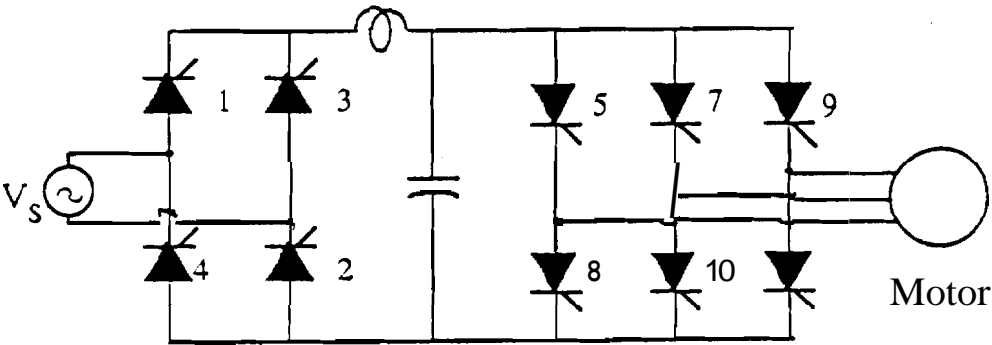


Figure 1.3 Voltage source inverter adjustable speed **drive**

1.4 Transformers

1.4.1 Distribution transformers

A distribution transformer is used to convert primary distribution voltage levels which typically range from 4kV to 13.8kV, to secondary voltage levels which are typically 120/240V for residential or 120/240/480V for commercial [17]. A two winding single phase transformer consists of a primary and a secondary of insulated wire wound around a laminated, usually iron, core. The alternating current voltages applied to the primary winding produces flux which travels **throughout** the low reluctance path of the iron core. The core is made up of many thin insulated slices, or laminations of iron to reduce the eddy current losses. The alternating flux **links** the secondary **windings** to produce a voltage on the secondary. The number of turns in the primary, N_1 , relative to the secondary windings, N_2 , can be changed to produce the desired voltage transformation ratio. Figure (1.4) illustrates the basic components of a transformer. A **classical** reference on transformers is the J & P Transformer Book [14]. The Handbook of Transformer Applications [15] is a reference which also describes the transformer and its applications in detail.

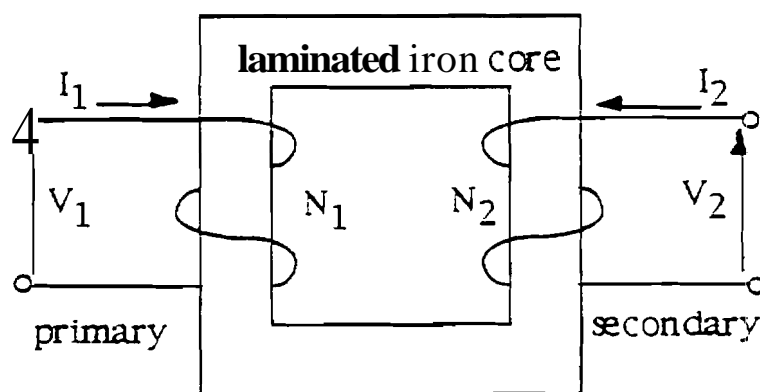


Figure 1.4 Transformer configuration

1.4.2 Transformer losses

Any real device **will** consume energy during operation, and the transformer is no exception. The losses in a transformer can be divided into the copper losses, stray losses, and the no-load or the excitation loss. The wire windings of the transformer have a small resistance. The current flowing through the windings will cause the I^2R copper losses. The stray losses are made up of the eddy current losses in the windings and in the other metal components of the transformer. This stray loss occurs because the leakage flux induces a voltage in the metal of the transformer which causes circular, or eddy, currents to flow. The metal has an electrical resistance so heat is produced by the eddy currents which is lost energy. The eddy current losses are proportional to the square of the load current multiplied by the square of the frequency [2].

1.4.3 Transformer thermal damage

The power lost in a transformer is converted to thermal energy. The thermal energy raises the temperature of the transformer. Transformer losses must be limited so that the internal temperature is not so high that damage to the **transformer** would result. Several of the methods used to cool a transformer are: oil bath **surrounding** the core and windings, a heat exchanger, and cooling fans.

Transformer damage resulting **from** increased internal temperature can occur in several ways. The highest temperature, often referred to as the hot spot, in the transformer must be limited so that the device is not permanently physically damaged. The operating lifetime of the transformer can also be reduced by high operating temperatures. The conventional insulation between conductors turn-to-turn used in **transformers** consists of lacquer and a paper or cloth material which contains cellulose. **Lacquer** is a complex

organic compound. Cellulose is a complex organic compound whose molecules are made up of 1000 to 1400 glucose monomers, which are a combination of carbon, oxygen, and hydrogen atoms [18]. Extreme heat will cause charring of the insulation. However, even moderately high temperatures cause a breakdown in the individual monomers in the large cellulose molecule. The thermal aging of cellulose insulation deteriorates its mechanical properties, such as tensile strength, burst, and tear properties. Although cellulose is adversely affected by water and oxygen, modern oil preservation systems are employed to minimize the water and oxygen content in a transformer. The transformer temperature is determined by the operating conditions primarily the load level, power factor, and duration of the load. Also, the temperature depends on the losses, which in part depend on the level and the total harmonic distortion of the current. Thus thermal operating conditions can reduce the useful operating lifetime of the transformer. Mechanical and dielectric stresses more frequently determine the transformer life, although thermally induced insulation deterioration can make a transformer more susceptible to mechanical or dielectric stresses.

1.4.4 American National Standards Institute document C57.110

The American National Standards Institute, ANSI, jointly with the IEEE, has estimated and quantified the reduction in transformer capacity when it is forced to carry nonsinusoidal load currents. This work appears in ANSI C57.110, "Recommended Practice for Establishing Transformer Capability when Supplying Nonsinusoidal Load Currents." A distribution transformer is designed to operate with sinusoidal voltages and currents at the fundamental frequency of 60 hertz. Loads such as incandescent lamps, induction motors, resistive heating, and power factor correction capacitors do not significantly distort the sinusoidal voltage and current waveforms. Since the voltage and

current waveforms are not distorted, the harmonic content in the current drawn by these loads is low.

The number of power electronic loads served by the distribution system has increased. The main power electronic load is the industrial rectifier. Other nonlinear loads are: fluorescent lighting, lighting dimmers, electronic devices such as televisions and computers, and drives for rotating machines. Power electronic drives use solid-state switches which interrupt the current drawn by a load and reconnect it during any portion of the cycle [13]. Although the operating characteristics of these drives can vary widely depending on the design, the current drawn by these power electronic loads is often not sinusoidal. In most cases the input current to a drive is a square wave or other non-sinusoidal wave, which contains a significant percentage of harmonics. A harmonic current is a sinusoidal wave with a frequency that is an integer **multiple** of the 60 hertz fundamental frequency. The harmonic is one term of the Fourier series **representation** of a periodic signal. Since the impedance of the power system source is lower than the impedance of the power electronic load, a power electronic load appears to the distribution line as a harmonic current source. The distribution transformer is forced to **carry** these non-sinusoidal currents which are injected into the distribution system. The higher **frequency** sinusoids which make up the distorted current waveforms cause extra losses in the transformer. Most energy lost in the transformer is converted to thermal energy which raises the operating temperature of the transformer. The factor which determines whether damage is done to the transformer is the hot spot temperature - the maximum temperature in the device. A high operating temperature can reduce the operating life of the transformer, thus it is important to **limit** transformer temperature. Since the losses rise with increasing harmonic currents, limiting **transformer** temperature can be accomplished by reducing the total current, and thus the apparent power through the transformer.

The winding eddy current loss is due to the flow of current resulting from the voltage caused by **flux**. The eddy current loss increases with frequency and is proportional to the square of the harmonic current amplitude times the square of the harmonic current frequency. The copper loss and the winding eddy current losses are dissipated in the windings of the transformer, and in the iron laminations. These quantities must be limited to limit the temperature of the transformer. The ANSI C57.110 recommended practice includes transformer characteristics and the magnitude of the current at each harmonic to produce a formula which yields a recommended operating capacity.

CHAPTER 2

ADJUSTABLE SPEED DRIVE HEAT PUMPS

2.1 Refrigeration cycle

The refrigeration cycle is used in a heat pump to absorb thermal energy from a low temperature source and to reject the thermal energy to a higher temperature medium. The refrigeration cycle can be used as an air conditioner to cool a building or as a heat pump to heat a building. The high efficiency air conditioner is installed with a reversible valve and dual-purpose controls so it can also operate as a heat pump. The heat pump operates during the winter and the cooler periods of the spring and fall to transfer thermal energy from the outside, cooler air to the interior of a residence. One heat **exchange** element is located outside the building and the other is located inside. The heat exchange unit is termed an evaporator if it is absorbing thermal energy and is termed a condenser if it is releasing thermal energy. For an air conditioner the refrigeration cycle is used to absorb thermal energy from a low temperature area and to reject the thermal **energy** to a higher temperature medium, usually the warmer outside air. The main advantage of the heat pump is that it has the capability to transfer several units of thermal energy, **typically** 7-12, for each unit of electrical energy consumed by the device [1]. The ratio of the thermal energy transferred divided by the electrical energy consumed is called the coefficient of performance (COP) or energy efficiency ratio (EER). The refrigeration cycle is used in many applications including air conditioners, heat pumps, **refrigerators**, and dehumidification systems. The operation and applications for the refrigeration cycle can

be found in greater detail in references such as the Handbook of HVAC Design, [16], and other references such as [10], and [11].

The components which are used in the refrigeration cycle are: a motor, compressor, expansion device, evaporator, condenser, cooling fans, a **control** system, and a refrigerant. A diagram of the refrigeration cycle is shown in Figure (2.1). A heat pump is typically equipped with a reversing valve so it can also operate as an air conditioner. Figure (2.2) is a block diagram of a reversible refrigeration cycle with the valve set for cooling operation. Figure (2.3) shows a block diagram of the same refrigeration cycle with the reversible valve set for heating operation. The location of the heat exchange unit does not change as the heat pump is changed to air conditioning operation, but the names used to describe each depend on whether the heat exchanger is absorbing or releasing thermal energy, and not on the actual location of the heat exchange units.

The following discussion will explain the operation of the refrigeration cycle, starting at the motor and continuing counter-clockwise around Figure (2.1). An electric motor is used to drive the compressor. This motor is typically a single phase, single speed induction motor in conventional, residential heat pumps. **Variable** speed, high efficiency heat pumps instead use a standard three phase induction motor that can run in the range of

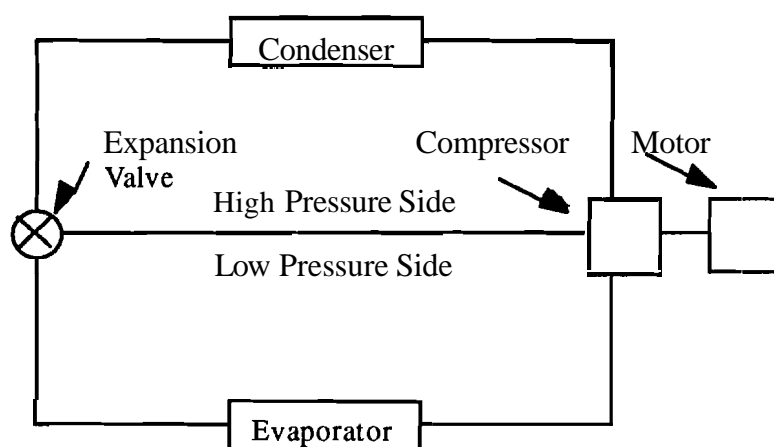


Figure 2.1 Refrigeration cycle block diagram

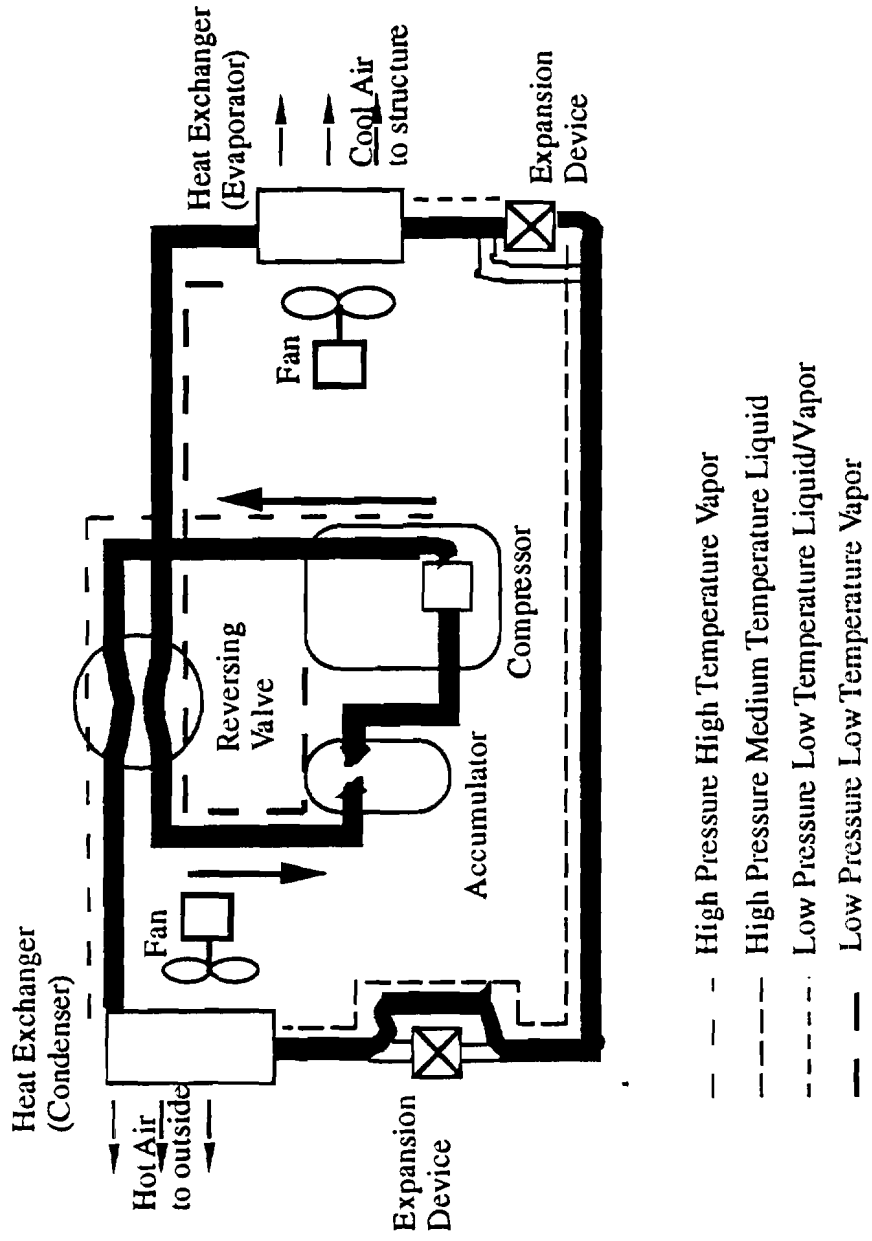
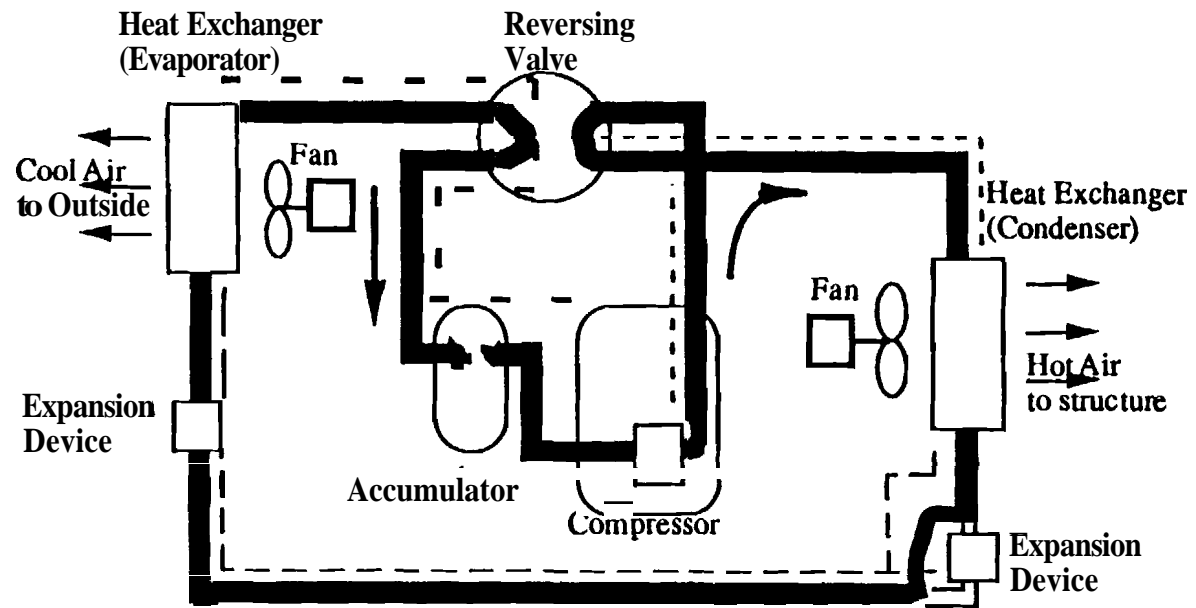


Figure 2.2 Reversible refrigeration cycle in cooling mode



Heating Operation
EPRI CU 6661, 12-89

- High Pressure High Temperature Vapor
- - - - High Pressure Medium Temperature Liquid
- Low Pressure Low Temperature Liquid
- - - - Low Pressure Low Temperature Vapor

Figure 2.3 Reversible refrigeration cycle in heating mode

about twenty percent to two hundred percent of rated speed for extended periods of time [12]. The motor is connected directly to the compressor, and the motor and compressor are usually enclosed in a common, sealed case. The compressor is used to pump the refrigerant around the loop. The compressor also raises the pressure **and** temperature of the evaporated refrigerant as it pumps the refrigerant to the condenser. The temperature of the refrigerant in the condenser is higher than the temperature of the medium, usually air, around the condenser. This difference in temperature allows the condenser to reject, or give off, heat to the surrounding medium. The refrigerant changes from a vapor to a liquid in the condenser and heat is given off during this change in phase. A small motor is used to drive a fan to increase the air flow through the condenser. This increased flow of air across the heat exchanger increases the rate of energy transfer. The condenser is constructed with narrow fins which provide extra radiating surface **area** to increase the effective surface area used for energy transfer. During heat pump operation the heat rejected by the condenser is used to warm the interior of a building. The condenser releases thermal energy to the outside air during air conditioning operation.

After the liquid refrigerant leaves the condenser it passes through an expansion device. The expansion device is simply a small restriction through which the refrigerant passes. The expansion device can be connected to a control mechanism and is changed in diameter in variable speed heat pumps. The refrigerant is changed from a high pressure, medium temperature liquid into a low pressure, low temperature **mixture** of vapor and liquid. This decrease in the temperature of the refrigerant is due to the increased volume that the refrigerant occupies, as evidenced by the lower pressure.

After leaving the expansion device the refrigerant next enters the: evaporator. The temperature of the refrigerant is lower than the temperature of the medium, usually air, **surrounding** the evaporator. This difference in temperature allows the refrigerant to absorb thermal energy in the evaporator. The refrigerant will change phase from a **mixture**

of vapor and liquid into a vapor. Energy is absorbed by the evaporator **during** this change in phase from a liquid to a vapor. One of the heat exchange units is located inside the building and one is located outside. These heat exchange units are termed the evaporator if it is absorbing thermal energy and the condenser if it is releasing thermal energy. In heat pump operation the evaporator is located outside the building and **absorbs** energy from the cooler, outside air. During air conditioning operation the evaporator is located inside the building and absorbs energy from the cooler interior of the building. **A fan** is also used on the evaporator to increase the rate of energy transfer. After leaving **the** evaporator the warmer, liquid refrigerant flows back to the compressor, whereupon the cycle repeats.

2.2 Adjustable speed drive heat pumps

Most conventional residential heat pumps and air conditioners in use today use a 230V, single phase induction motor. These classical designs used a motor speed of 1750 or 3000 revolutions per minute, and a few are designed to switch **between** these two operating speeds [1]. Most operate at only one speed, and the **compressor** is turning at the same speed as the motor. The thermal output of the refrigeration cycle is proportional to the compressor speed. Thus a conventional heat pump and air **conditioner** is either on at the maximum pumping and thermal transfer rate or is idle. Heat pumps and air conditioning units are designed for maximum output so that they can satisfy the thermal requirements of the coolest or warmest days, respectively.

The **full** output of the heat pump or air conditioner is not **required** to maintain the desired building temperature. Since the heat pump and air conditioning unit is typically oversized so that it will perform well even during the brief periods of temperature extremes, the unit will be required to frequently cycle on and off a large percentage of the time. Extra energy is required **as** the motor is energized to return the **components** of the

refrigeration cycle to their operating temperature. This is because the **temperature** of the **components** such as the condenser, evaporator, and compressor have been returning to the ambient, background temperature while the compressor is idle. The **energy** required to bring components to the operating temperature each time the unit is cycled on is wasted energy.

High efficiency, adjustable speed drive heat pumps are equipped with power electronic circuits so that the motor can operate over a wide range of speed for long periods of time [13]. A block diagram of an adjustable speed drive heat pump is shown in Figure (2.4). Variable speed operation offers several advantages. The thermal output of the heat pump and air conditioning unit is proportional to the speed of the motor and compressor. The compressor speed can be varied so that the thermal **output** of the heat **pump** and air conditioning unit more closely matches the energy that is required to maintain the building at a constant temperature. With operation in this manner, the heat pump can remain on for extended periods of time, which drastically reduces the cycling losses. The motor will be run at slower speeds when the heating demand is low, and will be run at high speeds for increased thermal output.

During a large portion of the operation of a heat pump or air **conditioning** unit the full thermal output of the unit will not be required. Therefore cycling losses can be significant. The adjustable speed drive heat pump drastically reduces the cycling losses since the unit remains on for much longer periods of time. If the heating demand is low the compressor can be run at a fraction of its rated speed, which produces a lower flow rate: in the refrigeration cycle. Besides the obvious advantage that the compressor requires **less** energy to pump at a lower rate, the overall coefficient of performance increases as the **flow** rate decreases. This inverse relationship between the coefficient of performance and the flow rate occurs because the refrigerant stays in the evaporator and the condenser for a longer period of time. The total amount of energy transferred in **the** evaporator or

condenser is greater with the slower flow rate since the refrigerant **stays** in the heat exchange unit for a longer period of time. Thus the refrigerant has time to accept or reject more thermal energy. The cooling fans can also be slowed down to consume less power during periods of low thermal demand. During those periods when the full output of the unit is required the compressor can be operated at a speed that is **greater** than the rated speed of the motor. It is for these reasons that the adjustable speed drive has been successfully applied to the refrigeration cycle to achieve significant energy savings. **An** average energy savings of 15% is estimated for the adjustable speed drive: heat pump [1].

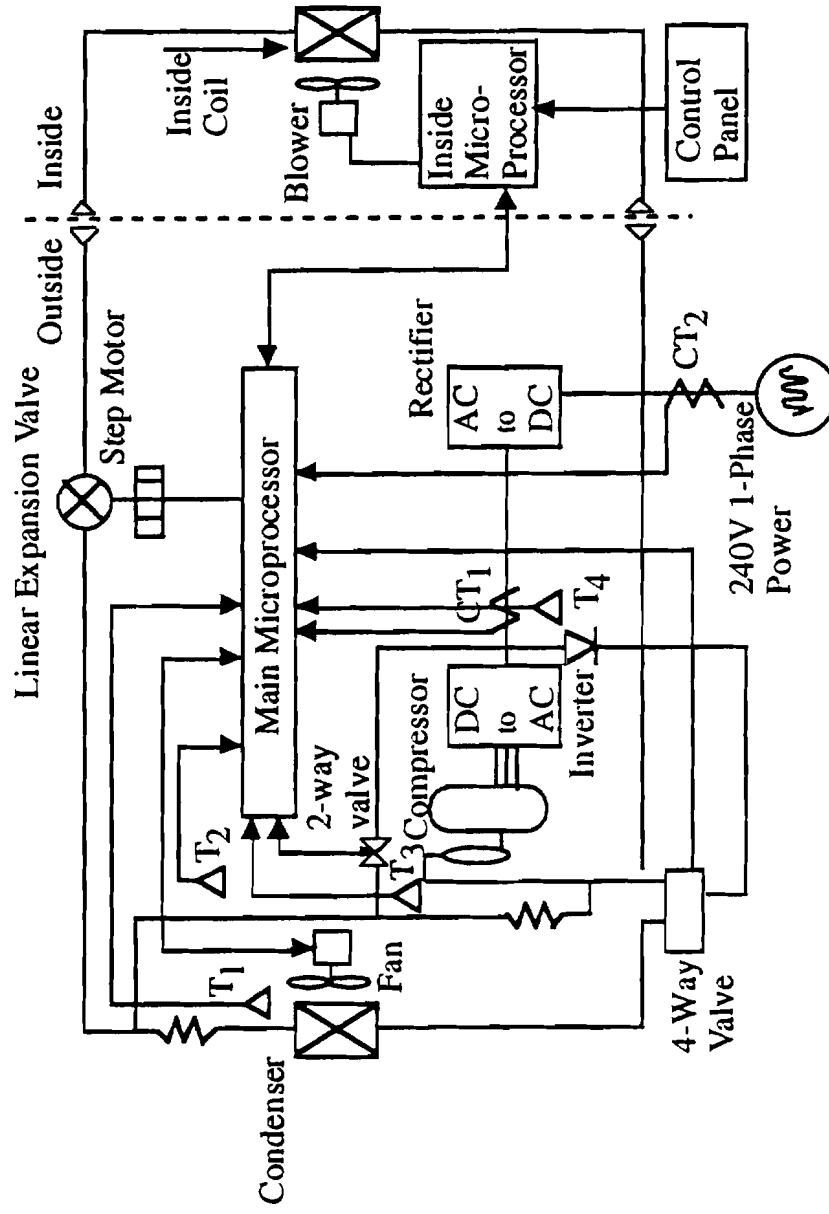


Figure 2.4 Block diagram of ASD heat pump

CHAPTER 3

MODELING OF THE ASD HEAT PUMP

3.1 Introduction

In this chapter, the components of an ASD heat pump are modeled and studied. Also, the supply distribution transformer is modeled. The objective is to assess the typical impact of an ASD heat pump on power distribution systems. The chapter is organized into five main topics, which include:

- modeling of the electric motor
- modeling of the power electronic drive
- modeling of the distribution transformer
- modeling of the compressor shaft load
- ACSL program explanation and listing .

The Advanced Continuous Simulation Language (ACSL) will be used to simulate the combination of the above components. This chapter will provide a detailed derivation of equations and an explanation of the method of operation of the components to be modeled. In addition, the last section contains the ACSL listing in sections, along with an explanation of the purpose of each section.

3.2 Modeling of the electric motor

A three phase induction motor is typically used to drive the compressor in an adjustable speed drive heat pump. The three phase induction motor is more efficient and is thus preferred over the single phase induction motor. Other high efficiency motors, such as permanent magnet rotor machines, are also being considered for use in this application. The efficiency of a motor can decrease with a decrease in motor speed. Since a power electronically driven motor must operate over a wide range of speeds the efficiency over the entire operating range must be considered to minimize: operating losses. Although other motors can be used with adjustable speed drives, the three phase induction motor is the most common for this application. Thus the induction motor will be modeled in the simulation of the electric motor used in ASD heat pumps. This section will show how the equations that describe the operation of an induction machine are derived.

The three phase induction machine consists of three sets of windings on the stator, which is the outer stationary part of the motor and three sets of windings on the rotor. Figure (3.1) shows the stator along with the rotor, which is the inner, rotating portion of the motor. This first figure also shows how a conductor is placed lengthwise in the machine. Typically one phase winding consists of many turns of insulated wire. The turns which make up the winding are distributed along the stator as shown in :Figure(3.2). The turns are distributed so that the air gap magneto-motive force (MMF) resulting from the flow of current through the windings is sinusoidal. The voltage harmonics are also minimized when the turns are distributed. Although the windings are actually distributed, it is convenient for analysis to represent each set of windings as one equivalent conductor.

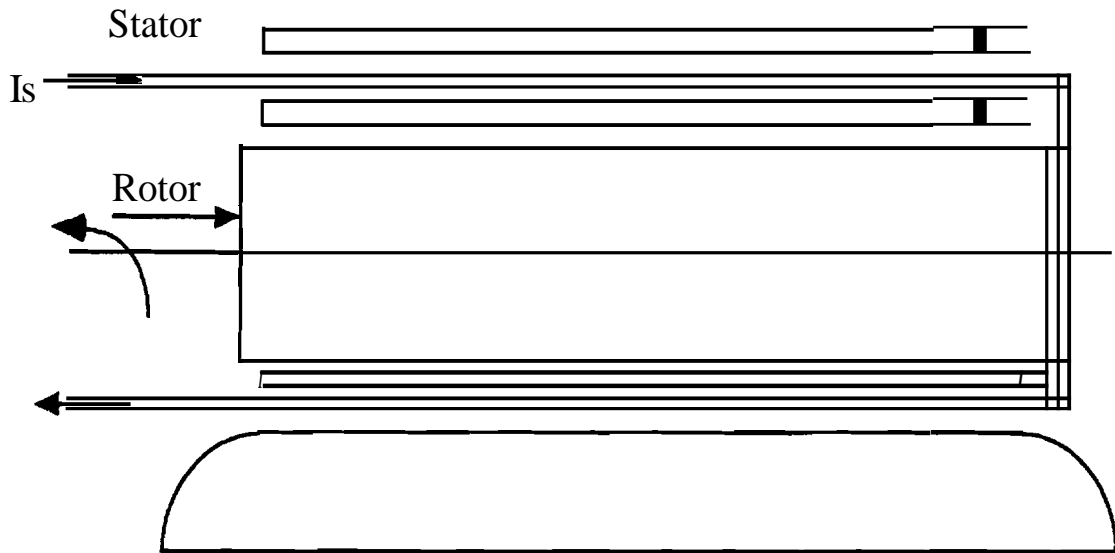


Figure 3.1 Side view of motor with stator winding

Figure (3.3) shows the cross-sectional view of a three phase induction motor, where each phase winding is represented by one equivalent winding. The three phase induction motor consists of the a, b, and c phase windings that are separated by 120 degrees from each other. These three windings on the stator would **typically** be connected to a three phase voltage during operation. The rotor windings can also **be** represented **as** three sets of windings, each separated from the other by 120 degrees. The rotor can rotate with respect to the stator windings. The angle between the as axis and **the** ar axis is given by θ_r . The stator and rotor circuits of the induction machine can also be represented as a balanced **wye** connected stator and rotor circuit consisting of a resistance and an inductance in series. The analysis is more involved than would appear from Figure (3.4) because there is mutual inductance between **all** of the inductors. In addition, the **mutual** inductance between the stator and rotor inductances is a function of the rotor position. The rotor position is also a function of time. A current flowing through a winding causes a magnetic flux to flow in the motor. This flux will pass through the other windings of the

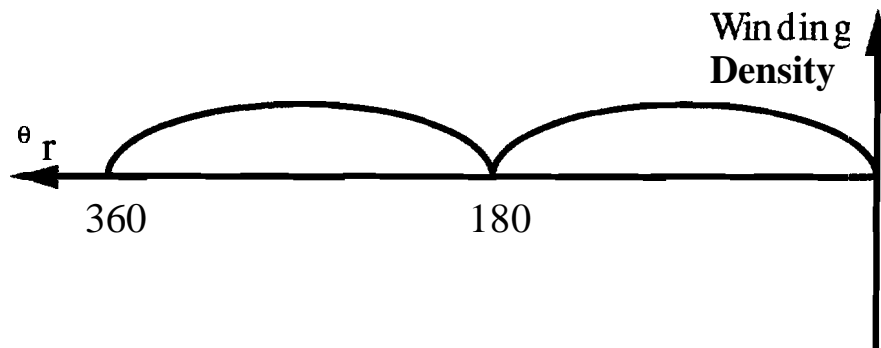


Figure 3.2 Winding turns density versus θ_r

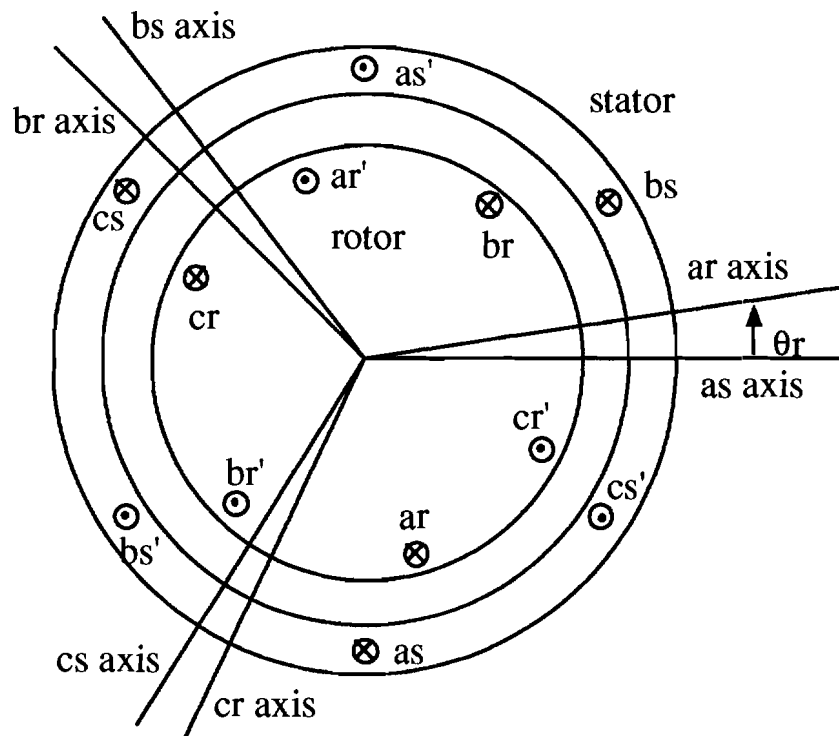


Figure 3.3 Cross-sectional view of induction motor showing the locations of the rotor and stator windings

machine to cause linkage between the windings.

The derivation of the machine equations for the three phase induction machine involves six voltage equations: three for the stator and three for the rotor circuit. For convenience and to make the equations more compact, matrix and vector notation will be used. The notation used in this section follows that used by Krause in [5]. The (p) operator will be used to denote the derivative operation with respect to time. The machine voltage equations can be written as shown below. The first equation shows the stator voltage equations in matrix form. The second equation shows the rotor voltage equations in matrix form. The matrix notation used is shown in the third and fourth equation for the stator and rotor, respectively,

$$V_{abcS} = r_{sm} I_{abcS} + p \lambda_{abcS}$$

$$V_{abcR} = r_{rm} I_{abcR} + p \lambda_{abcR}$$

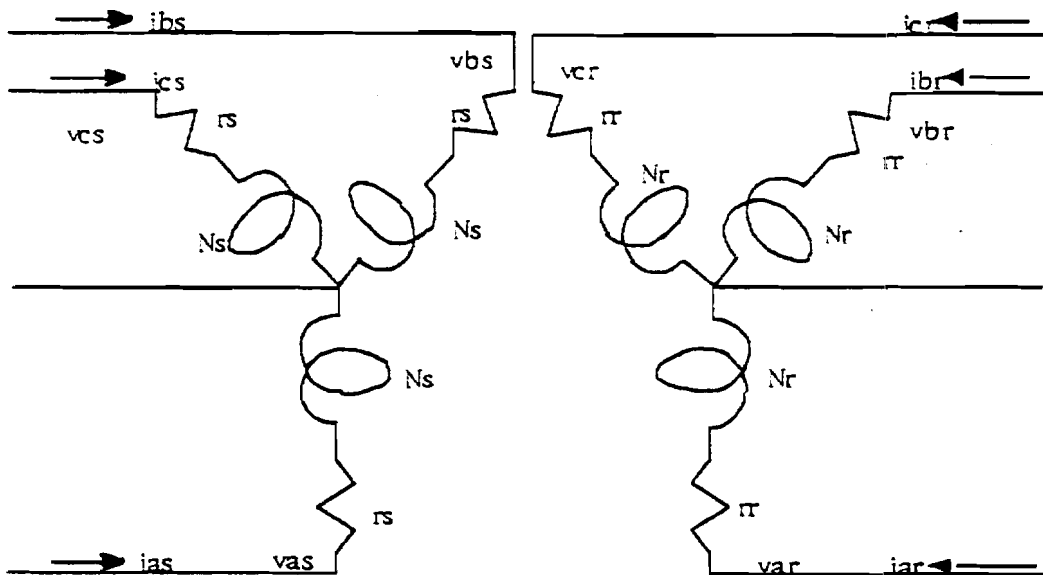


Figure 3.4 Equivalent circuit of induction machine

$$f_{abc s} = [f_{as} \quad f_{bs} \quad f_{cs}]^T$$

$$f_{a r} = [f_{ar} \quad f_{br} \quad f_{cr}]^T$$

$$r_{sm} = \begin{bmatrix} r_s & 0 & 0 \\ 0 & r_s & 0 \\ 0 & 0 & r_s \end{bmatrix}$$

$$r_{rm} = \begin{bmatrix} r_r & 0 & 0 \\ 0 & r_r & 0 \\ 0 & 0 & r_r \end{bmatrix}.$$

The flux linkage, λ , is written as an inductance times the current, as shown in Equation (3.1) for the stator and rotor circuits. The stator, rotor, and mutual inductance matrices are also shown following Equation (3.1). The leakage inductance L_{ls} and L_{lr} represents the flux produced by a stator or rotor winding, respectively, that does not link with any other winding. The mutual inductances L_{ms} and L_{mr} represent the flux linkage produced by a winding that links with, or passes through, other windings. Since the machine is assumed to be symmetric, these quantities are the same for the stator and rotor circuits. The $-\frac{1}{2}L_{ms}$ and $-\frac{1}{2}L_{mr}$ terms come about because the windings are separated by 120 degrees in the stator and rotor. The flux produced by the stator also links with the rotor windings and the flux produced by the rotor links with the stator windings. The amount of flux linking the stator and rotor windings changes with the angle between the stator and rotor. Hence the $\cos(\theta_r)$ term occurs,

$$\begin{bmatrix} abc s \\ \lambda_{abc r} \end{bmatrix} = \begin{bmatrix} L_s & L_{sm} \\ (L_{sm})^T & L_r \end{bmatrix} \begin{bmatrix} i_{abc s} \\ i_{abc r} \end{bmatrix} \quad (3.1)$$

$$\mathbf{L}_s = \begin{bmatrix} L_{ls} + L_{ms} & -\frac{1}{2} L_{ms} & -\frac{1}{2} L_{ms} \\ -\frac{1}{2} L_{ms} & L_{ls} + L_{ms} & -\frac{1}{2} L_{ms} \\ -\frac{1}{2} L_{ms} & -\frac{1}{2} L_{ms} & L_{ls} + L_{ms} \end{bmatrix}$$

$$\mathbf{L}_r = \begin{bmatrix} L_{lr} + L_{mr} & -\frac{1}{2} L_{mr} & -\frac{1}{2} L_{mr} \\ -\frac{1}{2} L_{mr} & L_{lr} + L_{mr} & -\frac{1}{2} L_{mr} \\ -\frac{1}{2} L_{mr} & -\frac{1}{2} L_{mr} & L_{lr} + L_{mr} \end{bmatrix}$$

$$\mathbf{L}_{srm} = \mathbf{L}_{sr} \begin{bmatrix} \cos(\theta_r) & \cos\left(\theta_r + \frac{2\pi}{3}\right) & \cos\left(\theta_r - \frac{2\pi}{3}\right) \\ \cos\left(\theta_r - \frac{2\pi}{3}\right) & \cos(\theta_r) & \cos\left(\theta_r + \frac{2\pi}{3}\right) \\ \cos\left(\theta_r + \frac{2\pi}{3}\right) & \cos\left(\theta_r - \frac{2\pi}{3}\right) & \cos(\theta_r) \end{bmatrix}.$$

In the analysis of a transformer the secondary parameters, such as the voltage, current, and impedance, are typically referred to the primary by **multiplying** by the appropriate turns ratio. In the same manner the analysis of the induction motor is made easier if the rotor variables are referred through the turns ratio to stator variables. This is done using the following equations for the current, voltage, flux linkage, and impedance where primed variables have been referred to the stator windings,

$$i'_{abc} = \frac{N_r}{N_s} i_{abc}$$

$$V'_{abc} = \frac{N_s}{N_r} V_{abc}$$

$$\lambda'_{abc} = \frac{N_s}{N_r} \lambda_{abc}$$

$$L_{ms} = \frac{N_s}{N_r} L_{sr}$$

$$L_r = \left(\frac{N_s}{N_r} \right)^2 L_r$$

$$r_r' = \left(\frac{N_s}{N_r} \right)^2 r_r$$

$$L'_{sr} = L_{ms} \begin{bmatrix} \cos(\theta_r) & \cos\left(\theta_r + \frac{2\pi}{3}\right) & \cos\left(\theta_r - \frac{2\pi}{3}\right) \\ \cos\left(\theta_r - \frac{2\pi}{3}\right) & \cos(\theta_r) & \cos\left(\theta_r + \frac{2\pi}{3}\right) \\ \cos\left(\theta_r + \frac{2\pi}{3}\right) & \cos\left(\theta_r - \frac{2\pi}{3}\right) & \cos(\theta_r) \end{bmatrix}$$

$$L_r' = \begin{bmatrix} L_r + L_{ms} & -\frac{1}{2} L_{ms} & -\frac{1}{2} L_{ms} \\ -\frac{1}{2} L_{ms} & L_r + L_{ms} & -\frac{1}{2} L_{ms} \\ -\frac{1}{2} L_{ms} & -\frac{1}{2} L_{ms} & L_r + L_{ms} \end{bmatrix}$$

The voltage equations are now written,

$$\begin{bmatrix} V_{abcs} \\ V'_{abcr} \end{bmatrix} = \begin{bmatrix} r_{sm} + p L_s & p L'_{sr} \\ p (L'_{sr})^T & r'_{rm} + p L'_r \end{bmatrix} \begin{bmatrix} i_{abcs} \\ i'_{abcr} \end{bmatrix}. \quad (3.2)$$

The implementation of the above voltage equation is difficult because it involves the derivative of a product of two variables that are a function of time, current and inductance. A transformation to the arbitrary reference frame will make the analysis less complicated. A transformation can be used to turn the time-varying mutual inductances L'_{sr} to a constant. This is accomplished by the following arbitrary reference frame transformation which converts the (abc) rotor variables to the (qdo) axis in the arbitrary reference frame,

$$f'_{qdor} = K_r f'_{abcr}$$

$$f'_{qdor} = [f'_{qr} \quad f'_{dr} \quad f'_{or}]^T$$

$$f'_{abcr} = [f'_{ar} \quad f'_{br} \quad f'_{cr}]^T$$

$$\beta = \theta - \theta_r$$

$$K_r = \frac{2}{3} \begin{bmatrix} \cos(\beta) & \cos\left(\beta - \frac{2\pi}{3}\right) & \cos\left(\beta + \frac{2\pi}{3}\right) \\ \sin(\beta) & \sin\left(\beta - \frac{2\pi}{3}\right) & \sin\left(\beta + \frac{2\pi}{3}\right) \\ \frac{1}{2} & \frac{1}{2} & \frac{1}{2} \end{bmatrix}$$

$$K_s = \frac{2}{3} \begin{bmatrix} \cos(\theta) & \cos\left(\theta - \frac{2\pi}{3}\right) & \cos\left(\theta + \frac{2\pi}{3}\right) \\ \sin(\theta) & \sin\left(\theta - \frac{2\pi}{3}\right) & \sin\left(\theta + \frac{2\pi}{3}\right) \\ \frac{1}{2} & \frac{1}{2} & \frac{1}{2} \end{bmatrix}.$$

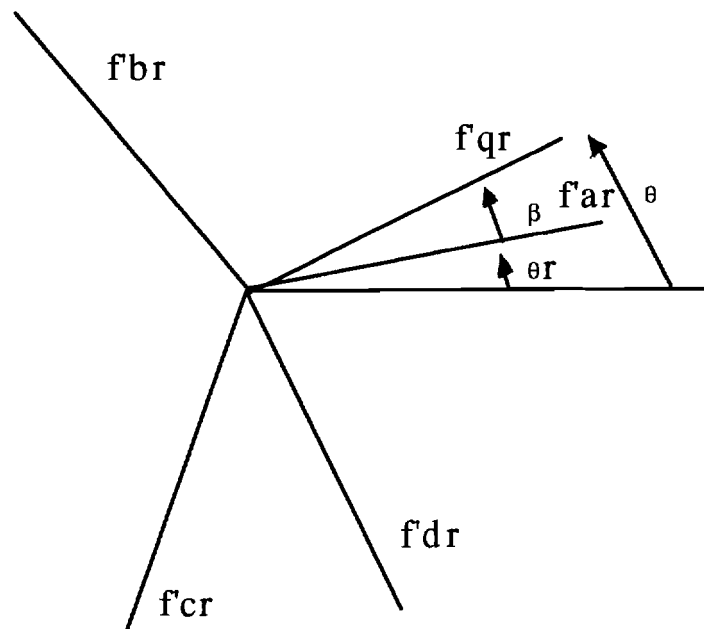


Figure 3.5 Figure showing relationship between (abc) and (qdo) variables

Figure (3.5) shows the relationship between the (abc) and qdo variables. When this transformation is applied to the previously developed machine voltage Equation (3.2) in the (abc) reference frame the following (qdo) equations result,

$$\mathbf{V}_{\text{qdos}} = \mathbf{r}_{\text{sm}} \mathbf{i}_{\text{qdos}} + \omega \lambda_{\text{dqs}} + \mathbf{P} \lambda_{\text{qdos}}$$

$$\mathbf{V}'_{\text{qdor}} = \mathbf{r}'_{\text{m}} \mathbf{i}'_{\text{qdor}} + (\omega - \omega_{\text{r}}) \lambda'_{\text{dqr}} + \mathbf{P} \lambda'_{\text{qdor}}$$

$$\lambda_{\text{dqs}} = [\lambda_{\text{ds}} \quad -\lambda_{\text{qs}} \quad 0]^{\text{T}}$$

$$\lambda'_{\text{dqr}} = [\lambda'_{\text{dr}} \quad -\lambda'_{\text{qr}} \quad 0]^{\text{T}}$$

$$\begin{bmatrix} \lambda_{\text{qdos}} \\ \lambda'_{\text{qdor}} \end{bmatrix} = \begin{bmatrix} \mathbf{K}_{\text{S}} \mathbf{L}_{\text{S}} (\mathbf{K}_{\text{S}})^{-1} & \mathbf{K}_{\text{S}} \mathbf{L}'_{\text{sr}} (\mathbf{K}_{\text{r}})^{-1} \\ \mathbf{K}_{\text{r}} (\mathbf{L}'_{\text{sr}})^{\text{T}} (\mathbf{K}_{\text{S}})^{-1} & \mathbf{K}_{\text{r}} \mathbf{L}'_{\text{r}} (\mathbf{K}_{\text{r}})^{-1} \end{bmatrix} \begin{bmatrix} \mathbf{i}_{\text{qdos}} \\ \mathbf{i}'_{\text{qdor}} \end{bmatrix}$$

$$\mathbf{M} = \frac{3}{2} \mathbf{L}_{\text{ms}}$$

$$\mathbf{K}_{\text{S}} \mathbf{L}_{\text{S}} (\mathbf{K}_{\text{S}})^{-1} = \begin{bmatrix} \mathbf{L}_{\text{S}} + \mathbf{M} & 0 & 0 \\ 0 & \mathbf{L}_{\text{S}} + \mathbf{M} & 0 \\ 0 & 0 & \mathbf{L}_{\text{S}} \end{bmatrix}$$

$$\mathbf{K}_{\text{S}} \mathbf{L}'_{\text{sr}} (\mathbf{K}_{\text{r}})^{-1} = \mathbf{K}_{\text{r}} (\mathbf{L}'_{\text{sr}})^{\text{T}} (\mathbf{K}_{\text{S}})^{-1} = \begin{bmatrix} \mathbf{M} & 0 & 0 \\ 0 & \mathbf{M} & 0 \\ 0 & 0 & 0 \end{bmatrix}.$$

The voltage equations are now written in expanded form as shown below,

$$V_{qs} = r_s i_{qs} + \omega \lambda_{ds} + p \lambda_{qs}$$

$$V_{ds} = r_s i_{ds} - \omega \lambda_{qs} + p \lambda_{ds}$$

$$V_{os} = r_s i_{os} + p \lambda_{os}$$

$$V_{qr} = r_r' i_{qr} + (\omega - \omega_r) \lambda_{dr}' + p \lambda_{qr}'$$

$$V_{dr} = r_r' i_{dr} - (\omega - \omega_r) \lambda_{qr}' + p \lambda_{dr}'$$

$$V_{or} = r_r' i_{or}' + p \lambda_{or}'$$

$$\lambda_{qs} = L_{ts} i_{qs} + M(i_{qs} + i_{qr}')$$

$$\lambda_{ds} = L_{ts} i_{ds} + M(i_{ds} + i_{dr}')$$

$$\lambda_{os} = L_{ts} i_{os}$$

$$\lambda_{qr}' = L_{tr} i_{qr}' + M(i_{qs} + i_{qr}')$$

$$\lambda_{dr}' = L_{tr} i_{dr}' + M(i_{ds} + i_{dr}')$$

$$\lambda_{or}' = L_{tr} i_{or}'$$

Each voltage equation now contains the derivative of only one variable, λ , so the simulation of this set of equations is more straight-forward. These equations are valid for any value of ω , but the equations are simpler if the arbitrary reference frame velocity equals zero. The ACSL simulation uses the stationary reference frame.

3.3 Modeling of the adjustable speed drive

3.3.1 Introduction

There are many types of ASD circuit topologies and switching strategies. Most convert the input ac waveform to dc with a rectifier, then use an inverter to reconstruct an ac waveform which is used to supply the machine. The voltage source inverter employs one of the simplest switching strategies and has been favored because of the low switching frequency requirements and its rugged design. Due to the low switching frequency the rectifier and inverter switches are modeled as ideal. The disadvantages of the voltage source inverter include poor power factor at low speeds and low speed pulsations [8]. The voltage source inverter is modeled in this simulation. The circuit diagram of the voltage source inverter is shown in Figure (3.6) Each of the ten thyristors are numbered to facilitate later reference.

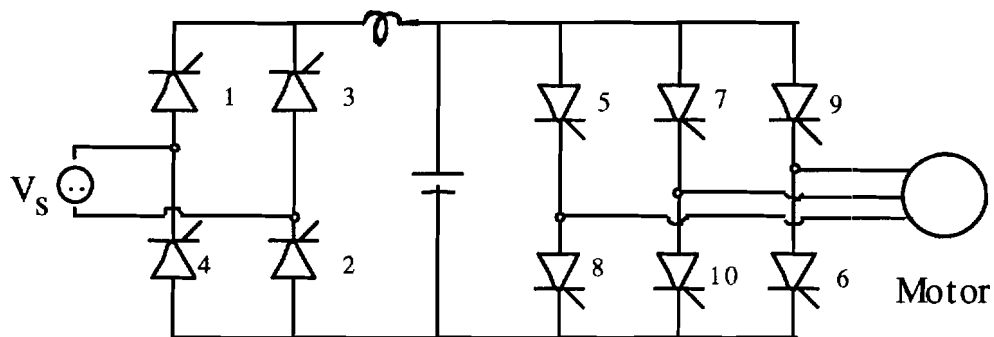


Figure 3.6 Voltage source inverter adjustable speed drive

The input is single phase ac and the three phase output voltage waveform is a six-step waveform as shown in Figure (3.7). A silicon controlled rectifier (SCR) is used in the rectifier. The SCR will conduct if it is forward biased and is subjected to either: gate pulses, high forward voltages, transient voltage spikes, or high temperatures. During normal operation the solid state switch will only turn on with the application of a current to the gate terminal. The SCR will turn off if the current through it tries to reverse. The rectifier uses an SCR so that the turn on point can be changed to control the dc voltage produced. This is important so that a constant volts/hertz ratio can be maintained in the induction motor. If the voltage applied to an induction machine is not reduced at lower speeds, the machine flux will increase, which may cause saturation. The operation of the voltage source inverter adjustable speed drive is explained in a subsequent section describing the inverter. Also, an explanation of the operation of the rectifier is given.

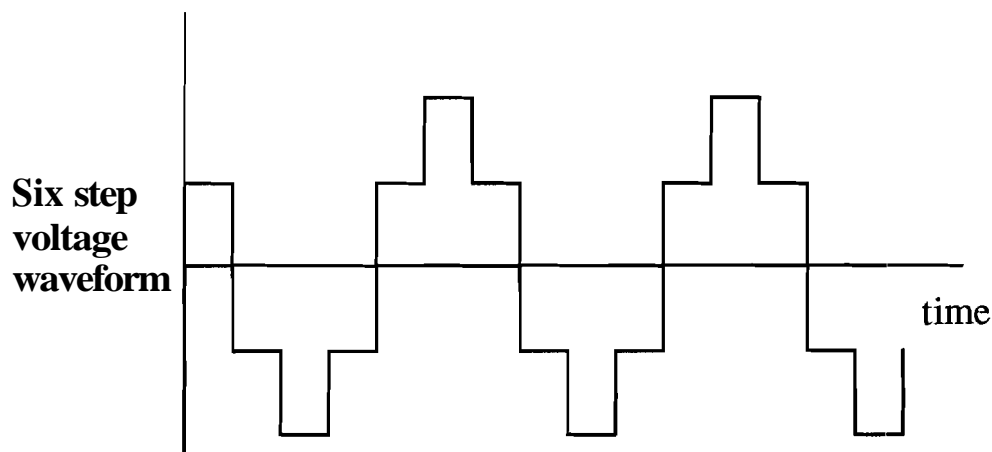


Figure 3.7 Six step voltage waveform

3.3.2 VSI-ASD inverter

The inverter is the portion of the voltage source inverter ASD depicted by thyristors five through ten in Figure (3.8). The inverter converts the relatively constant capacitor voltage into a three phase, six-step voltage waveform shown in Figure (3.10). This is accomplished by controlling the switches according to the following switching strategy. A short would occur across the capacitor if both switches on the same leg of the inverter are turned on simultaneously. A leg of the inverter is, for example, the leg containing switches five and ten. The switching strategy that will produce the desired waveform is to turn on one switch on a phase leg for 180 electrical degrees, then turn it off and turn the other switch on for the other 180 electrical degrees. If the 180 degree switching pattern is offset by 120 electrical degrees from a on each of the legs connected to the b and c phases of the motor winding, a three phase voltage waveform will result. Figure (3.9), a timing diagram which shows the switch state for each switch in the inverter, explains in greater detail the switching strategy for the inverter.

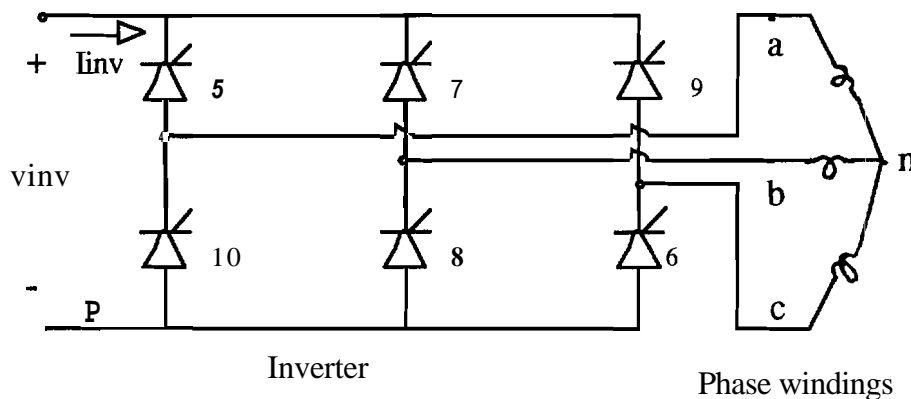


Figure 3.8 Voltage source inverter, 3-phase

If the inverter switches are controlled according to the switching strategy shown in the timing diagram in Figure (3.9), the phase voltages will be alternately connected to ground or to the input voltage V_{inv} . The following equations are used to determine the phase to neutral voltages produced by the 180 degree switching strategy. The voltage equations for the inverter are written as follows,

$$V_{ap} = V_{as} + V_{np}$$

$$V_{bp} = V_{bs} + V_{np}$$

$$V_{cp} = V_{cs} + V_{np}$$

$$V_{as} + V_{bs} + V_{cs} = 0$$

$$V_{np} = \frac{1}{3} (V_{ap} + V_{bp} + V_{cp})$$

$$V_{as} = \frac{2}{3} V_{ap} - \frac{1}{3} (V_{bp} + V_{cp})$$

$$V_{bs} = \frac{2}{3} V_{bp} - \frac{1}{3} (V_{ap} + V_{cp})$$

$$V_{cs} = \frac{2}{3} V_{cp} - \frac{1}{3} (V_{ap} + V_{bp})$$

Since the output of the inverter is connected to the induction machine, the sum of the three individual phase voltages will equal zero. The last three equations determine the three individual phase voltages which are applied to the motor.

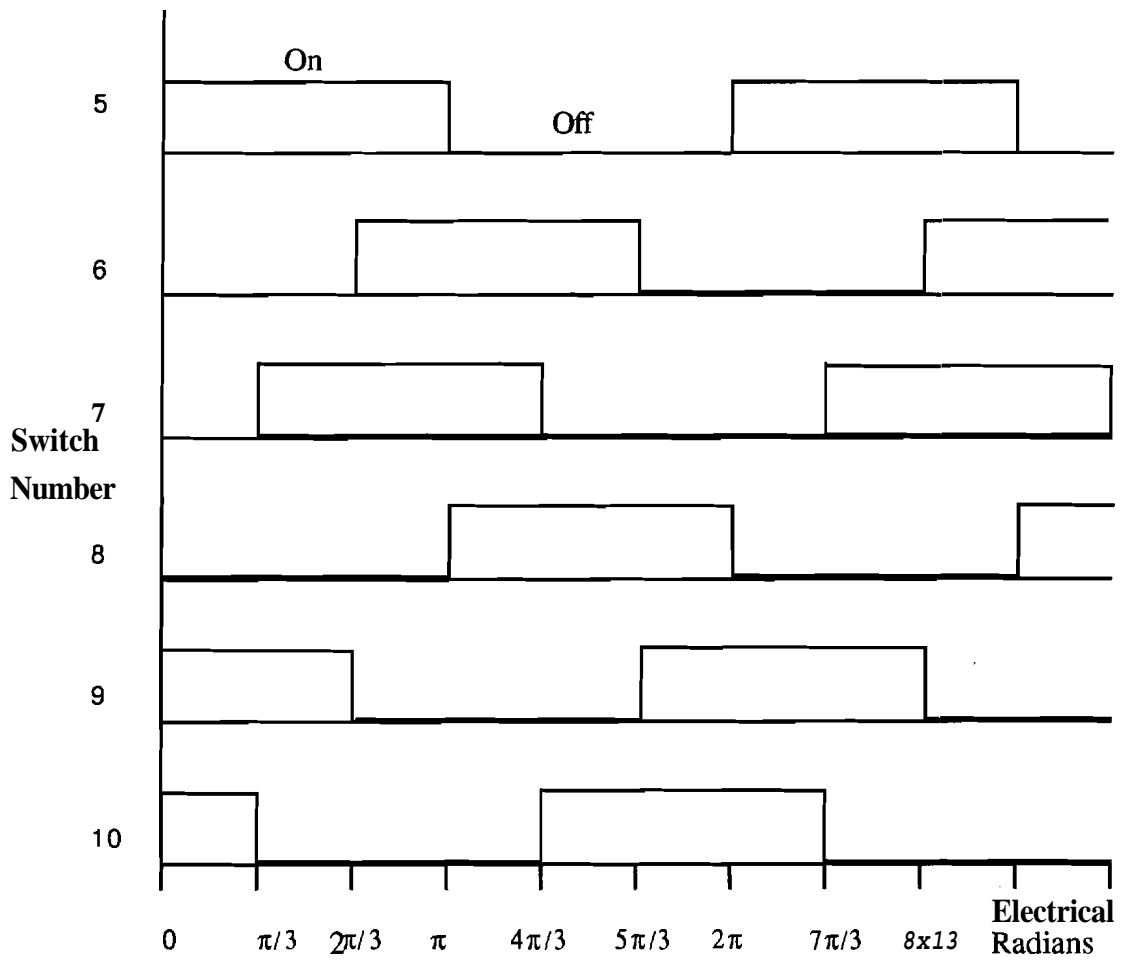


Figure 3.9 Inverter switching strategy

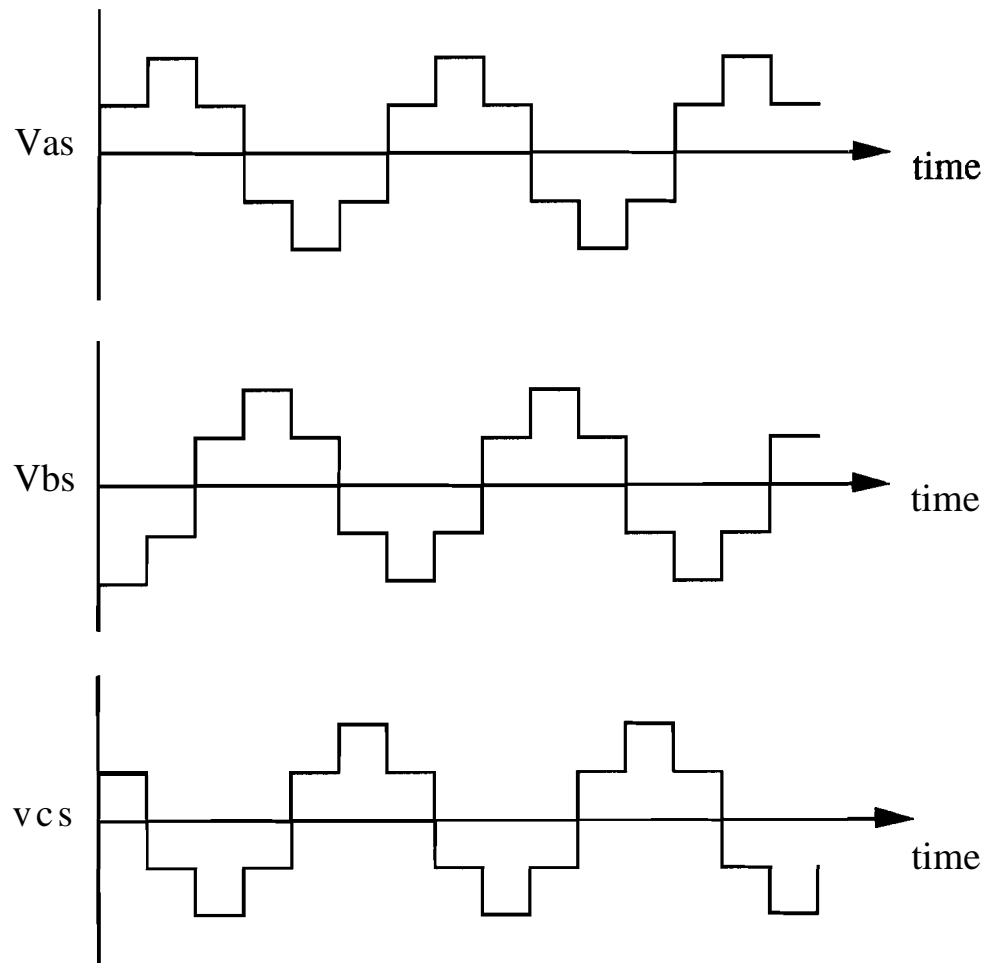


Figure 3.10 Six step inverter waveform

Each of V_{as} , V_{bs} , and V_{cs} is a six-step waveform, as shown in Figure (3.10), and the frequency of the voltages applied to the motor is determined by the switching frequency of the inverter,

3.3.3 VSI-ASD rectifier operation

The rectifier uses four thyristors to convert the applied single phase voltage into dc. The rectifier is connected through a series inductor and a parallel capacitor to the inverter. The inductor and capacitor filter the output voltage of the rectifier for a more constant applied voltage to the inverter. The circuit diagram of a single phase rectifier is shown in Figure (3.11). The input current to the rectifier, I_{rec} , will be equal to zero when all four switches are off. There are three possible switching states in the operation of the single phase rectifier: the first switching state occurs when thyristor one and thyristor four are conducting, which can only occur when the source voltage, V_{rec} , is greater than the output dc voltage, V_{inv} , and a signal is applied to gate terminals one and four. The second possible switching state occurs when the source voltage, V_{rec} , is less than the negative value of the output voltage, or $-V_{inv}$, and a signal is applied to the gate terminal of switches two and three. The third possible switching state occurs when all four switches are turned off. Thus the input current to the rectifier is equal to zero, unless the absolute value of the source voltage is greater than the output voltage and a signal is applied to the gate terminal of the appropriate switches.

The rectifier uses a thyristor instead of a diode. With the controllable solid state switch the output voltage of the rectifier can be reduced by delaying the firing angle of the thyristors. The thyristor will turn on and conduct current when the applied voltage is positive and a voltage is applied to the thyristor gate terminal. The switch will remain on

until the current through the device goes to zero. The equations which describe the rectifier can be described in two sets: one set of equations when a rectifier thyristor is conducting, and one set of equations for the case when the rectifier thyristors are off. The following equations describe the operation of the rectifier when the thyristor is on,

$$pV_{inv} = \frac{1}{C_f} (i_l - i_{inv})$$

$$pi_l = \frac{1}{L_f} (V_{rec} - V_{inv}) .$$

The thyristor will turn off when the current through it goes to zero. The equations which describe the operation of the rectifier during this portion of the voltage cycle are found directly from the previous equations. Since the rectifier is off the current through the inductor is now equal to zero. The current through the inductor will remain at zero until the switch is turned on, which can be accomplished by setting the time derivative of the current through the inductor, I_l to zero. When the switches of the rectifier are turned off the output voltage is simply the exponentially decaying voltage across the capacitor C_f as shown by the following equations,

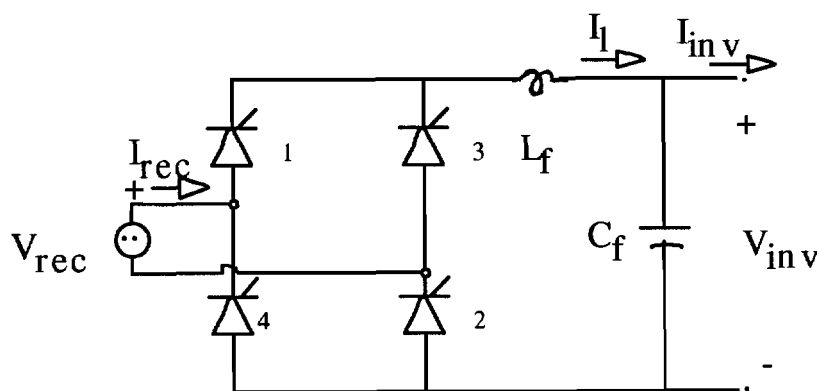


Figure 3.11 Single phase rectifier with LC filter

$$pV_{inv} = \frac{1}{C_f} (-i_{inv})$$

$$p i_1 = 0 .$$

3.4 Modeling of the distribution transformer

The distribution transformer consists of two windings on a laminated, usually iron core. The distribution transformer is used to reduce the distribution voltages to the lower voltages used by individual residential and commercial customers. Additional information on the transformer is given in Section 1.4. The equations which describe the operation of the transformer are written as follows. The voltage across the primary or secondary winding is equal to the current through the winding times the winding resistance plus the time derivative of the flux linkage, as shown in the following equations,

$$V_1 = i_1 r_1 + p \psi_1$$

$$V_2 = i_2 r_2 + p \psi_2$$

$$\psi_1 = \omega_b \lambda_1 = X_{11} \dot{i}_1 + \psi_m$$

$$\psi_2 = \omega_b \lambda_2 = X_{12} \dot{i}_2 + \psi_m$$

$$X_{11} = \omega_b L_{11}$$

$$x_{12} = \frac{N_1^2}{N_2^2} \omega_b L_{12}$$

$$i_2 = \frac{N_2}{N_1} i_2$$

$$V_2 = \frac{N_1}{N_2} V_2$$

$$r_2 = \frac{N_1^2}{N_2^2} r_2$$

$$L_{12} = \frac{N_1^2}{N_2^2} L_{12} .$$

The previous equations describe the primary and secondary voltages. The secondary parameters are referred to the primary using the primed quantities defined above. The voltage equations defined above can be used to simulate the operation of the transformer with the flux linkage per second, Ψ , as the state variables in the simulation. The flux linkages per second and the transformer currents can be defined as follows, where L_{m1} is equal to the mutual inductance,

$$\psi_m = \omega_b L_{m1} (i_1 + i_2) = x_m (i_1 + i_2)$$

$$\psi_m = x_M \left(\frac{\psi_1}{x_{11}} + \frac{\psi_2}{x_{12}} \right)$$

$$x_M = \frac{1}{\frac{1}{x_m} + \frac{1}{x_{11}} + \frac{1}{x_{12}}}$$

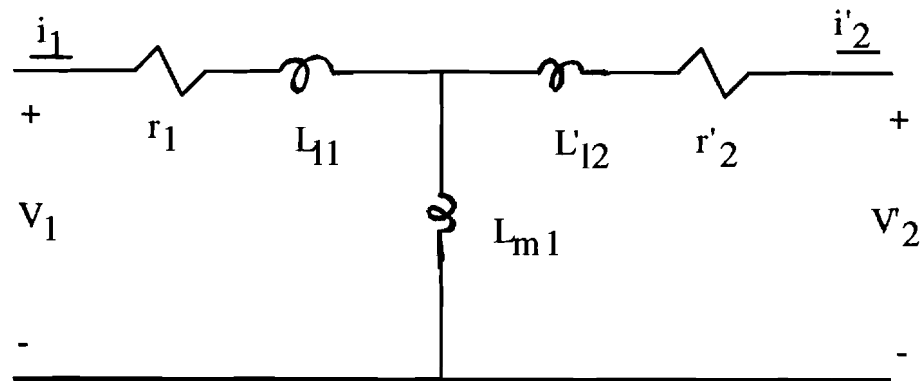


Figure 3.12 Transformer equivalent circuit diagram

$$i_1 = \frac{\psi_1 - \psi_m}{x_{11}}$$

$$i_2 = \frac{\psi_2 - \psi_m}{x_{12}}$$

These last equations, along with the voltage equations defined previously, are used to simulate the operation of a single phase transformer. The turns ratio defines the ratio of the input voltage to the output voltage. Figure (3.12) shows the equivalent circuit of a transformer.

3.5 Modeling of the compressor shaft load

The dynamic model of the induction motor developed in Section 3.2 is valid for transient and steady state operating conditions. The load torque placed on the motor can be modeled as time varying. The torque needed to drive a compressor load is a function of the shaft angle. A four-stroke piston compressor requires less power during the intake than it does during the compression portion of the cycle. The speed of the compressor is equal to the speed of the induction machine shaft, which is denoted by ω_{shaft} . The

compressor load is modeled as a constant value plus a sinusoidally varying quantity, which accounts for the fact that the compressor load varies with position. This equation is,

$$T_l = T_{\text{cons}} \tan t + T_{\text{var}} \cos(\omega_{\text{shaft}} / 2) .$$

The parameters of this equation can be changed to model the capacities and characteristics of different compressors. This equation is only an estimate of the compressor torque, as the time varying portion of the compressor torque is not sinusoidal.

3.6 ACSL program simulation and listing

The Advanced Continuous Simulation Language, ACSL, will be used to simulate the combination of the motor, drive, and distribution transformer. ACSL offers several advantages over a general programming language. The ACSL program is simply a list of the differential and algebraic equations which describe a system. The state variables are those variables which are integrated to find the system behavior. The state variables are entered as the time derivative of a state variable set equal to a function of the other state variables or functions, as required for the model. ACSL allows one to choose from a variety of pre-written integration algorithms, such as Runge-Kutta, Adams-Moulton, and Gear's stiff, to find the solution to the state variables. One of the other main advantages of ACSL is that the program will sort the equations, so they can be entered in any order. ACSL also allows the user to change the model parameters while the simulation is running to aid in the simulation of a variety of system conditions. ACSL also allows for analysis and plotting of the results of the simulation. The results of the ACSL simulation run can also be transferred to Matlab for further analysis. Matlab is used to find the frequency spectrum of selected model parameters.

The following ACSL program was written to simulate the single phase distribution transformer, single phase rectifier, smoothing dc filter, three phase six-pulse inverter, and three phase induction machine connected to a compressor load. The program listing is indented and will be separated into sections, preceded by an explanation of the purpose of each main section.

The program statement is used to name the program. The ACSL program is organized into blocks. The initial block is only executed once at the beginning of the simulation run and is used to set the initial conditions, which end in -ic, of the state variables. In this simulation all initial conditions are set to zero, except for *Vinvic*, which is set to 200 volts. Any statement placed after an exclamation point in an ACSL program is a comment statement, and will be left in this listing to facilitate the explanation of the program.

```

program vector
  initial
    ! induction motor state variable initial conditions
    Siqssic = 0.0
    Sidssic = 0.0
    Siqrsic = 0.0
    Sidrsic = 0.0
    wric = 0.0
    ! transformer state variable initial conditions
    Silpric = 0.0
    Si2ic = 0.0
    ! control ramp signal initial conditions
    rampic = 0.0
    ramppic = 0.0
    ! smoothing LC filter initial conditions
    Vinvic = 200.
    ilic = 0.0
    ! base frequency=377rad/sec
    wb = 2*60*3.14159
    we = wb
    twopi = 2*3.14159

```

end ! of initial

The dynamic statement contains constants which are used in the simulation. The constant statement is preferred over a simple assignment statement because the value of any variable which is defined using an assignment statement can be changed during runtime. The first set of statements define the motor parameters, and the second set of statements define the parameters of the dc filter, input voltage magnitude, inverter output frequency, and delay angle on the rectifier. The logical statements denote the logical variables, which can only take on the value of true or false. These logical variables are used in the switching logic of the rectifier and inverter.

The next set of statements are used to define the parameters for the integration algorithms. The `maxinterval` statement sets the maximum step size per integration point, while the `mininterval` statement sets the minimum step size for each integration point. The `cinterval` statement sets the time between each data point that is recorded for the purposes of graphing and displaying the resulting system parameters. `Cint` is set so that 2048 samples are taken each second. The `tstop` statement sets the time for the termination of the simulation. The `algorithm` statement is used to select the desired integration algorithm. Setting `ialg = 9` employs a fourth order Runge Kutta Fehlberg integration algorithm, which is a variable-step algorithm.

```
dynamic
  ! induction motor parameters
  constant P = 4
  constant rs = 0.435
  constant rr = 0.816
  constant Xls = 0.754
  constant XM = 26.13
  constant J = 0.089
  constant Xlr = .745
  ! dc filter and drive parameters
  constant Lf = .0005
```

```

constant Cf = 0.01
constant Vmag = 250
constant Fme = 40.
constant alpha = .01
! transformer parameters
constant r1 = .25
constant r2pr = .134
constant xmtran = 708.8
constant x11 = .056
constant x12pr = .056
Ntrans = 1.0
constant Rload = 100
logical SA, SB, SC
logical gtzero
logical Ron
! ACSL integration parameters
maxterval maxt = 2E-6
mininterval mint = 1E-6
cinterval cint = 4.882E-4
constant tstop = .2
termt (t.gt.tstop)
algorithm ialg = 9
merror wr = 1E-3
xerror wr = 1E-2

```

The derivative block contains the system equations which are evaluated at each time step. All variables which are the derivatives of time are denoted by the p- prefix. The first section contains the equations which describe the three phase induction machine. These equations were described in detail in Section 3.2.

DERIVATIVE

```

Tm = 1./Fme ! inverter output voltage period
Vng = (Vag + Vbg + Vcg)/3.0
Vas = Vag - Vng
Vbs = Vbg - Vng
Vcs = Vcg - Vng
Vab = Vas - Vbs
vqss = (2./3.)*(Vas-0.5*Vbs-0.5*Vcs)
vdss = (2./3.)*0.86602*(-Vbs+Vcs)
vqrs = 0.0
vdrs = 0.0

```

$$\begin{aligned}
X_{aq} &= 1./((1./X_M + 1./X_{ls} + 1./X_{lr})) \\
X_{ad} &= X_{aq} \\
i_{as} &= i_{qss} \quad ! \quad f_{abcs} = \text{inv}(K_s) * f_{qdos} \\
i_{bs} &= -0.5 * i_{qss} - 0.86602 * i_{dss} \\
i_{cs} &= -0.5 * i_{qss} + 0.86602 * i_{dss} \\
\text{sim}_q &= X_{aq} * (S_{iqss}/X_{ls} + S_{iqrs}/X_{lr}) \\
\text{sim}_d &= X_{ad} * (S_{idss}/X_{ls} + S_{idrs}/X_{lr}) \\
p_{Siqss} &= w_b * (v_{qss} + (r_s/X_{ls}) * (\text{sim}_q - S_{iqss})) \\
p_{Sidss} &= w_b * (v_{dss} + (r_s/X_{ls}) * (\text{sim}_d - S_{idss})) \\
p_{Siqrs} &= w_b * (v_{qrs} + (w_r/w_b) * S_{idrs} + (r_r/X_{lr}) * (\text{sim}_q - S_{iqrs})) \\
p_{Sidrs} &= w_b * (v_{drs} - (w_r/w_b) * S_{iqrs} + (r_r/X_{lr}) * (\text{sim}_d - S_{idrs})) \\
p_{wr} &= (P/(2.*J)) * (T_e - T_l) \\
w_r &= \text{integ}(p_{wr}, w_{ric}) \\
w_{rb} &= w_r / (\text{twopi} * F_{me}) \\
w_{sl} &= \text{twopi} * F_{me} - w_r \\
S_{iqss} &= \text{integ}(p_{Siqss}, S_{iqssic}) \\
S_{idss} &= \text{integ}(p_{Sidss}, S_{idssic}) \\
S_{iqrs} &= \text{integ}(p_{Siqrs}, S_{iqrsic}) \\
S_{idrs} &= \text{integ}(p_{Sidrs}, S_{idrsic}) \\
i_{qss} &= (S_{iqss} - \text{sim}_q) / X_{ls} \\
i_{dss} &= (S_{idss} - \text{sim}_d) / X_{ls} \\
i_{qrs} &= (S_{iqrs} - \text{sim}_q) / X_{lr} \\
i_{drs} &= (S_{idrs} - \text{sim}_d) / X_{lr} \\
T_e &= (3./2.) * (P/2.) * (1./w_b) * (S_{idss} * i_{qss} - S_{iqss} * i_{dss}) \\
\Pi &= T_{\text{constant}} + T_{\text{var}} * \cos(w_r * t / 2)
\end{aligned}$$

The following equations describe the operation of the single phase distribution transformer. The input transformer voltage is equal to V_1 and is a sinusoidal waveform. The derivation of the transformer equations are discussed in detail in Section 3.4. The primary parameters, such as the voltage, current and impedances, are all referred to secondary quantities by the appropriate turns ratio.

$$\begin{aligned}
r_{lpr} &= r_1 / N_{\text{trans}}^2 \\
x_{l1pr} &= x_{l1} / N_{\text{trans}}^2 \\
x_{mtranpr} &= x_{mtran} / N_{\text{trans}}^2 \\
r_2 &= r_{2pr} * N_{\text{trans}}^2 \\
x_{l2} &= x_{l2pr} * N_{\text{trans}}^2 \\
V_1 &= V_{\text{mag}} * \cos(\omega_e * t) \\
v_{l1pr} &= V_1 / N_{\text{trans}} \\
S_{im} &= x_{\text{capm}} * (S_{i1pr} / x_{l1pr} + S_{i2} / x_{l2}) \\
x_{\text{capm}} &= 1. / (1./x_{mtranpr} + 1./x_{l1pr} + 1./x_{l2})
\end{aligned}$$

$$\begin{aligned}
i_{1pr} &= (S_{i1pr} - S_{im})/x_{11pr} \\
i_1 &= i_{1pr}/N_{trans} \\
i_2 &= (S_{i2} - S_{im})/x_{12} \\
V_2 &= -R_{load}*(i_{ltran} + i_2) \\
pS_{i1pr} &= \omega_b*(v_{1pr} - r_{1pr}*((S_{i1pr} - S_{im})/x_{11pr})) \\
pS_{i2} &= \omega_b*(V_2 - r_2*i_2) \\
S_{i1pr} &= \text{integ}(pS_{i1pr}, S_{i1pric}) \\
S_{i2} &= \text{integ}(pS_{i2}, S_{i2ic}) \\
V_m &= 10*\cos(\omega_b*t/T_m)
\end{aligned}$$

The following equations are used to model the dynamics of the series inductor and parallel capacitor which is used to filter the output of the rectifier. This provides for a more constant input voltage to the inverter. V_{inv} is used to denote the voltage across the capacitor and i_l denotes the current through the inductor. Since the input rectifier converts the negative applied voltage to a positive voltage, the derivative of the inductor current must be defined with two different equations. The variable p_{il} is used when the input rectifier voltage is greater than zero, and the variable p_{ilnms} is used when the input rectifier voltage is less than zero. The RSW switch is used to set the value of p_{il} , which applies when the rectifier switches are on. The variable p_{il} is equal to p_{ilnms} when the rectifier is on, and is set equal to zero when the rectifier is turned off.

$$\begin{aligned}
pV_{inv} &= (1./C_f)*(i_l - i_{inv}) \\
V_{inv} &= \text{integ}(pV_{inv}, V_{invic}) \\
p_{il} &= (1./L_f)*(V_{rec} - V_{inv}) \\
p_{ilnms} &= (1./L_f)*(-V_{rec} - V_{inv}) \\
p_{il} &= \text{RSW}(gtzero, p_{il}, p_{ilnms}) \\
p_{il} &= \text{RSW}(R_{on}, p_{il}, 0.0) \\
i_l &= \text{integ}(p_{il}, i_{lic}) \\
V_{rec1} &= V_{mag}*(3./4.)*\cos(\omega_b*t) \\
V_{rec} &= V_{2pr} \\
\text{schedule commute .XN. } i_l & \text{ ! sets } p_{il} \text{ to zero when } i_l = 0
\end{aligned}$$

The inverter output voltage waveform depends on the switching pattern of the inverter. This simulation includes a controller that controls the inverter switches according to the timing diagram shown in Fig. (3.9). A ramp function with a period equal

to the inverter output voltage is defined in the following sections by the variable ramp. The ramp function is used because it is convenient to determine the position in the cycle for switching purposes. The variable rampp defines a ramp function with a frequency equal to the input voltage and is used in the rectifier switching logic. A procedural block is executed at every time step of the simulation run. The following procedural blocks are necessary since the negative applied voltage is turned around by the rectifier switches. The current through the smoothing inductor is always greater than or equal to zero, while the input current is positive when the applied voltage is greater than zero, and is negative when the applied voltage is negative.

```
pramp=1.0
ramp=integ(pramp,rampic)
schedule zero .XP. Vm ! sets ramp to zero
prampp = 1.0
rampp = integ(prampp,ramppic)
schedule zeroo .XZ. Vrec1 ! sets rampp to zero
```

```
procedural(iltran=il,Vrec1)
  if(Vrec1.lt.0.) iltran = -il
  if(Vrec1.gt.0.) iltran = il
end
```

```
procedural(gtzero=Vrec) ! flag = .t. if Vrec>0
  if(Vrec.gt.0.) gtzero=.true.
  if(Vrec.lt.0.) gtzero=.false.
end
```

```
procedural(Ron=rampp,Vrec,alpha)
  if(Vrec.lt.0) Vrecc = - Vrec
  if(Vrec.gt.0) Vrecc = Vrec
  if((rampp.gt.alpha/60.).and.(Vrecc.gt.Vinv)) Ron = .true.
end ! of procedural to determine rectifier turn-on time
```

```
procedural(Vag,Vbg,Vcg=Vinv,SA,SB,SC)
  Vag = 0
  Vbg = 0
  vcg = 0
  if(SA) Vag = Vinv
```

```

    if(SB) Vbg = Vinv
    if(SC) Vcg = Vinv
end ! of procedural to determine inverter voltages

procedural(Iinv=SA,SB,SC,ias,ibs,ics)
    Iinv = 0.0
    if(SA) Iinv = ias
    if(SB) Iinv = Iinv + ibs
    if(SC) Iinv = Iinv + ics
end ! of procedural to calculate inverter current Iinv
procedural(SA,SB,SC=ramp,Tm)
! This procedural block controls the switch states, SA,
! SB, SC to produce a six-step output voltage waveform
SA = .false.
if((ramp-(Tm/2.)).lt.0) SA = .true.
SB = .false.
if((ramp.lt.(5.*Tm/6.)).and.(ramp.gt.(Tm/3.)))SB=.true.
SC = .false.
if((ramp.gt.(2.*Tm/3.)).or.(ramp.lt.(Tm/6.)))SC=.true.
end ! of procedural
end ! of derivative

```

A discrete block is executed whenever directed by the schedule operator. The following blocks are used to set the ramp functions to zero at the appropriate times. The discrete block named commute is used to turn off the rectifier switches. Each block must be concluded with an end statement.

```

discrete zero
    ramp=0.0
end ! of discrete to re-set the inverter ramp to zero
discrete zeroo
    rampp = 0.0
end ! of discrete to re-set the rectifier ramp to zero
discrete commute
! this block switches from Vcon to Vcoff if Ron is .true.
    if(Ron) Ron = .false.
end ! of discrete
end ! of dynamic
end ! of program

```

Figure (3.13) is a block diagram of the transformer and drive modeled by the ACSL program with program variables labeled.

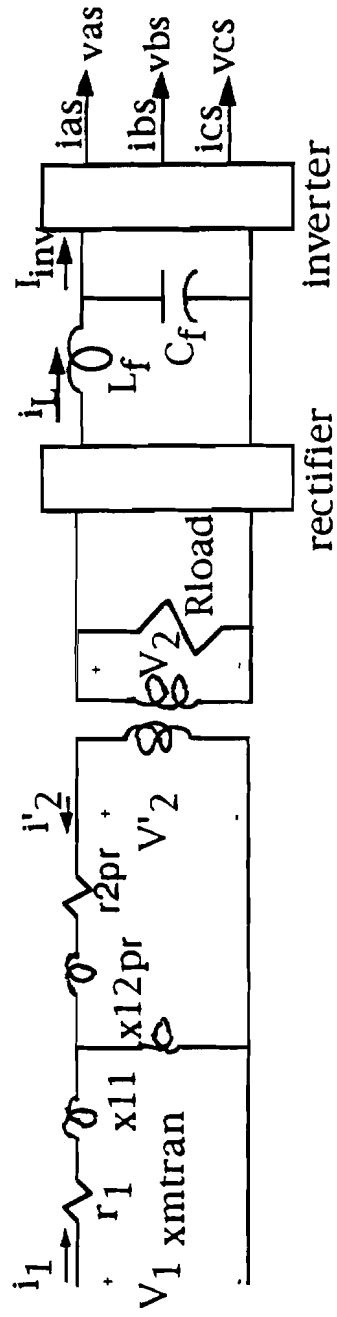


Figure 3.14 Transformer and drive with ACSL program parameters

CHAPTER 4

SIMULATION RESULTS AND ANALYSIS

4.1 Introduction

The ACSL program which simulates the transient and steady state operation of the distribution transformer, six step voltage source inverter adjustable speed drive, three phase induction motor, and compressor load is described in detail in Section 3.6. Simulation output for various operating conditions is presented in this chapter. These figures illustrate the operating characteristics of the motor and drive combination. Also, the figures clearly show the characteristics of the voltage supplied to and the current drawn by the drive. These figures were obtained by transferring the prepared variables from ACSL to Matlab for plotting the variables as a function of time or frequency. To determine the harmonic content of selected waveforms, the fast Fourier transform (FFT) Matlab command was used to obtain the frequency spectrum of selected waveforms. The input rectifier current and the inverter output voltage waveforms have a significant harmonic content.

The parameters used in the simulation are given in the ACSL program listing in Section 3.6. The induction motor parameters are for an induction motor with rated values of 220 volts, 3 horsepower, and 1710 rpm were taken from [20]. The transformer parameters are for a 240/120V, single phase transformer [21]. The values for the smoothing filter between the rectifier and inverter were chosen so that the current through the inductor and the voltage across the capacitor would not change too rapidly or too

slowly to yield undesired simulation output waveforms. In an actual system the parameters of the drive would be determined by other factors. The switches in the rectifier and inverter are modeled as ideal: they are either on or off, can be switched instantaneously, and have a zero forward voltage drop. The ideal switch approximation is justified because of the low switching speeds in the voltage source inverter and the single phase rectifier.

As discussed in Section 1.4.4, ANSI C57.110 provides a method which can be used to determine the transformer derating when supplying nonsinusoidal loads. The hannonic content of the input currents drawn by the drive and motor in the simulation are used to determine the transformer derating, assuming that the transformer is loaded to its **fill** capacity with all ASD and one half ASD loading levels. Also, plots taken from an actual, installed heat pump are included for qualitative comparison to the waveforms produced by the simulation. The plots cannot be directly compared to the simulation results because the parameters of the measured system were not available:. The derating of the distribution transformer for the actual installation is also presented. The total hannonic distortion, THD, is also calculated for the primary and secondary transformer current. Also, the IEEE Standard 519-1992, which includes recommended limits on the current distortion for individual consumers of electric energy, is presented. The total harmonic distortion of the simulated and measured current waveforms are used to determine if the IEEE Standard 519-1992 limits are violated in either case.

4.2 Simulation results

The ACSL simulation is valid for transient and steady state operating conditions. Several cases are presented to show the operation of the system during startup and steady state conditions for zero applied load torque, a simulated compressor load, and step

changes in motor speed. The induction motor and transformer parameters used in the simulation are shown in the ACSL program listing in Section 3.6. The simulation was run for several cases. The cases studied are divided into three types:

- No load representative cases of the ASD
- Loaded representative cases of the ASD
- Field measured cases.

The first of these cases is depicted by a series of figures which are listed in Table (4.1). Figures (4.1) to (4.12) were obtained with a zero applied induction motor load torque and a 1:1 transformer turns ratio. Figures (4.13) to (4.43) were obtained with the induction motor applied torque as shown in Figure (4.15) and a transformer turns ratio of 4:1.

Figure	Volts	Amps	Power	Primary	Inverter	Speed	Torque	FFT
(4.1)	x			x				
(4.2)		x		x				
(4.3)			x	x				
(4.4)	x				x			
(4.5)	x				x			
(4.6)	x				x			
(4.7)						x		
(4.8)							x	
(4.9)	x				x			
(4.10)					x			x
(4.11)				x				x
(4.12)					x			x

Table 4.1 ASD figure description, no load case

Figure (4.1) shows the transformer primary applied sinusoidal voltage. Figure (4.2) shows the transformer input current, which clearly shows the nonsinusoidal current drawn by the **ASD**. Figure (4.3) shows the instantaneous power drawn by the transformer. Figures (4.4), (4.5), and (4.6) show the six-step, three phase inverter output voltages for the a, b, and c phase, respectively. Note that the frequency of the inverter output voltage is equal to 40 hertz. Figures (4.7), (4.8), and (4.9) show the induction motor rotor speed, electrical torque, and inverter applied voltage versus time, respectively. Figure (4.10) shows the frequency spectrum of the six step inverter output voltage. Note that the inverter fundamental frequency f_0 is 40 hertz, and the harmonic components are present at $(6h-1)f_0$ and $(6h+1)f_0$, where f_0 is the frequency of the fundamental component and h is an integer. Figure (4.11) shows the frequency spectrum of the secondary current through the transformer. Note that the frequency spectrum of the current drawn by the **ASD** contains odd harmonics. Figure (4.12) shows the frequency spectrum of the current drawn by the induction motor. The frequency spectrum of the current drawn by the induction motor has components at the same frequency as the inverter output voltage shown in Figure (4.10).

The loaded cases are also depicted by the figures which are listed in Table (4.2). Figures (4.13) through (4.43) were obtained from the simulation of the **ASD** system with the applied load torque shown in Figure (4.15). Figure (4.13) shows the induction motor speed, which decreases as the load torque is increased. Figure (4.14) shows the induction motor electrical torque, which increases with the applied load torque. Figure (4.16) shows the transformer secondary current, which is large during motor startup, and then increases as the applied load torque increases. Figure (4.17) shows the transformer primary instantaneous power, which increases as the load torque is increased. Figure (4.18) shows the inverter input voltage, which decreases slightly as the load torque is increased.

Load number	Figure	Time interval	Percent load
1	(4.19) to (4.23)	0 - 1 seconds	0
2	(4.24) to (4.28)	1 - 1.5 seconds	25
3	(4.29) to (4.33)	1.5 - 2 seconds	50
4	(4.34) to (4.38)	2 to 2.5 seconds	75
5	(4.39) to (4.43)	2.5 to 3 seconds	100

Table 4.2 Simulated motor load torque cases

Expanded views of selected steady state power, current, and frequency spectrum waveforms resulting from the five load torque levels shown in Figure (4.15) are presented in Figures (4.19) to (4.43).

Table (4.2) gives the figure numbers associated with each load case. The five figures shown for each of the five cases are the transformer primary current, secondary current, primary power, frequency spectrum of transformer secondary current, and the frequency spectrum of the transformer primary current. The frequency spectrum plots are normalized so that the amplitudes are displayed as the percentage of the fundamental. This is more convenient since the per unit values are needed for the transformer derating calculations. As the load torque is increased, the current drawn by the ASD increases. Also, the current waveform becomes more sinusoidal as the input current becomes larger. Also, the transformer primary current is more sinusoidal than the secondary current because of the filtering effects of the transformer.

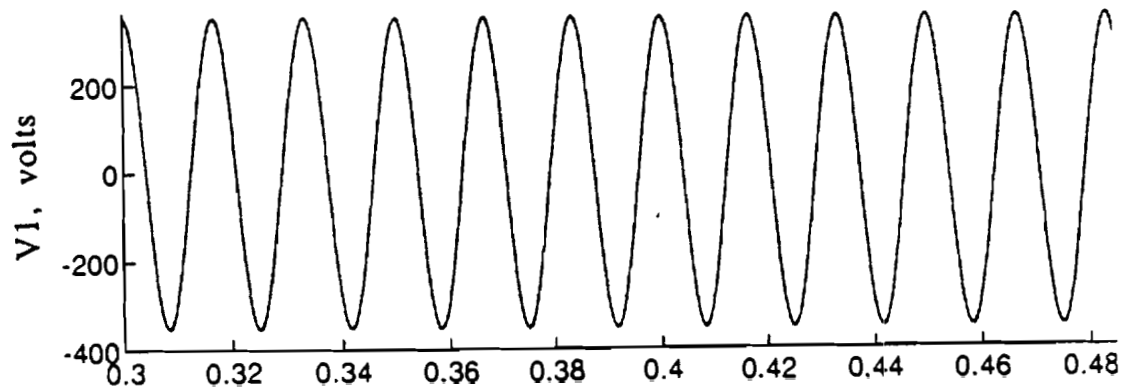


Figure 4.1 Transformer primary voltage versus time

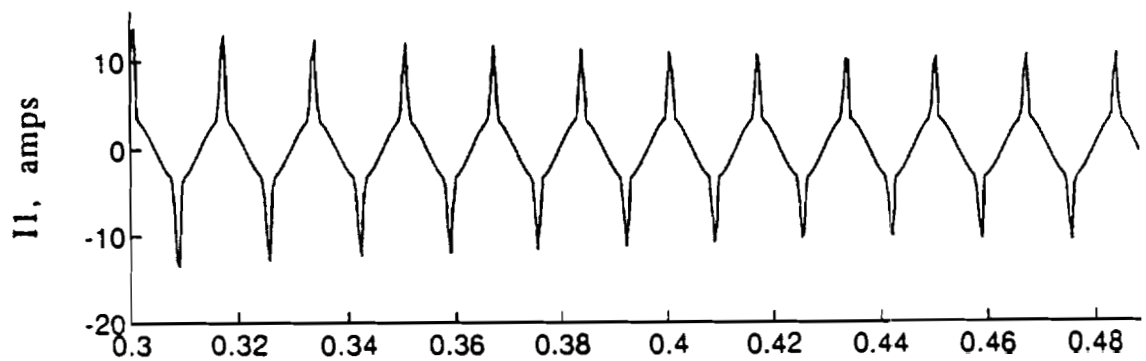


Figure 4.2 Transformer input current versus time

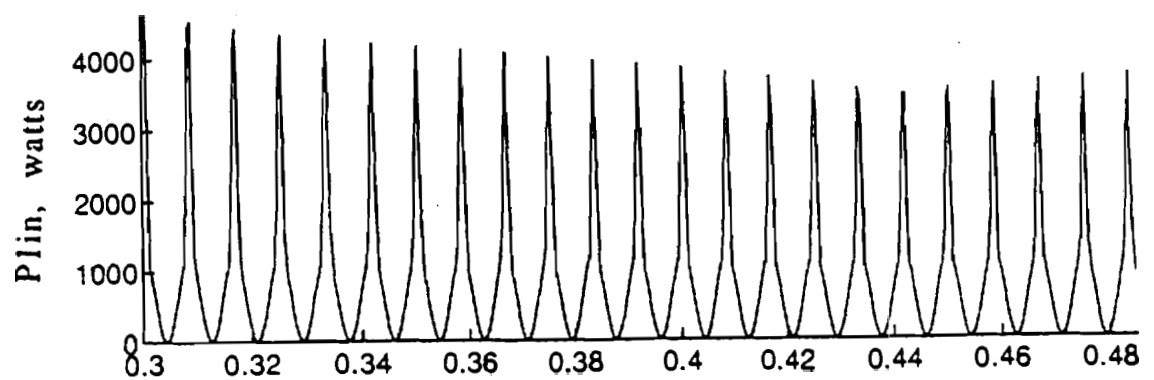


Figure 4.3 Transformer instantaneous power versus time

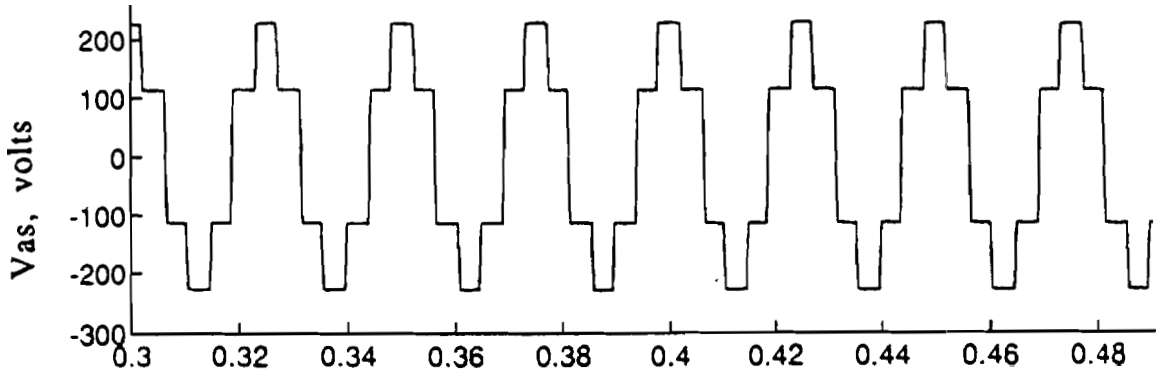


Figure 4.4 Phase a inverter six step output voltage versus time

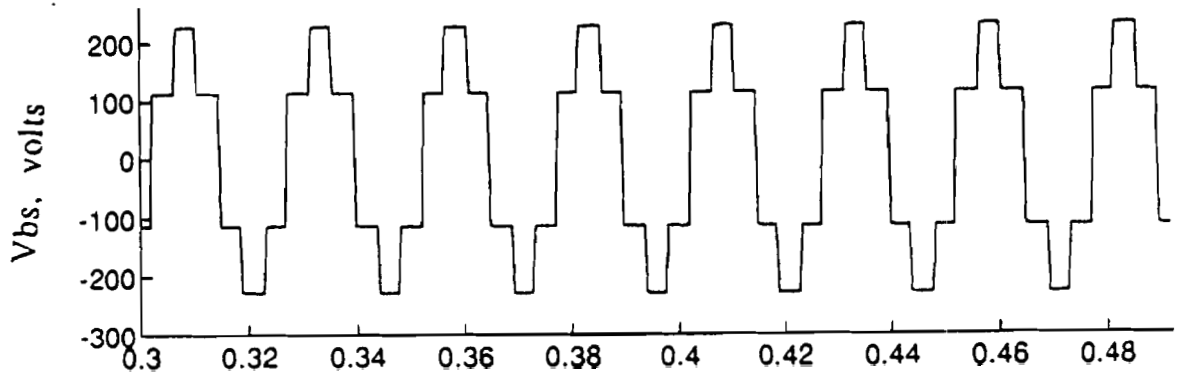


Figure 4.5 Phase b inverter six step output voltage versus time

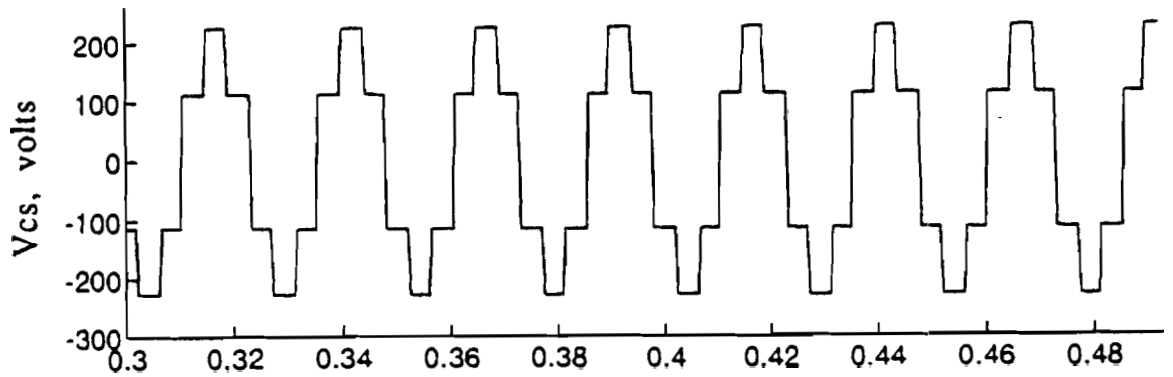


Figure 4.6 Phase c inverter six step output voltage versus time

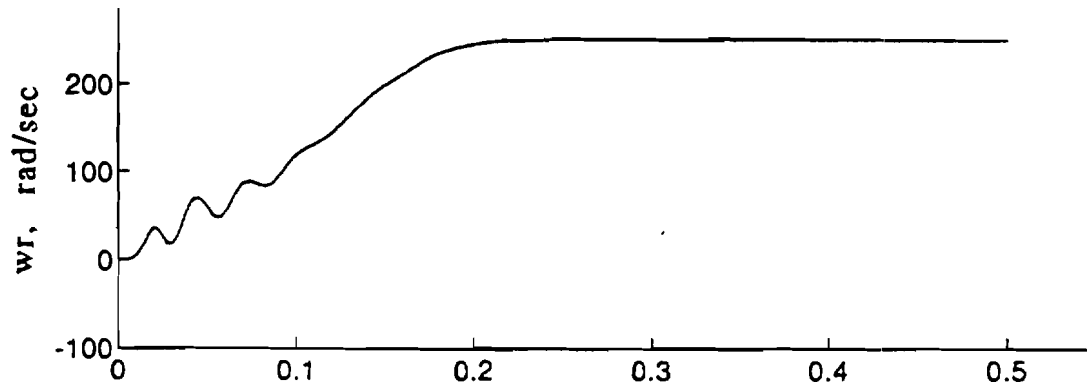


Figure 4.7 Induction motor speed versus time

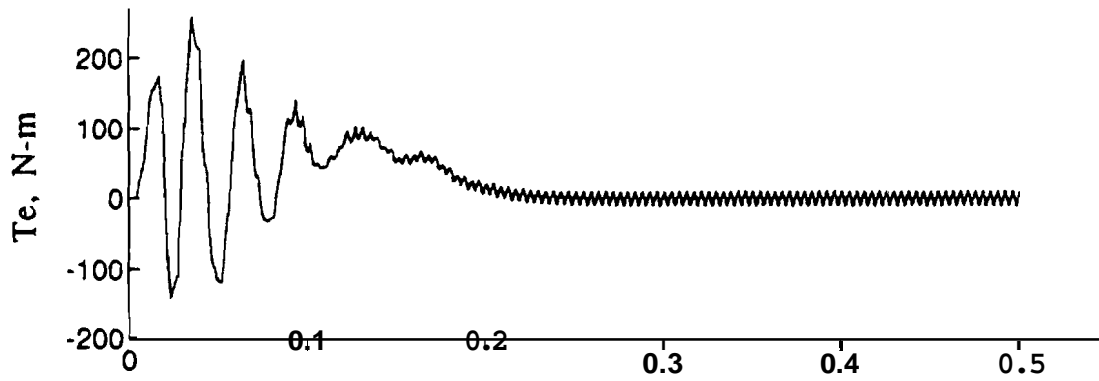


Figure 4.8 Induction motor electrical torque versus time

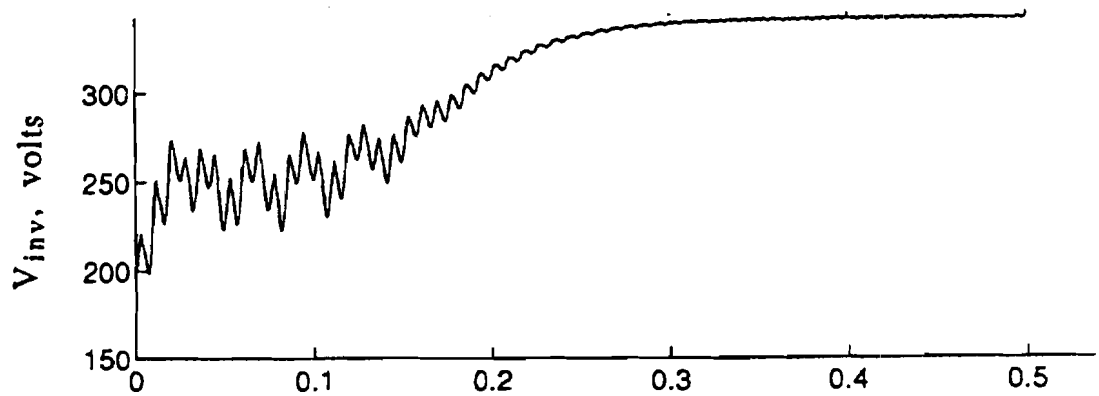


Figure 4.9 Inverter input voltage V_{inv} versus time

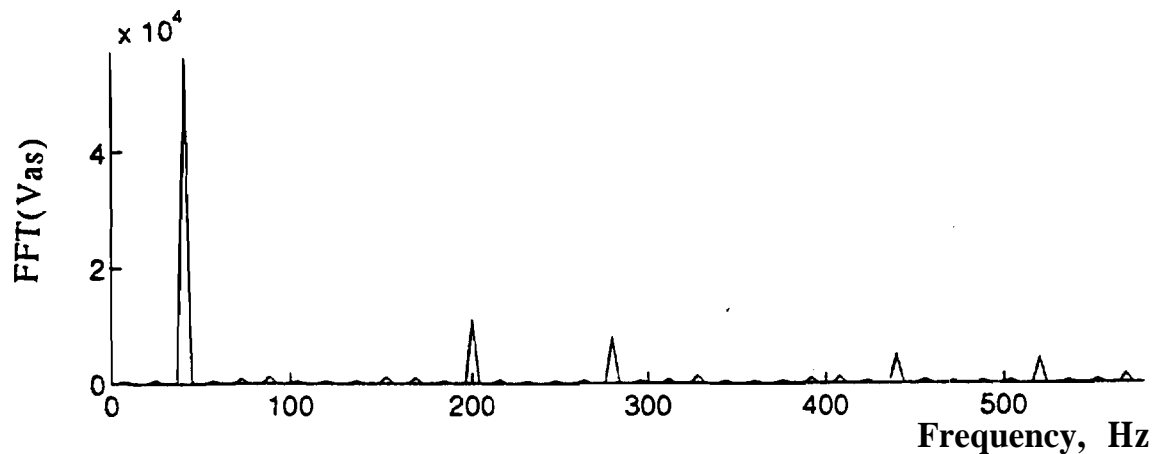


Figure 4.10 Frequency spectrum of inverter output voltage V_{as}

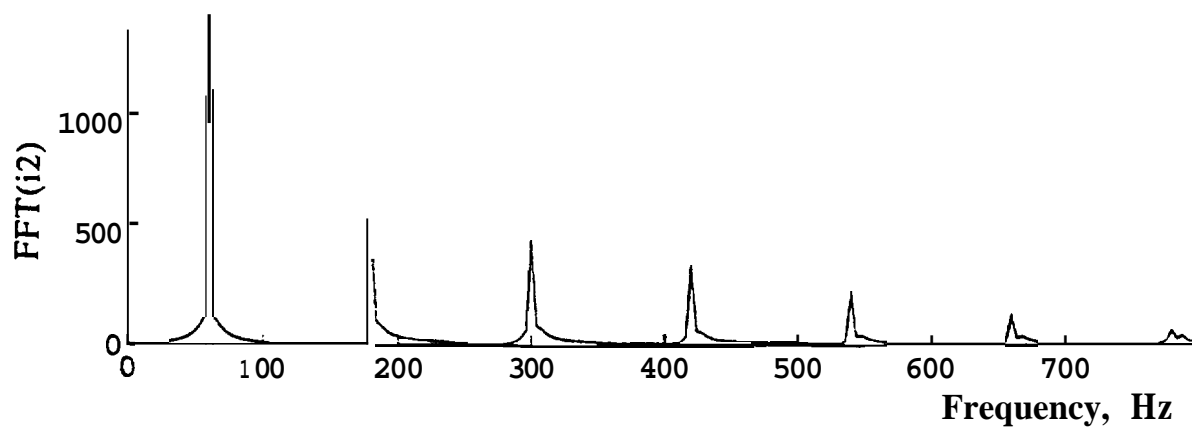


Figure 4.11 Frequency spectrum of transformer secondary current

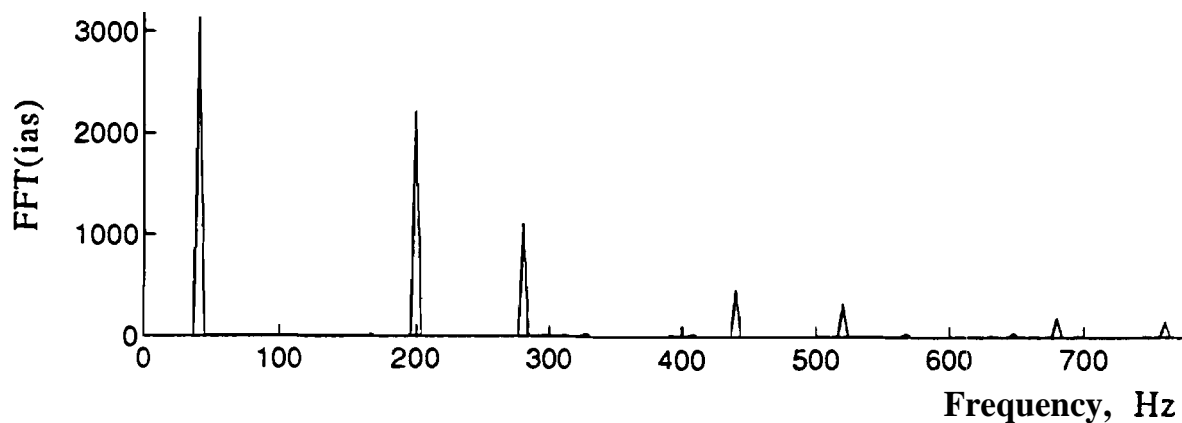


Figure 4.12 Frequency spectrum of phase a motor stator current

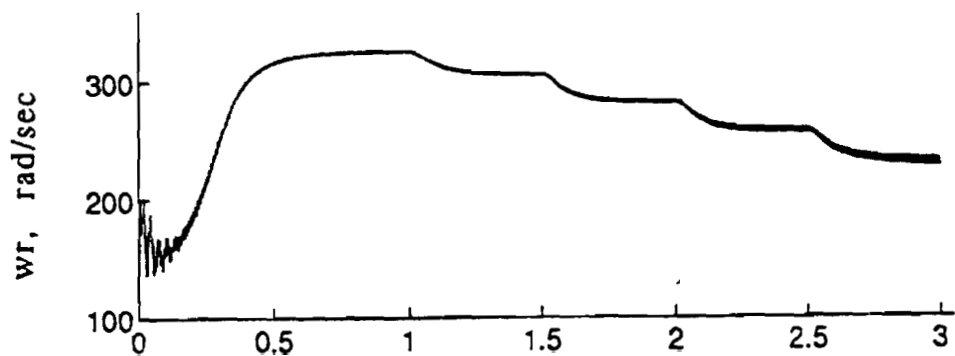


Figure 4.13 Induction motor speed versus time

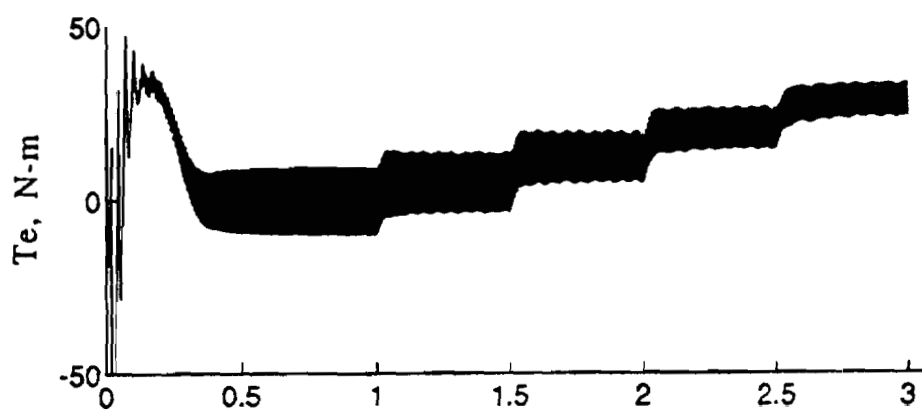


Figure 4.14 Induction motor electrical torque versus time

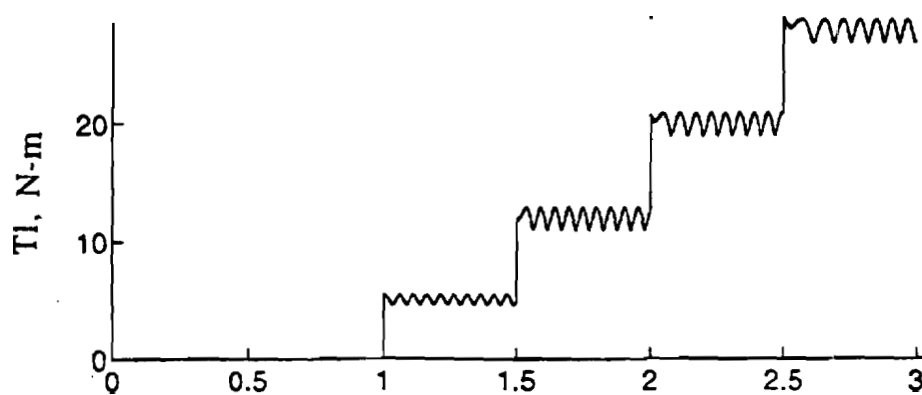


Figure 4.15 Applied load torque versus time

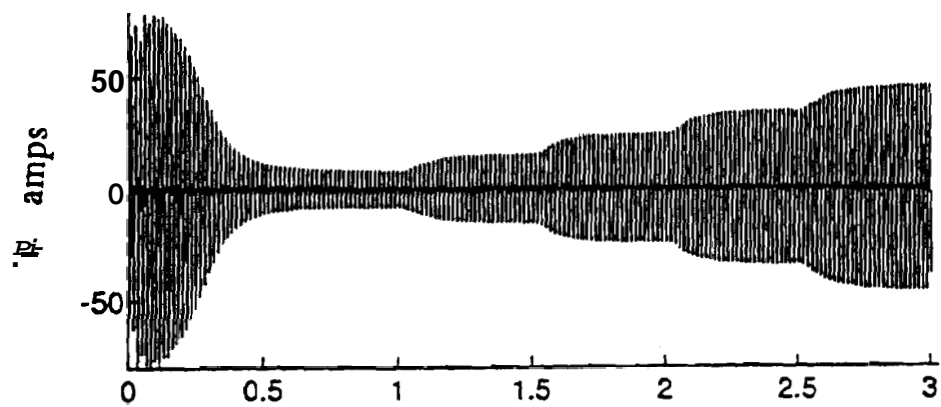


Figure 4.16 Transformer secondary current versus time

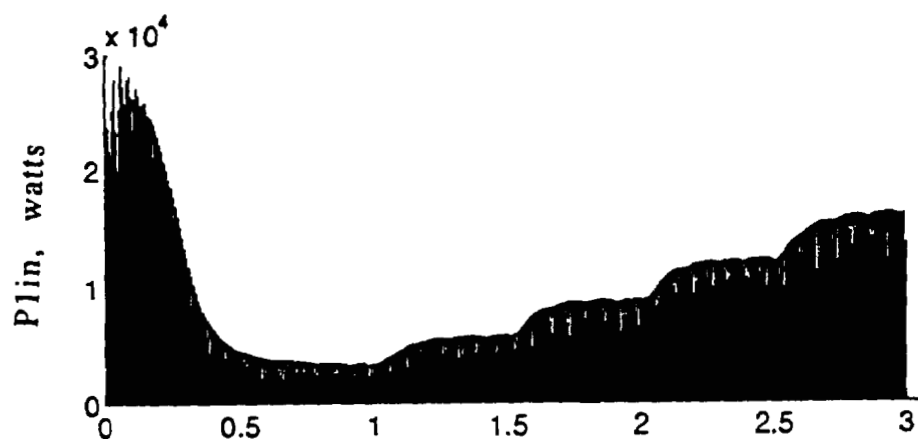


Figure 4.17 Transformer primary instantaneous power versus time

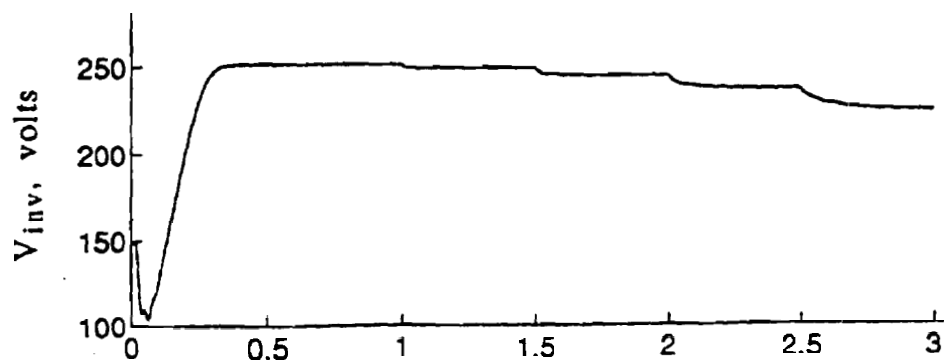


Figure 4.18 Inverter input voltage versus time

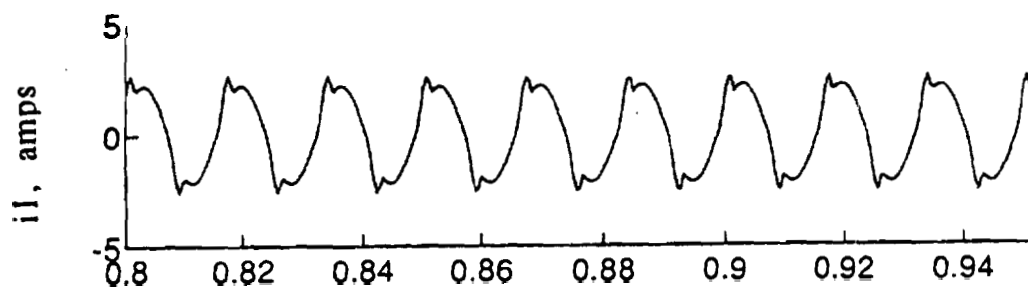


Figure 4.19 Load 1, Transformer primary current versus time

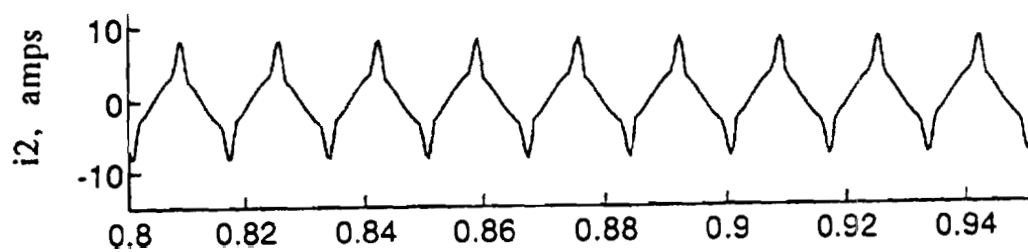


Figure 4.20 Load 1, Transformer secondary current versus time

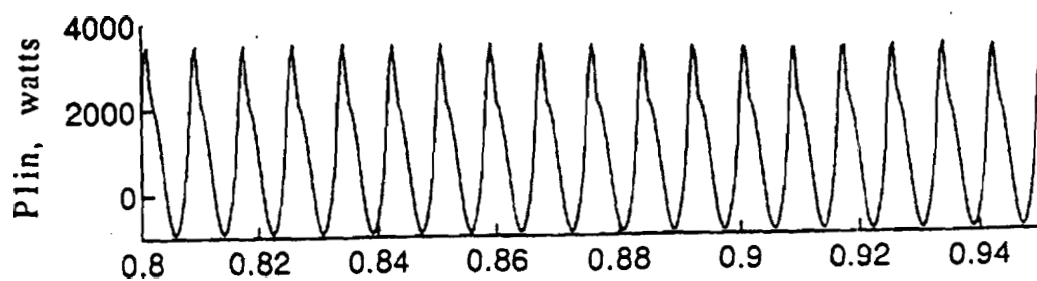


Figure 4.21 Load 1, Transformer primary instantaneous power

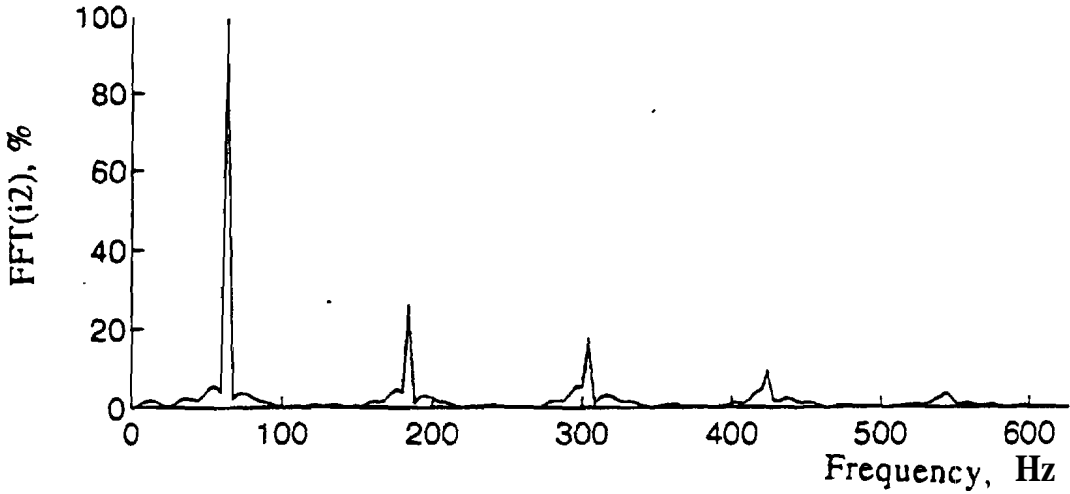


Figure 4.22 Load 1, Frequency spectrum of transformer secondary current expressed as a percentage of the fundamental

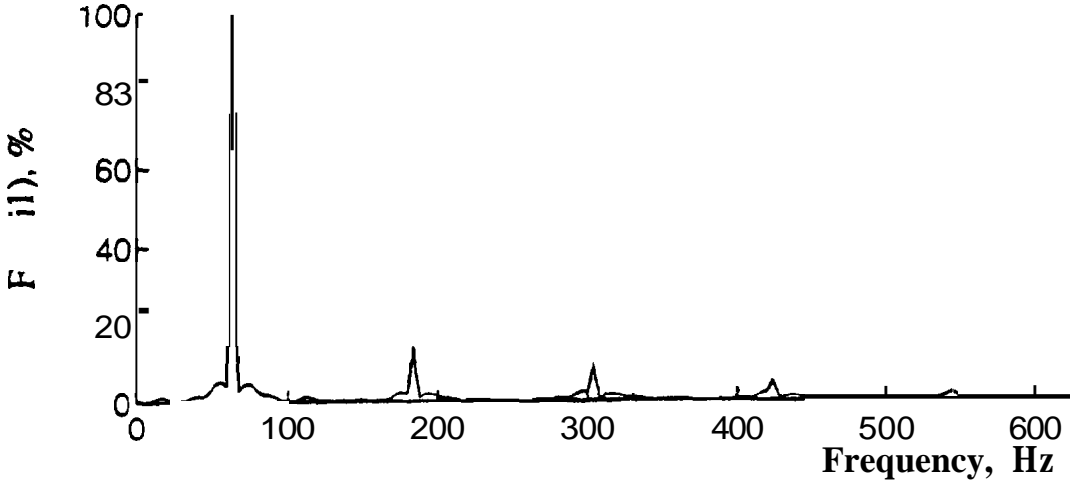


Figure 4.23 Load 1, Frequency spectrum of transformer primary current expressed as a percentage of the fundamental

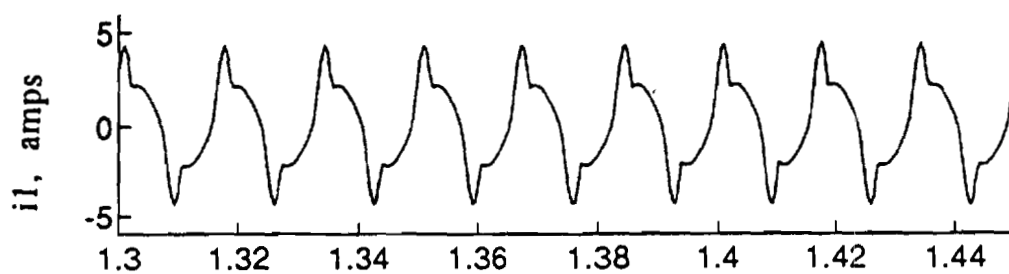


Figure 4.24 Load 2. Transformer primary current versus time

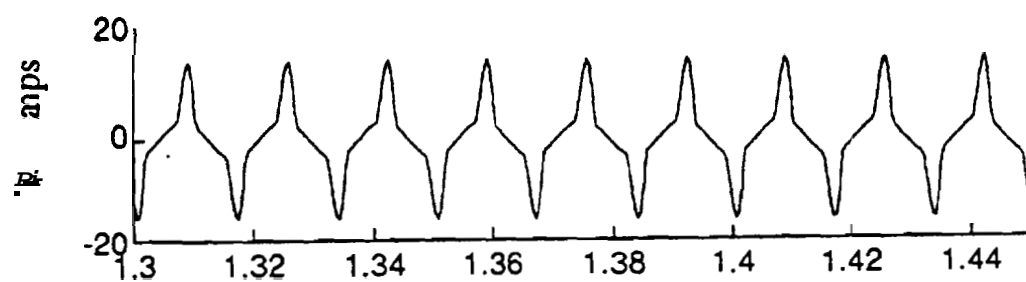


Figure 4.25 Load 2, Transformer secondary current versus time

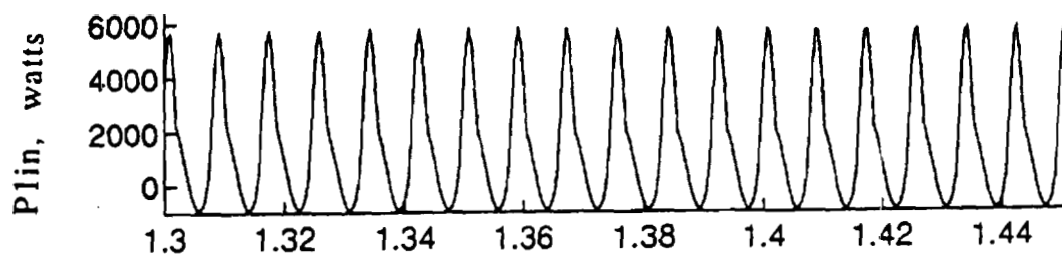


Figure 4.26 Load 2, Transformer primary instantaneous power

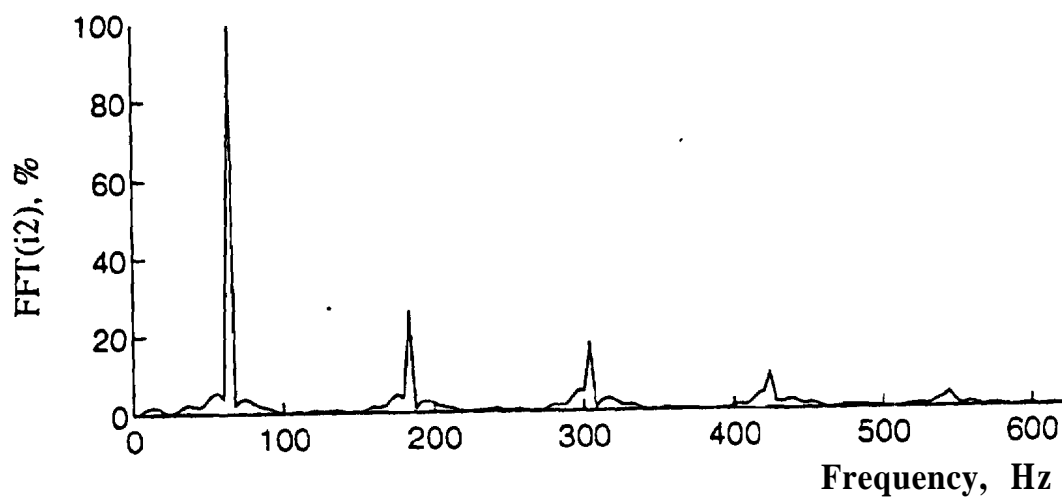


Figure 4.27 Load 2, Frequency spectrum of transformer secondary current expressed as a percentage of the fundamental

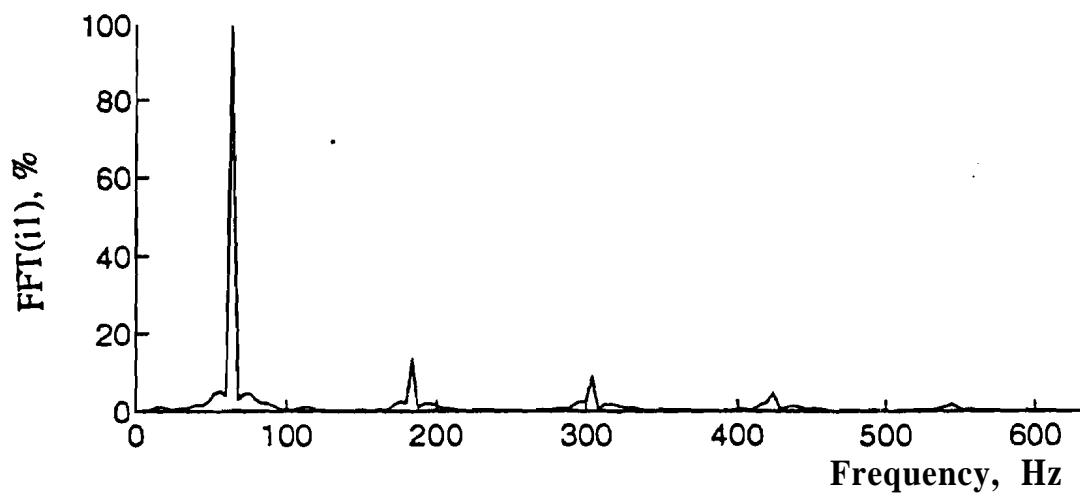
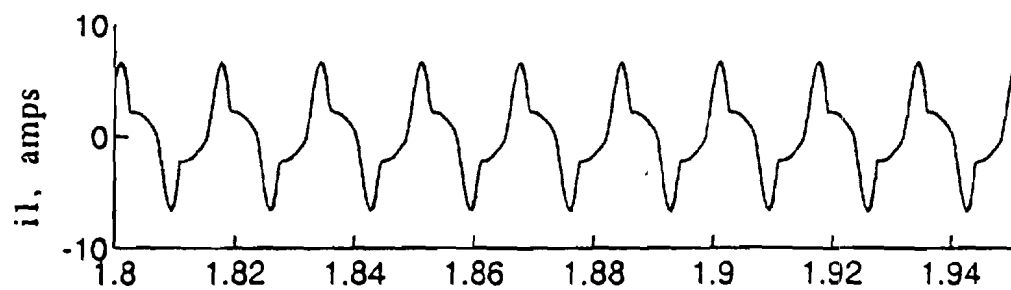


Figure 4.28 Load 2, Frequency spectrum of transformer primary current expressed as a percentage of the fundamental



Figure, 4.29 Load 3, Transformer primary current versus time

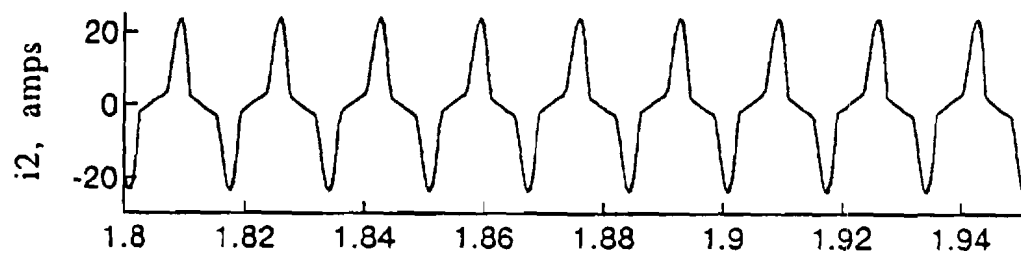


Figure 4.30 Load 3, Transformer secondary current versus time

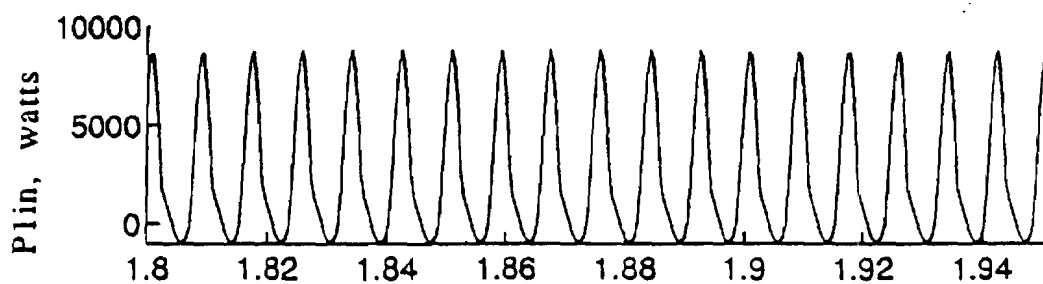


Figure 4.31 Load 3, Transformer primary instantaneous power

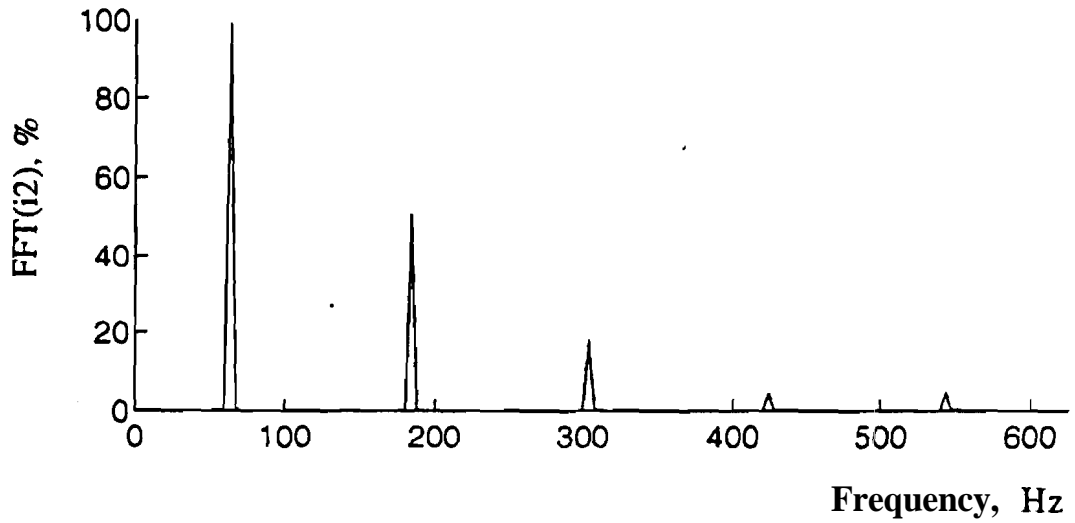


Figure 4.32 Load 3, Frequency spectrum of transformer secondary current expressed as a percentage of the fundamental

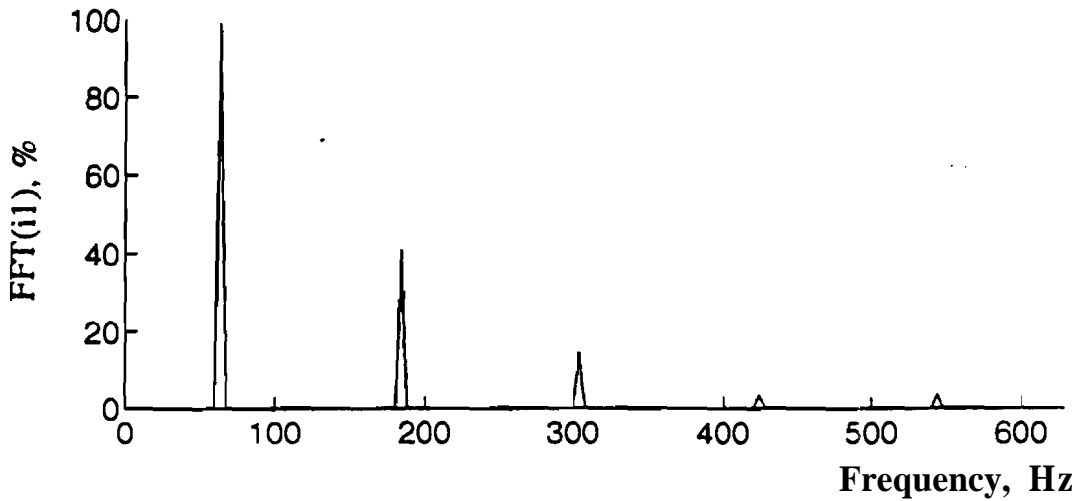


Figure 4.33 Load 3, Frequency spectrum of transformer primary current expressed as a percentage of the fundamental

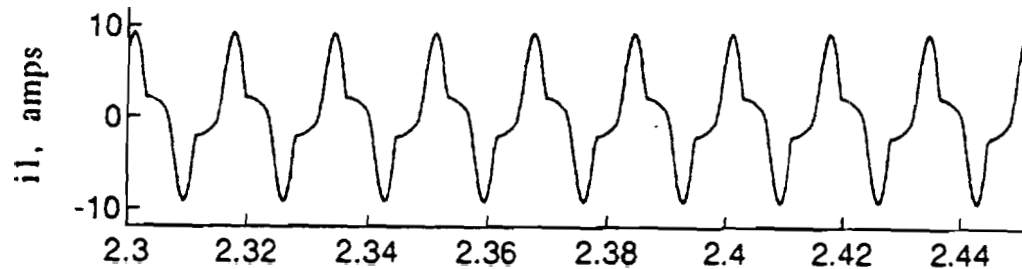


Figure 4.34 Load 4, Transformer primary current versus time

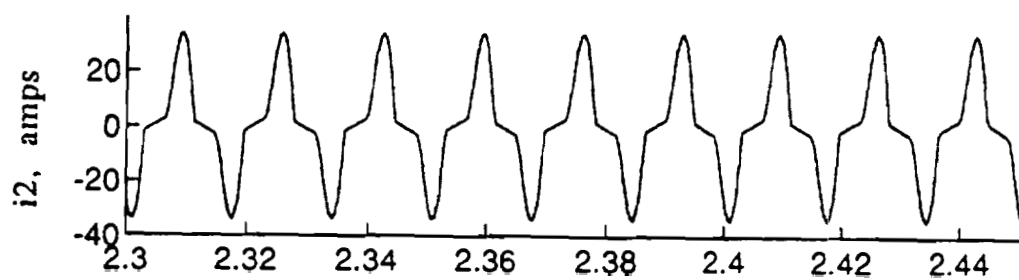


Figure 4.35 Load 4, Transformer secondary current versus time

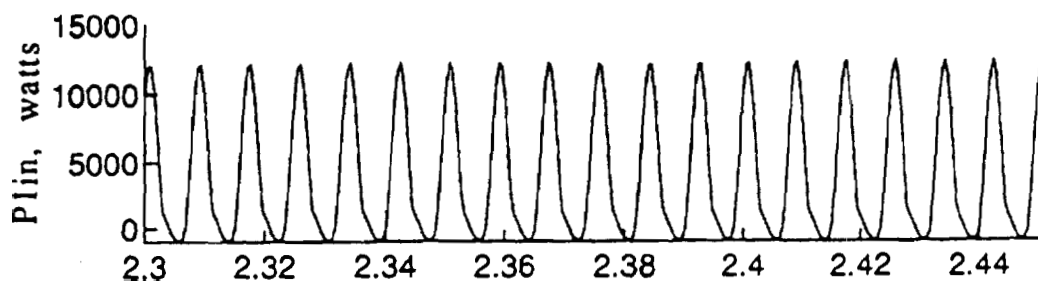


Figure 4.36 Load 4, Transformer primary instantaneous power

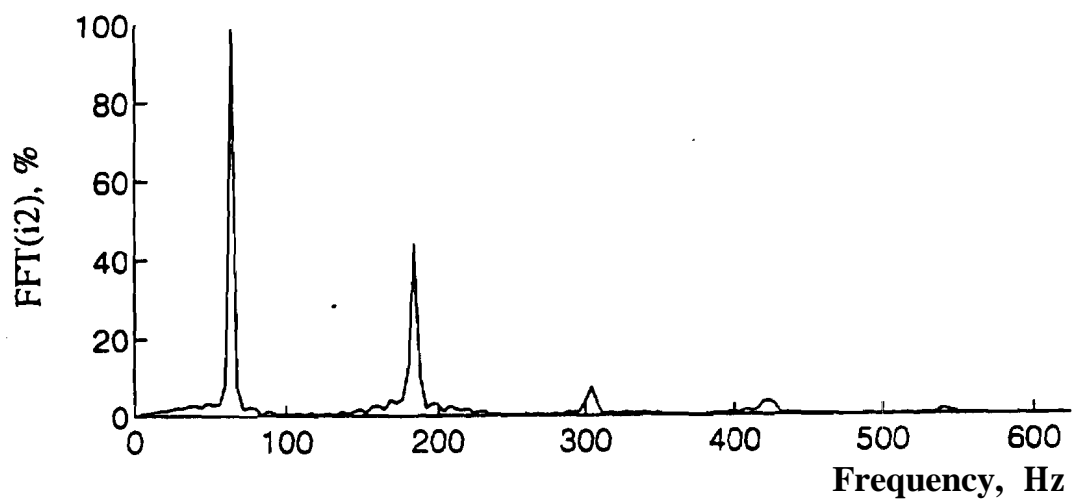


Figure 4.37 Load 4, Frequency spectrum of transformer secondary current expressed as a percentage of the fundamental

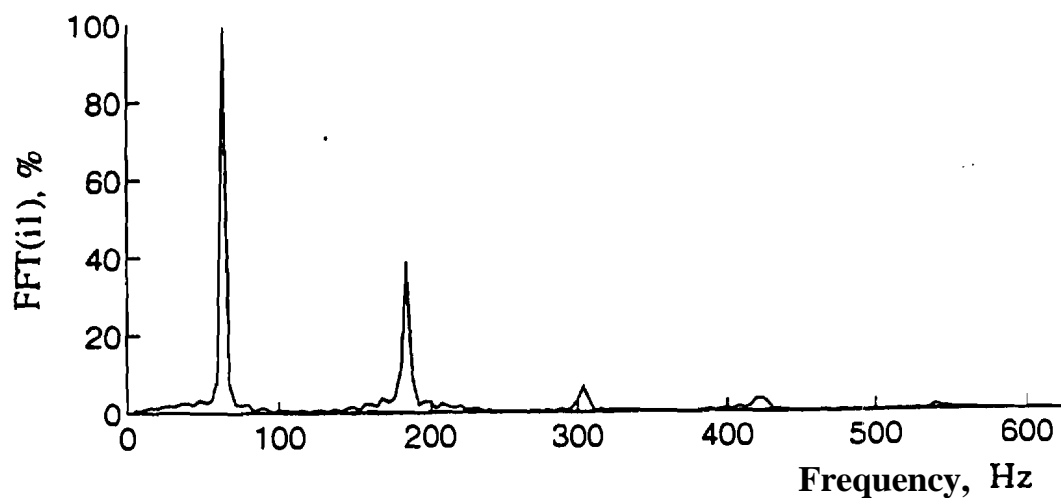


Figure 4.38 Load 4, Frequency spectrum of transformer primary current expressed as a percentage of the fundamental

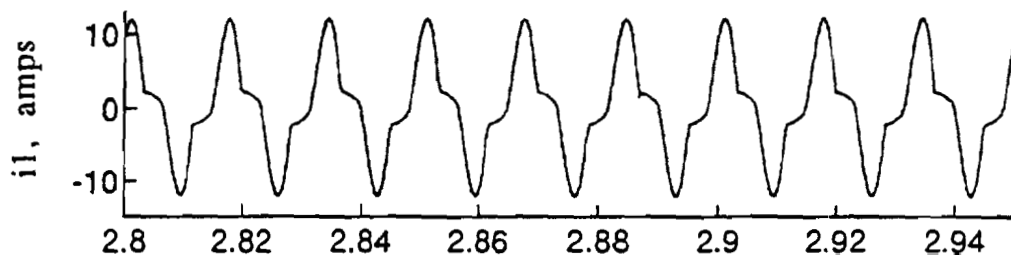


Figure 4.39 Load 5, Transformer primary current versus time

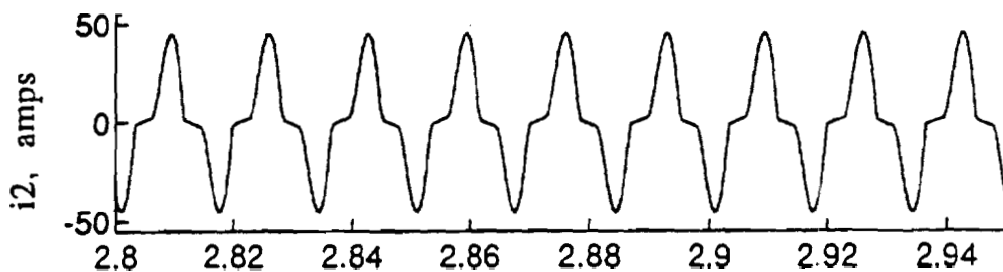


Figure 4.40 Load 5, Transformer secondary current versus time

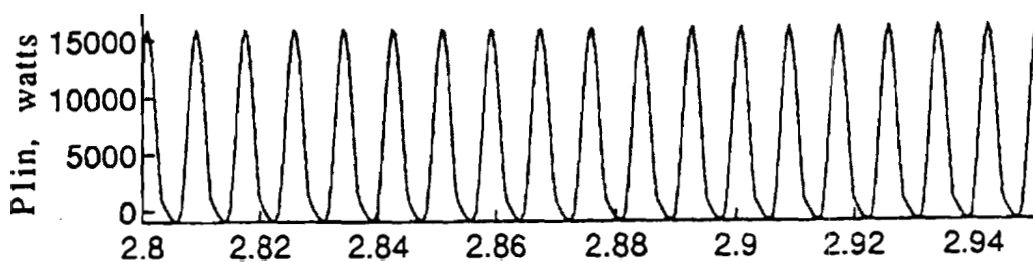


Figure 4.41 Load 5, Transformer primary instantaneous power

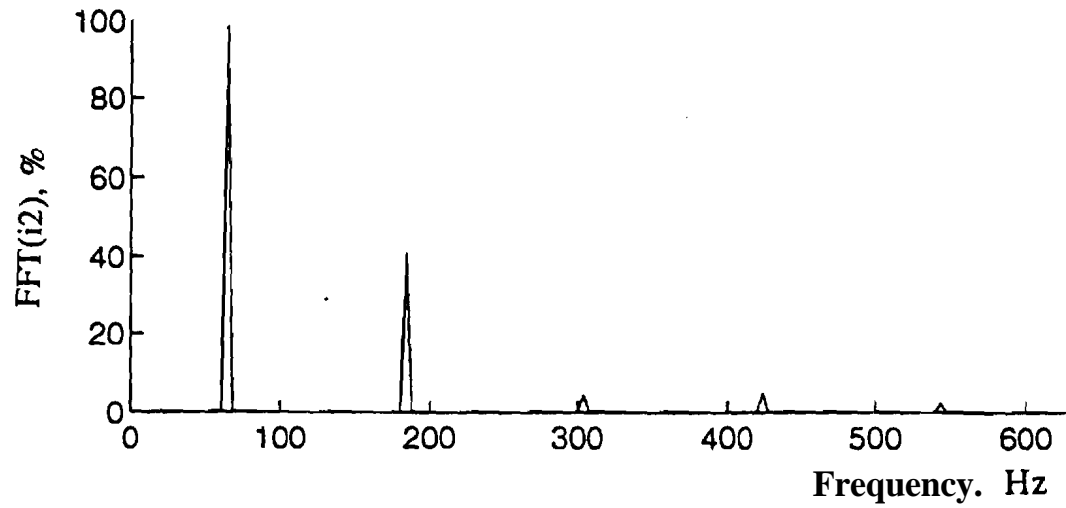


Figure 4.42 Load 5, Frequency spectrum of transformer secondary current expressed as a percentage of the fundamental

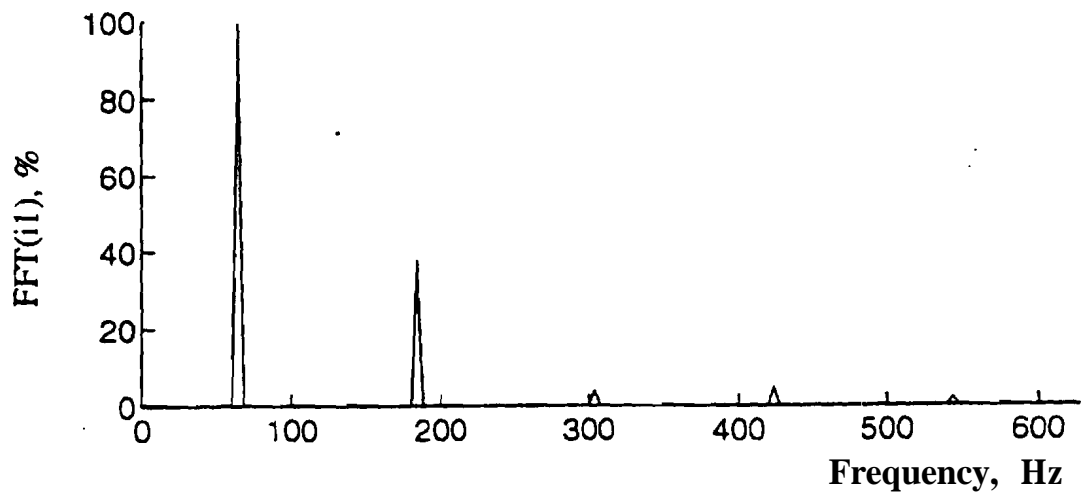


Figure 4.43 Load 5, Frequency spectrum of transformer primary current expressed as a percentage of the fundamental

4.3 Field measurement cases

This section contains figures which were obtained from field measurements of an operating adjustable speed drive heat pump taken at an all-electric residence. A Trane model XV1500 variable speed Weathertron heat pump was installed. Table (4.3) lists the waveforms obtained from the field measurements. Figures (4.44) to (4.47) show the voltage, current, power, frequency spectrum of the distribution transformer secondary voltage, and the frequency spectrum of the transformer secondary current, respectively, for the case when the heat pump is off. Figures (4.48) to (4.51) show the voltage, current, power, frequency spectrum of the transformer secondary voltage, and the frequency spectrum of the transformer secondary current, respectively, for the case when the heat pump is on.

Fig. #	HP on	HP off	Volts	Amps	Power	FFT
(4.44)		x	x	x		
(4.45)		x			x	
(4.46)		x	x			x
(4.47)		x		x		x
(4.48)	x		x	x		
(4.49)	x				x	
(4.50)	x		x			x
(4.51)	x			x		x

Table 4.3 Figure descriptions of field measurements

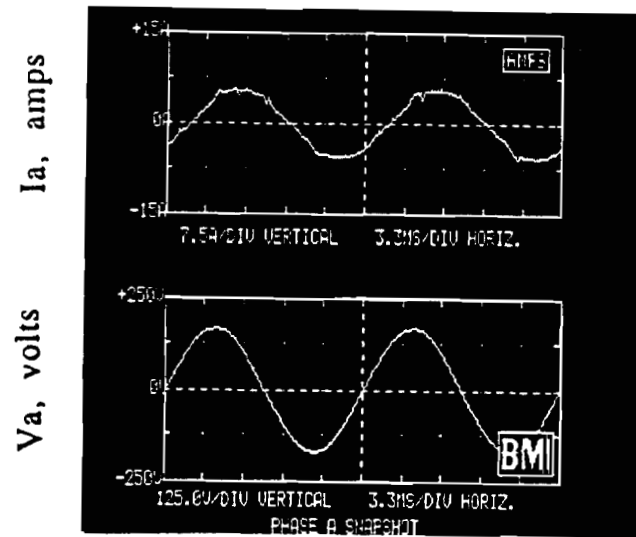


Figure 4.44 Phase a current and voltage snapshot, heat pump off

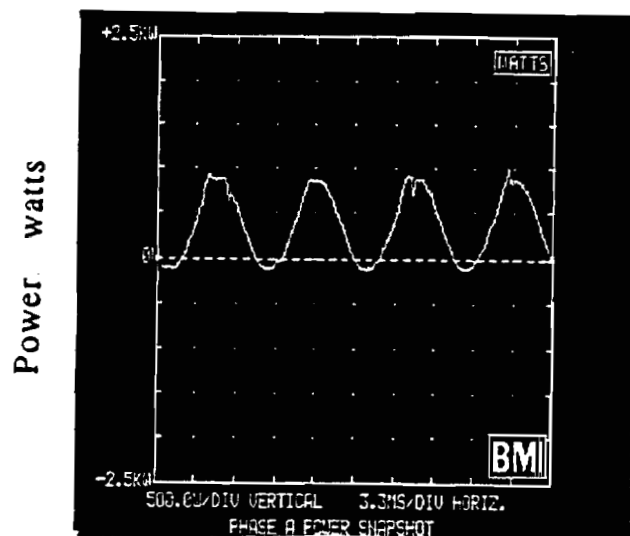


Figure 4.45 Phase a instantaneous power. heat pump off

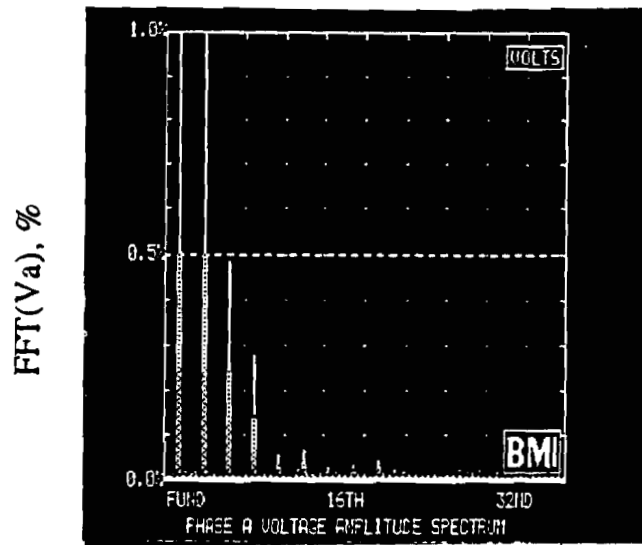


Figure 4.46 Phase a voltage amplitude spectrum, heat pump off

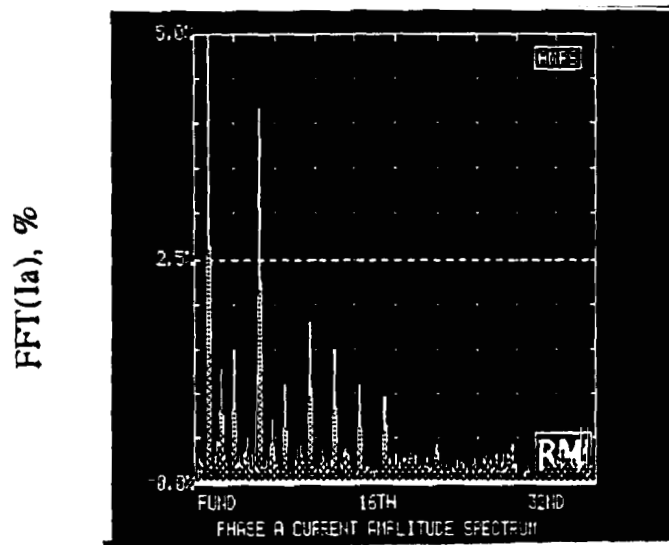


Figure 4.47 Phase a current amplitude spectrum, heat pump off

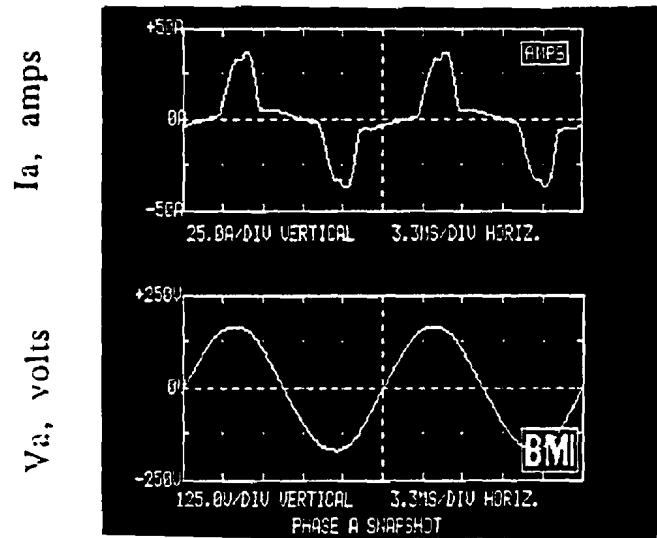


Figure 4.48 Phase a current and voltage snapshot, heat pump on

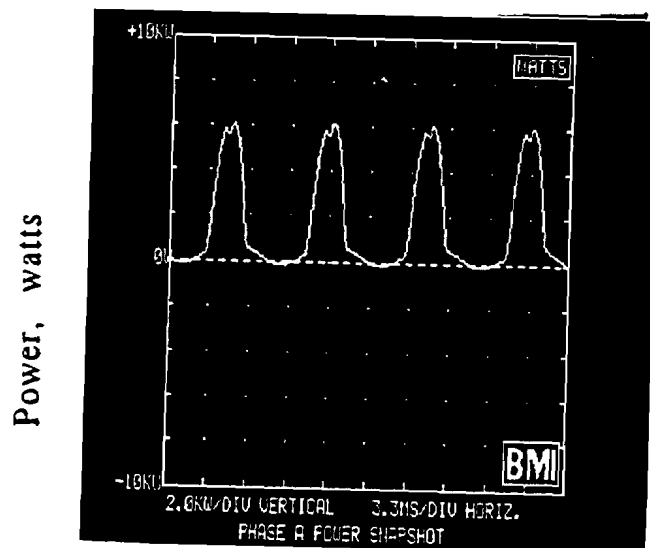


Figure 4.49 Phase a instantaneous power, heat pump on

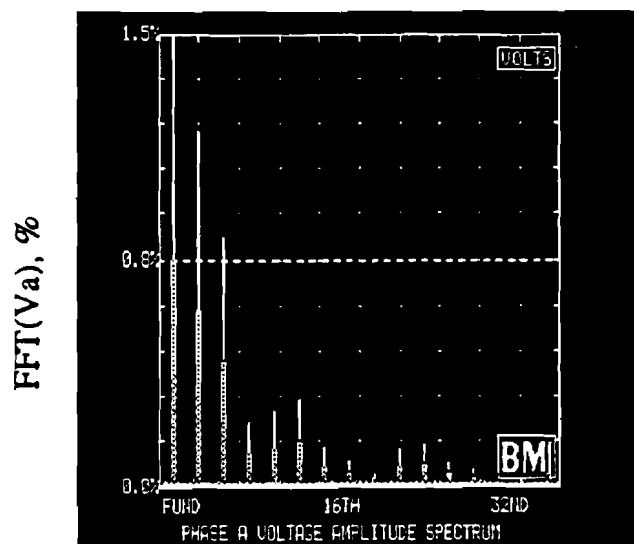


Figure 4.50 Phase a voltage amplitude spectrum, heat pump on

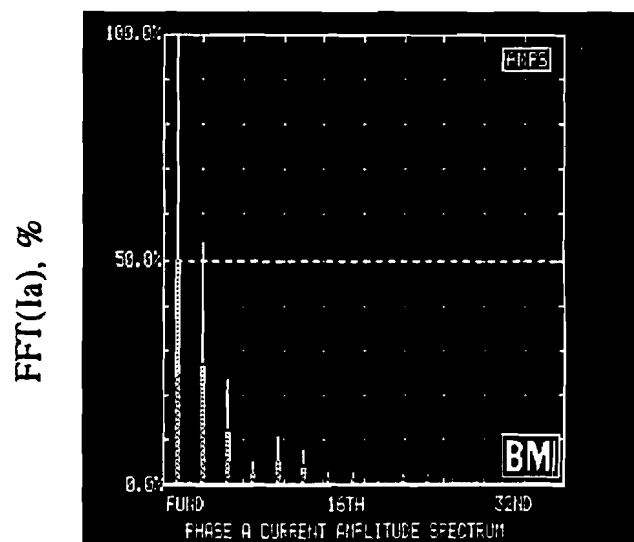


Figure 4.51 Phase a current amplitude spectrum, heat pump on

4.4 Transformer derating calculations

4.4.1 ANSI C57.110 example calculation

The distribution transformer incurs additional losses when it is supplying harmonic currents, as is the case for both the simulation results and the measured waveform obtained from an actual installation. The ANSI C57.110 Standard is used to determine the transformer derating, or reduction in power transfer capability, due to the flow of harmonic currents [2]. This recommended practice has been described in more detail in Section 1.4.4. The equation which determines the transformer derating is shown below. To aid in the explanation of the calculation of the transformer derating, the following example is included, which was taken from ANSI C57.110. The harmonic current spectrum and other calculations are shown in Table 4.4. The variable f_h is the ratio of the harmonic current magnitude divided by the magnitude of the fundamental component of current. The current magnitudes are all given in per unit quantities. The transformer winding eddy-current loss density ($P_{EC-R}(pu)$) is 15% of the local I^2R loss, therefore $P_{LL-R}(pu) = 1.15 pu$,

$$I_{\max}(pu) = \sqrt{\frac{P_{LL-R}(pu)}{1 + \left\{ \left(\frac{\sum_{h=1}^{h_{\max}} f_h^2 h^2}{\sum_{h=1}^{h_{\max}} f_h^2} \right) P_{EC-R}(pu) \right\}}}}$$
$$I_{\max}(pu) = \left[\frac{1.15}{1 + \frac{2.849}{1.0459} 0.15} \right]^{1/2} = 0.9035 .$$

h	I_h	I_h^2	h^2	$I_h^2 h^2$	f_h	f_h^2	$f_h^2 h^2$
1	0.987	0.957	1	0.957	1.00	1.00	1.00
5	0.171	0.029	25	0.731	0.175	0.0306	0.7643
7	0.108	0.012	49	0.571	0.110	0.0122	0.5975
11	0.044	0.002	121	0.234	0.045	0.002	0.2449
13	0.028	0.0008	169	0.133	0.029	0.0008	0.1385
17	0.015	0.0002	289	0.065	0.015	0.0002	0.068
19	0.0098	0.0001	361	0.035	0.01	0.0001	0.0362
Σ		1.00		2.726		1.0459	2.8494

Table 4.4 ANSI C57.110 transformer derating example:

A transformer which is supplying current at the given magnitude of harmonic component has a capability which is only 90.3% of the full-load rated value. Thus the transformer is not able to transmit its full rated power due to the current harmonics drawn by the load. A transformer that will supply a load that produces harmonic currents must be oversized to ensure that the transformer temperature does not exceed design limits.

4.4.2 Transformer derating of actual system

The waveforms presented in Section 4.3 were obtained from an operating heat pump. Table 4.5 gives the magnitude of each current harmonic and other calculations that are needed to evaluate the derating. The transformer derating is calculated to be equal to 0.9368 in this case,

$$I_{\max} = \sqrt{1 + \frac{\frac{750/90}{(13.7455)(75)}}{(1.3484)(90)}} = 0.9368 .$$

h	I_h	I_h^2	h^2	$I_h^2 h^2$	f_h	f_h^2	$f_h^2 h^2$
1	0.8615	0.7422	1	0.7422	1.000	1.000	1.000
3	0.3077	0.0947	9	0.8520	0.3572	0.1276	1.1483
5	0.2769	0.0767	25	1.9170	0.3214	0.1033	2.5824
7	0.2077	0.0431	49	2.1135	0.2411	0.0581	2.8483
9	0.1615	0.0261	81	2.1135	0.1874	0.0351	2.8466
11	0.1154	0.0133	121	1.6109	0.1339	0.0179	2.1711
13	0.0615	0.0038	169	0.6400	0.0714	0.0051	0.8612
15	0.0308	0.0009	225	0.2130	0.0358	0.0031	0.2876
					Σ	1.3484	13.745

Table 4.5 Transformer active power loss estimates for the actual measurements

The transformer in this case has 7620/240/120 V, 25kVA, single phase, 1.8% rated values. Although the exact data is not known, the full load losses are estimated to be approximately 3% of the kVA rating, and core losses are estimated to be 10% of the full load loss. Thus for this operating heat pump, the 6.3% of the transformer capability is not available because of the harmonics drawn by the power electronic load.

4.4.3 Transformer derating for simulation results

The waveforms produced by the simulation of the single phase transformer, drive, and induction motor are shown in Section 4.2. The transformer secondary current spectrum for the simulation results are shown in Figures (4.22), (4.27), (4.32), (4.37), and (4.42). Each figure is the frequency spectrum for a different applied motor torque. Each frequency spectrum shows that the transformer secondary current contains a significant percentage of odd harmonics. The ANSI C57.110 Standard is used to calculate the transformer derating for the simulation results. The root mean squared value of the current containing harmonics, I_h , through the transformer is assumed to be equal to the transformer rated current, thus the sum of I_h is equal to 1.0 per unit of the transformer rating. This assumption may not be valid for the partial load cases, since if the ASD is partially loaded, the transformer will not be fully loaded. Also, the transformer winding eddy-current loss density is assumed to be 15% of the local copper loss. Table 4.6 contains the data taken from Figure (4.32), which is load 3 case.

$$I_{\max} (\text{pu}) = \left[\frac{1.15}{1 + \frac{5.29}{1.294} \cdot 0.15} \right]^{1/2} = 0.844$$

h	I _h , %	I _h (pu)	I_h^2	$I_h^2 h^2$	f _h	f_h^2	$f_h^2 h^2$
1	100.0	0.525	0.276	0.276	1.00	1.00	1.00
3	46.31	0.243	0.059	0.532	0.4631	0.2145	1.93
5	25.55	0.134	0.018	0.450	0.256	0.066	1.638
7	8.32	0.044	.0019	0.093	0.0832	0.007	0.339
9	4.03	0.021	.00045	0.036	0.0403	0.0016	0.132
11	3.99	0.0209	.00044	0.0531	0.0399	0.0016	0.193
13	1.85	0.0097	.00009	0.0159	0.0185	0.0034	0.058
			Σ	1.456		1.294	5.29

Table 4.6 Transformer active power loss estimates for the simulation results, load 3

For the cases shown, the transformer derating is, at most, **90%**. The **84.4%** calculated above for the simulation results may appear to be low, but the figure was calculated assuming that the entire current through the transformer is the result of an ASD load and the 100 ohm resistor across the transformer secondary. The **93%** derating calculated using the actual system measurements (Section 4.4.2) included other, linear loads which would not reduce the transformer derating due to the larger fundamental current component. The figure calculated above is for the case of load 3. The transformer derating calculations for the other four cases are not shown, but follow exactly the same method as shown above for load 3. The total harmonic distortion of the **primary** and secondary transformer current is shown in Table 4.7 for each case. The total transformer derating was calculated for the simulation results assuming the transformer was loaded at rated capacity. Table 4.8 contains the transformer derating for the one-half

ASD and the full ASD load simulation cases. The full ASD load case is calculated by normalizing the total transformer current to 1 per unit. To determine the effect on the transformer derating, the same calculations are repeated with a fundamental magnitude of current equal to twice the value for the full ASD case. This is approximately what would occur if a transformer were to serve an equally sized ASD and linear load. The transformer is not derated as severely in these cases. Note that the total harmonic distortion, THD, is defined by

$$\text{THD} = \frac{\sqrt{\sum_{n=2}^{h_{\max}} (I_n)^2}}{I_1}$$

Load Number	Loadin level	Primar THD	Secondar THD
		36.8%	53.9%
3	50%	43.9%	54.2%
4	75%	39.2%	44.7%
5	100%	38.1%	41.6%

Table 4.7 Transformer primary and secondary current total harmonic distortion for the five load cases

Load Number	Loading level	One-half ASD load derating	Full ASD load derating
1	0%	97.1%	90.4%
2	25%	94.4%	84.4%
3	50%	95.4%	86.6%
4	75%	97.3%	91.5%
5	100%	97.6%	92.1%

Table 4.8 Transformer derating for the five load cases, transformer at rated load, one-half ASD and full ASD load cases

4.5 IEEE Standard 519-1992

The IEEE "Recommended Practices and Requirements for Harmonic Control in Electric Power Systems," is a recommended practice which addresses harmonic producing devices present on typical power systems and lists problems that may result from excessive harmonics [11]. Section 10, Recommended Practices for Individual Consumers, describes the current distortion limits that apply to individual consumers of electrical energy. Table 4.9 was taken from IEEE Standard 519-1992 and lists the current distortion limits for general distribution systems with voltage levels ranging from 120 volts to 69,000 volts.

I_{sc}/I_L	$h < 11$	$11 \leq h < 17$	$17 \leq h < 23$	$23 \leq h < 35$	$35 \leq h$	TDD
<20	4.0	2.0	1.5	0.6	0.3	5.0
20<50	7.0	3.5	2.5	1.0	0.5	8.0
50<100	10.0	4.5	4.0	1.5	0.7	12.0
100<1000	12.0	5.5	5.0	2.0	1.0	15.0
>1000	15.0	7.0	6.0	2.5	1.4	20.0
Even harmonics are limited to 25% of the odd harmonic limits above.						
Current distortions that result in a dc offset are not allowed.						
I_{sc} = maximum short-circuit current at PCC						
I_L = maximum demand load current at PCC						
PCC - point of common coupling						

Table 4.9 IEEE Standard 519-1992 Current distortion limits for general distribution systems (120 volts through 69,000 volts) [11]

This standard applies to individual consumers of electrical energy. The THD levels for the load cases are shown in Table (4.7). These levels range from a minimum of 17.5% to a maximum of 53.9%. These THD levels only include even harmonics up to the thirteenth harmonic. The harmonics greater than the 13th are ignored because they are small compared to the lower order harmonics. The THD levels found in the simulation waveforms clearly violate all of the THD limits recommended by IEEE Standard 519-1992 for any short circuit ratio. The frequency spectrum of the current waveform found in the field measurement (Figure (4.51)) has a THD of 60.3 for the harmonics less than 11,

and 8.6 for the harmonics between 11 and 16). Both of these harmonic distortion levels violate the IEEE Standard 519-1992 for the short circuit levels between 50 and 100.

The significance of the violation of the IEEE Standard 519-1992 are:

- Excessive losses may occur in the distribution transformer,
- The distribution transformer may experience heating,
- The secondary distribution voltage waveform may be excessively distorted,
- Other services on the common distribution **feeder** may be impacted.

CHAPTER 5

CONCLUSIONS AND RECOMMENDATIONS

5.1 Conclusions

The power electronic adjustable speed drive has found many applications where a variable, controlled motor speed is required. This drive technology has been applied to heat pumps and air conditioners to achieve an increase in efficiency. These drives often have an input current waveform with a significant harmonic content. The harmonic current waveform subsequently passes through the distribution transformer, causing additional transformer core losses, a possible reduction in life, and an effective reduction in the transformer rating. The extra losses are difficult to measure in an actual installation since the transformer losses are small compared to the power flowing through the transformer. Also, in field conditions, the transformer load may vary with time in such a way that a measurement of the primary active power and the secondary (activepower may result in considerable error in the transformer loss due to nonsimultaneous measurements. A simulation was developed which models the behavior of the transformer, drive, induction motor, and compressor load. Output of the simulation is included in Chapter 4, which shows that the input current contains a significant percentage of harmonics. Plots obtained from an actual installation are included for comparison with simulation results. The transformer derating due to the nonsinusoidal load currents was determined for the simulation results and actual measurements.

Typical current THD and transformer deratings obtained from the simulation and field results, using the method given in ANSI C57.110, are given in Table (5.1). Both the simulation and the measured results show that the harmonic level of the currents drawn by the drive are significant. The IEEE Standard 519-1992 limits on the total harmonic distortion of the current drawn by a load are violated for all cases.

Loading level	Primary THD	Secondary THD	Derating
0% *	17.5%	33.3%	90.4%
25% *	36.8%	53.9%	84.4%
50% *	43.9%	54.2%	86.6%
75% *	39.2%	44.7%	91.5%
100% *	38.1%	41.6%	92.1%
Field results **	--	60.6%	93.6%

* Simulated

** Measured

Table 5.1 THD and transformer derating results for simulated and measured waveforms

5.2 Recommendations

The simulation described in this model was used to determine the output waveforms of an adjustable speed drive system. This simulation should be expanded to include several drives served by a common distribution transformer to determine the

effects of several drives on a single distribution transformer. Similarly, the case of a common primary feeder energizing several distribution transformers all of which have ASD heat pump loads should be studied. Also, future work in this area should focus on the maximum levels of harmonic currents that can be allowed in the **distribution** system. It is recommended to study alternative methods to reduce distribution system harmonic content including active filtering, passive filtering, alternative ASD design, and an increase in distribution transformer reactance. It is recommended to assess the economic tradeoffs in these techniques including the effects of distribution transformer loss of life and derating.

BIBLIOGRAPHY

BIBLIOGRAPHY

- [1] Alexander Domijan, Omar Hancock, and Craig Maytrott, 'A Study and Evaluation of Power Electronic Based Adjustable Speed Motor Drives for Air Conditioners and Heat Pumps with an Example Utility Case Study of the Florida Power and Light Company,' IEEE Transactions on Energy Conversion, Vol. 7, No. 3, pp. 396-404, September 1992 .
- [2] American National Standards Institute, Inc., 'Recommended Practice for Establishing Transformer Capability when Supplying Nonsinusoidal Load Currents.,'The Institute of Electrical and Electronic Engineers, Inc. 345 East 47th Street, New York, NY ANSI/IEEE C57.110-1986 .
- [3] Karl Johnson, Robert Zavakil, 'Assessing the Impacts of Nonlinear Loads on Power Quality in Commercial Buildings - An Overview,' 1991 IEEE Industry Application Society Annual Meeting,' IEEE Service Center, Piscataway, NJ, pp. 1863-1869 .
- [4] Muhammad Harunur Rashid, 'Power Electronics, Circuits, Devices, and Applications,' 1988, Prentice Hall, Inc. Englewood Cliffs, New Jersey .
- [5] Paul C. Krause, 'Analysis of Electric Machinery,' 1986, McGraw-Hill, New York .
- [6] P. C. Krause, 'Simulation of Unsymmetrical 2-Phase Induction Machines,' IEEE Transactions on Power Apparatus and Systems, vol. 84, No. 11, pp. 1025-1037, November 1965 .
- [7] N. Mohan, T. M. Undeland, W. P, Robbins, 'Power Electronics: Converters, Applications, and Design,' 1989, John Wiley & Sons, New York .
- [8] Howard Huffman, 'Introduction to Solid-State Adjustable Speed Drives,' IEEE Transactions on Industry Applications, Vol. 26, No. 4, pp. 671-678, July-August 1990 .
- [9] Robert. A. Hanna, 'Harmonics and Technical Barriers in Adjustable Speed Drives,' IEEE Transactions on Industry Applications, Vol. 25, No. 5, pp. 894-900, September-October 1989.

- [10] N. Richard Friedman, Morton H. Blatt, 'Handbook of High-Efficiency Electric Equipment and Cogeneration System Option options for Commercial Buildings,' Electric Power Research Institute, Inc. Final Report, December 1989 .
- [11] 'IEEE Recommended Practices and Requirements for Harmonic Control in Electrical Power Systems,' The Institute of Electrical and Electronic Engineers, Inc. 345 East 47th Street, New York, NY, IEEE Std. 519-1992.
- [12] Thomas A. Lipo, 'Recent Progress in the Development of Solid-State AC Motor Drives,' IEEE Transactions on Power Electronics, Vol. 3, No. 2, pp. 105-117, April 1988
- [13] Gordon R. Slemon, 'Electric Machines and Drives,' Addison-Wesley Publishing Company, 1992.
- [14] Stanley A. Stigan, 'The J & P Transformer Book, A Practical Technology of the Power Transformer,' 1973, Newnes-Butterworths, London .
- [15] William F. Flanagan, 'Handbook of transformer applications,' 1986, McGraw Hill, New York .
- [16] Nils R. Grimm, Robert C. Rosaler, "Handbook of HVAC Design," 1990, McGraw-Hill, New York .
- [17] Cyril M. Harris, "Handbook of Utilities and Services for Buildings," 1990, McGraw-Hill, New York .
- [18] W. J. McNutt, "Insulation Thermal Life Considerations for Transformer Loading Guides," IEEE Transactions on Power Delivery, Vol. 7, No. 1, 392-401, Jan. 1992 .
- [19] Advanced Continuous simulation Language (ACSL) Reference Manual, 1991, Mitchell & Gauthier Associates (MGA) Inc., Concord, MA .
- [20] L. Sulstede, "Applying Power Electronics to Residential HVAC -- the Issues," Conference Proceedings, IEEE Applied Power Electronics Conference and Exhibition - APEC, The Institute of Electrical and Electronic Engineers, Inc. 345 East 47th Street, New York, NY, pp. 615-621.
- [21] A. A. Girgis, F. M. Ham, "A Quantitative Study of Pitfalls in the FFT," IEEE Transactions on Aerospace and Electronic Systems, Vol. AES-16, No. 4, July 1980, pp. 434-439 .
- [22] M. Swartz, "The Operation and Application of Variable Speed Drive Heat Pumps," IEEE Power Engineering Society Summer Power Meeting, Vancouver BC July 1993

[23] M. Kempker, "A Case Study of a Residential ASD Heat Pump," IEEE Power Engineering Society Summer Power Meeting, Vancouver BC July 1993

[24] J. Balda, "A First Attempt to Quantify the Impact of a Large Concentration of ASD Heat Pumps in Residential Distribution Circuits," IEEE Power Engineering Society Summer Power Meeting, Vancouver BC July 1993